BIOANALYSIS OF SMALL AND LARGE MOLECULES USING LC AND LC-MS

I. BIOANALYSIS OF THIAMINE, ITS METABOLITES AND ANALOGS

II. METABOLITE IDENTIFICATION OF THERAPEUTIC OLIGONUCLEOTIDES

by

JAEAH KIM

(Under the Direction of Michael G. Bartlett)

ABSTRACT

In the pharmaceutical industry, LC-MS has been generally applied for quantitative (bio)analysis, biomarker analysis, impurity profiling, and metabolite identification. This dissertation focuses on the development, validation, and application of LC-MS methods in the bioanalysis of small and large molecules and is largely divided into two categories: bioanalysis of thiamine, its metabolites and analogs, and metabolite identification of therapeutic oligonucleotides. Chapter 1 of the thesis comprises the introduction section and gives a general overview of LC-MS methods in association with the studies investigated in the dissertation. The chapter therefore contains the prefaces of two categories, which helps to orient readers on the purpose of the research described in the dissertation. Chapter 2 presents a validated LC-UV method for the bioanalysis of two lipophilic thiamine analogs, benfotiamine and sulbutiamine, in cancer cells. Chapter 3 focuses on the development and validation of an LC-MS method for the simultaneous determination of stable isotope-labeled and unlabeled thiamine, thiamine monophosphate, and thiamine pyrophosphate in cancer cells. Chapter 4 describes the metabolite

identification of an investigational therapeutic oligonucleotide, eluforsen, using an LC-MS method. Finally, Chapter 5 presents an LC-MS method for the determination of the impact of chemical modifications of oligonucleotides on their metabolic stability.

INDEX WORDS: Bioanalysis, Metabolism, Quantitation, Thiamine, Thiamine monophosphate, Thiamine pyrophosphate, Phosphorothioate, Antisense oligonucleotides, Liquid chromatography-mass spectrometry, Ion-pairing agents, Alkylamines, Fluorinated alcohols

BIOANALYSIS OF SMALL AND LARGE MOLECULES USING LC AND LC-MS

I. BIOANALYSIS OF THIAMINE, ITS METABOLITES AND ANALOGS

II. METABOLITE IDENTIFICATION OF THERAPEUTIC OLIGONUCLEOTIDES

by

JAEAH KIM

B.S., Konkuk University, South Korea, 2008

M.S., Seoul National University, 2012

A Dissertation Submitted to the Graduate Faculty of The University of Georgia in Partial Fulfillment of the Requirements for the Degree

DOCTOR OF PHILOSOPHY

ATHENS, GEORGIA

2019

BIOANALYSIS OF SMALL AND LARGE MOLECULES

USING LC AND LC-MS

I. BIOANALYSIS OF THIAMINE, ITS METABOLITES AND ANALOGS

II. METABOLITE IDENTIFICATION OF THERAPEUTIC OLIGONUCLEOTIDES

by

JAEAH KIM

Major Professor:	Michael G. Bartlett
Committee:	Jason A. Zastre Shelley B. Hooks Arthur Roberts Ron Orlando

Electronic Version Approved:

Suzanne Barbour
Dean of the Graduate School
The University of Georgia
May 2019

DEDICATION

Dear my mom, late dad, and brother,

Thanks for always being there for me, love me, and care for me.

ACKNOWLEDGEMENTS

I would very much like to thank Dr. Michael Bartlett, my wonderful major advisor, for all his extraordinary guidance, support, and patience during the past five years. I will be forever grateful that he accepted me in the lab and gave me the great opportunities to work on my projects. He was consistently there as a great mentor and always willing to offer me not only educational support but also personal and career-related advice. Without his unlimited support, I cannot imagine that I could have completed my PhD journey.

I would also like to thank my graduate committee members: Dr. Jason A. Zastre, who gave me a great opportunity and a lot of guidance as a great collaborator in thiamine projects; Dr. Shelley Hooks, who helped me to build my biological insight into my project and gave me a wonderful introduction to the PBS program; Dr. Arthur Roberts, who greatly inspired me about what I should know as a scientist; and Dr. Ron Orlando who helped deepen my knowledge of mass spectrometry. I am extremely thankful for the valuable time they freely gave to give me great advice, to offer me guidance, and to broaden my insight into sciences.

I am thankful to all of my previous and current lab mates: Dr. Xiangkun Yang, who always encouraged and supported me across experiments and career paths, both as a wonderful senior lab mate and as a dear friend; Dr. Babak Basiri, who gave me a lot of impressive inspirations regarding how to fix instruments and taught me about thiamine and oligonucleotide projects; and Dr. Darren Gullick, who was always willing to help me in all circumstances. I would also like to thank to my other lab mates: dear Dr. Shirin Hooshfar, Dr. Ning Li, Dr. Noha El Zahar, Michael Sutton, Shogo,

Louis, Clinton, Helen, Vidya, and all the undergraduate students who have worked by my side throughout this process.

It was also my great pleasure to meet my best friends through my PhD journey, like Sukhneeraj Kaur, Derrick Afful, Ju-dong, and the rest of my friends in the PBS program. Additionally, I should thank all the faculty and staff in the College of Pharmacy at the University of Georgia and the collaborators at ProQR therapeutics.

TABLE OF CONTENTS

Page

CHAPTER 1

INTRODUCTION

Analytical chemistry, a study area focusing on how to separate, identify and quantify analytes, has been applied in numerous areas including forensic science, materials analysis, environmental analysis, and bioanalysis. Among the many analytical chemistry techniques, liquid chromatography-mass spectrometry (LC-MS) has been widely used for the characterization and quantification of drugs, metabolites, and endogenous compounds in biological matrices (e.g., tissues, blood, plasma, and urine) (Jemal 2000). LC is a physical separation method used to isolate components in a mixture by distributing them between two immiscible phases (i.e., mobile phase and stationary phase). Among the different separation techniques (i.e., partition chromatography, size-exclusion chromatography, affinity chromatography, adsorption chromatography, and ion-exchange chromatography), the reversed-phase (RP) mode of partition (liquid-solid) chromatography has been the most widely used to separate analytes. The process depends on the hydrophobic interaction of the analytes with the mobile phase and the stationary phase (i.e., n-octylsilyl- (C8) or n-octadecylsilyl- (C18, ODS) moieties on silica). In RP chromatography, the most hydrophobic analytes are eluted last through the stationary column containing hydrophobic groups, including octyl, butyl, or phenyl. The broad applicability, and more reproducible properties of RPLC compared to normal-phase LC (which is its opposite mode), have allowed RPLC to dominate applications involving nonpolar, polar, ionizable, and ionic compounds.

Ionic components (i.e., organic ions and partly ionized organic compounds) are very hydrophilic and hence their retention on a traditional C18 column is problematic under RPLC conditions. Ion-pair chromatography is a useful RPLC variant in terms of affecting retention of ionic compounds by adding an ionic surfactant. N-alkylamines that are characterized by tetrahedral nitrogen centers have traditionally been used as ion-pairing (IP) agents for acidic, negatively charged analytes (Basiri, Sutton et al. 2016). The hydrophobic moieties of IP agents allow for hydrophobic interactions within stationary phases. Additionally, IPRP chromatography has been actively used as a versatile platform for biological analysis (e.g., RNAs (Azarani and Hecker 2001, Nwokeoji, Kung et al. 2017)), food analysis (e.g., water-soluble vitamins (Albala´-Hurtado, Veciana-Nogue´s et al. 1997, Basiri, Sutton et al. 2016), lactose determination (Erich, Anzmann et al. 2012)), and pharmaceutical analysis for the determination of impurities in dosage forms (Vojta, Hanzlík et al. 2015).

Mass spectrometry is an essential analytical technique that ionizes molecules in an ionization source and sorts these ions based on their specific mass-to-charge ratio (*m/z*) in a mass analyzer, then measures the relative abundance of chemical species within the detector. Electrospray ionization (ESI), which is a soft ionization method for producing intact ions, has been commonly used for large molecules and for fragile polar molecules (Fenn, Mann et al. 1989). Although MS provides high accuracy and sensitivity, another separation process is ideally required when the analysis of components of interest in highly complex mixture are needed in order to separate molecules that have similar molecular masses and fragmentation patterns.

Coupling of LC with MS that is a more advanced technology than typical detectors (e.g., ultraviolet (UV), fluorescence (FL), or refractive index) used for LC and ensures higher sensitivity, broader dynamic range, and improved resolving power. Due to normally limited amounts of

biological samples, a high level of sensitivity is desirable for detection of drugs together with their metabolites. The emergence of LC-MS as a powerful analytical tool has accelerated successful quantitative and qualitative bioanalysis of small and large molecules (e.g., oligonucleotides, proteins, lipids, and carbohydrates). Especially, LC-MS methods have been indispensably applied to various studies for the identification and quantification of drugs and their metabolites in biological matrices, which is an important part of the drug development process.

The successes associated with LC-MS use in the bioanalysis of small molecules has led to its application for the bioanalysis of large molecules (e.g., peptides, proteins, or oligonucleotides) with molecular weights exceeding more than ten thousand Daltons. The distinguishing feature in large molecule analysis is the mass spectral complexity that arises from coherent sequences of peaks from multiply-charged ions. In contrast, small molecule analysis often utilizes a single *m/z* species for identification and quantification.

In the development of bioanalytical methods, the reliability of the methods has been evaluated by several important factors such as sensitivity, detection limit, selectivity, accuracy, precision, linear range, and robustness. To obtain fully validated bioanalytical methods, proper, robust, and stable sample preparation techniques together with analytical methodologies are required for the sample analysis in biological matrices. Depending on the properties of analytes, sample preparation methods should be appropriately modified. The most common methods used for isolation and extraction of analytes of interest are protein precipitation, liquid-liquid extraction (LLE), and solid-phase extraction (SPE). These methods can be used either alone or in combination.

Preface to thiamine analysis

Cancer continues to be a life threatening, yet unconquered disease. Cancer cells adaptively regulate the expression of many metabolic enzymes such as those involved in glycolysis for survival. One of the thiamine derivatives, thiamine pyrophosphate, is an essential coenzyme that plays a pivotal role in many enzyme reactions including glucose metabolism. Although numerous studies have pursued a better understanding of the role of thiamine in cancer metabolism, there is still a significant lack of knowledge regarding the physiological functions of thiamine itself and its phosphorylated forms. Additionally, it is unknown whether intracellular thiamine levels that control the cofactor and non-cofactor roles of its metabolites are regulated (Zastre, Sweet et al. 2013).

Due to its central role, thiamine has drawn attention as a potential nutraceutical therapeutic. Therefore, the study of lipophilic thiamine analogs that have improved therapeutic properties including higher bioavailability has become necessary. In Chapter 2, we developed and validated a robust LC-UV method to determine the synthetic thiamine analogs (i.e., benfotiamine and sulbutiamine) in cancer cells and cell media as part of an effort to determine their effects on cancer cell proliferation.

The need to understand the role of thiamine comes with a better mechanistic understanding of its metabolic fate in cancer cells. Specific isotope-labeled tracers are generally used to explore metabolic flux and specific pathways (Metallo, Walther et al. 2009, Chokkathukalam, Kim et al. 2014, Zhang, Ahn et al. 2014). In Chapter 3, we developed and validated a sensitive and accurate liquid chromatography-triple quadrupole mass spectrometry (LC-QqQ-MS) method for the determination of unlabeled and stable isotope-labeled thiamine and its metabolites in an effort to explore the metabolic fate of thiamine by tracking the movement of an isotope-labeled backbone.

Generally, either liquid chromatography (LC) or gas chromatography (GC) combined with mass spectrometry is widely used to separate and analyze molecules. Since thiamine and its metabolites are thermally unstable and highly polar, LC is a good choice to separate these molecules instead of GC that is typically used for volatile and less polar molecules. Mass spectrometry analysis is necessary to quantify the molecules as well as to distinguish isotope-labeled molecules from unlabeled ones. Electrospray ionization is well-suited for polar molecules that have ionizable functional groups and a triple quadrupole (QqQ) mass analyzer provides increased sensitivity and specificity using a multiple reaction monitoring (MRM) function. Thus, LC-ESI-QqQ-MS/MS was used to determine both the isotope-labeled and unlabeled forms of underivatized thiamine and its metabolites, such as TMP and TPP, for the study of the metabolic fate of thiamine in cancer cells.

Preface to antisense oligonucleotide analysis

Antisense oligonucleotides (ASOs) are short, synthetic, single-stranded oligonucleotides (DNA/RNA), which are with typically 15-25 nucleotides in length (Dias and Stein 2002, Bartlett, Kim et al. 2019) and act as therapeutic agents. ASOs modulate gene expression through various mechanisms including RNase H activation, inhibition of 5'-cap formation or RNA splicing, and steric hindrance of ribosomal subunit binding (Chan, Lim et al. 2006, Geary, Norris et al. 2015).

Metabolite profiling of investigational drugs is indispensable for providing comprehensive insight into compounds as part of the effort to conduct nonclinical safety assessment in the drug development process. Metabolism studies for the identification and characterization of drug metabolites have been completed on a number of other oligonucleotide therapeutics. The investigation of drug metabolism in animals is pivotal for evaluating nonclinical toxicity in order

to predict potential risks in humans. In Chapter 4, we first developed an LC-MS/MS method, then applied the method for the determination of *in vitro* and *in vivo* metabolism of eluforsen—a potential first-in-class RNA-based oligonucleotide designed for chronic inhalation treatment of patients with cystic fibrosis (CF) with the F508del mutation.

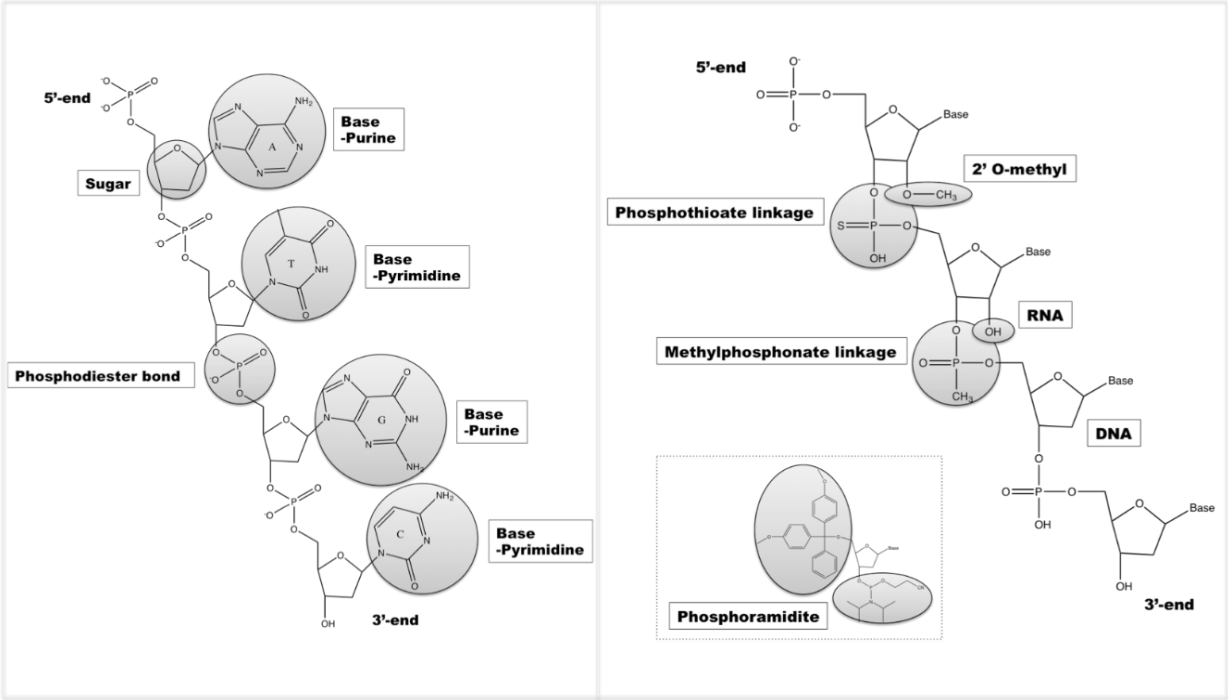

Figure 1. The structure of unmodified and modified oligonucleotides.

[From (Bartlett, Kim et al. 2019)]

Due to the susceptibility of unmodified phosphodiester oligonucleotides to intracellular nucleases (primarily 3'-exonucleases) under physiological conditions, several chemical modifications (**Figure 1**) have been developed to improve nuclease resistance while maintaining the affinity and specificity to target mRNA (Blackburn 2006, Chan, Lim et al. 2006, Faria and Ulrich 2008, Bartlett, Kim et al. 2019). To evaluate the impact of chemical modifications on the *in vitro* metabolic stability testing of ASOs, we developed an LC-MS/MS method for the

metabolite identification of unmodified, phosphorothioate-modified, both phosphorothioate- and 2'-*O*-modified ASOs in Chapter 5.

For both studies presented in Chapter 4 and Chapter 5, we developed quadrupole time-of-flight (QTOF) mass spectrometry-based methods for each study to gather information regarding the metabolic properties of the oligonucleotides. Specifically, negative ion mode is the preferred approach for the acquisition of oligonucleotide tandem mass spectra due to its greater sensitivity. Additionally, the main advantage of the QTOF for this work is to provide accurate mass measurements of both the precursor and product ions, which is necessary to identify numerous metabolites at the same time. Hence, this method provides great accuracy and sensitivity for the determination of a subset of compounds.

CHAPTER 2

DEVELOPMENT OF A NOVEL METHOD FOR THE BIOANALYSIS OF BENFOTIAMINE AND SULBUTIAMINE IN CANCER CELLS [1]

[1] Jaeah Kim, Christopher P. Hopper, Kelsey H. Connell, Parisa Darkhal, Jason A. Zastre, and Michael G. Bartlett. 2016. *Analytical Methods*. 8(28): 5596-5603

Reprinted here with permission of the publisher.

Abstract

Quantification of benfotiamine and sulbutiamine, synthetic thiamine analogs, in biological samples is an essential step toward understanding the role of these thiamine analogs on cancer cell proliferation. A sensitive method to quantitate benfotiamine and sulbutiamine in cells and media was successfully developed using reversed-phase HPLC. Accuracy, precision, specificity and robustness were evaluated to assess the reliability of this method in accordance with U.S. FDA guidelines. The method provided a linear range from 100-50000 nM for benfotiamine and from 500-30000 nM for sulbutiamine in both cells and media. The method was validated and the precision was found to be within 15% relative standard deviation (RSD), and the accuracy to be within 15% relative error (RE). Benfotiamine and sulbutiamine were used as internal standards for each other to achieve a high level of reproducibility. This method has been successfully applied to the study of benfotiamine and sulbutiamine to determine their uptake and disposition between mammalian cells and cell media. The method can contribute to future studies to determine the effect of benfotiamine and sulbutiamine as novel thiamine analogs on cancer cell proliferation.

1. Introduction

Thiamine (Vitamin B1) is an important enzyme cofactor that is critical in a variety of metabolic pathways, especially glucose metabolism. Nutritional supplementation with thiamine has been widely studied especially with respect to its role in cancer cell proliferation. Thiamine has been found to influence a variety of different types of cancer. However, there is a still controversy about the role of thiamine in cancer. The general thought is that thiamine supplementation may contribute to increasing cancer cell proliferation since an increased metabolic rate would be required for this process. Supporting evidence for this mechanism is that increasing thiamine supplementation was observed to contribute toward the growth of Ehrlich's ascites tumor xenografts (Comin-Anduix, Boren et al. 2001). In addition, thiamine supplementation was shown to decrease hypoxia-mediated apoptosis in rat cardiomyocytes (Shin, Choi et al. 2004). As a dichotomous effect of thiamine supplementation on cancer growth, an anti-proliferative effect with no increase in tumor growth in comparison with control has been observed at high doses (Comin-Anduix, Boren et al. 2001). In this scenario, high-doses of thiamine have been suggested to reduce cancer cell proliferation by inhibiting pyruvate dehydrogenase kinases (PDKs) (Hanberry, Berger et al. 2014).

Synthesized lipophilic thiamine derivatives can readily diffuse across plasma membranes and thereby have high bioavailability while thiamine is generally transported at low rates by high affinity carriers (Bitsch, Wolf et al. 1991, Bettendorff and Wins 1994, Loew 1996, Greb and Bitsch 1998, Volvert, Seyen et al. 2008, Portari, Vannucchi et al. 2013). These lipid-soluble thiamine derivatives can be converted to thiamine inside cells and utilized (Volvert, Seyen et al. 2008). Therefore, improvement of the pharmacokinetic properties of thiamine analogs has been considered as an effective strategy to alleviate symptoms due to thiamine deficiency. Among the lipid-soluble thiamine analogs, benfotiamine and sulbutiamine (Fig. 1) are two of the more

promising synthetic derivatives. Benfotiamine and sulbutiamine have excellent bioavailability (Bettendorff, Weekers et al. 1990, Bitsch, Wolf et al. 1991, Bettendorff 1994, Loew 1996, Greb and Bitsch 1998, Portari, Vannucchi et al. 2013) and are known to easily cross cell membranes and increase intracellular thiamine levels (Bettendorff, Weekers et al. 1990, Bettendorff 1994, Volvert, Seyen et al. 2008, Varadi, Zhu et al. 2015). Benfotaimine, an *S*-acyl derivate of thiamine, was discovered to stimulate transketolase (TKT) activity involved in glucose metabolism and prevent diabetic nephropathy in a similar manner to high-dose thiamine (Babaei-Jadidi, Karachalias et al. 2003, Hammes, Du et al. 2003, Rabbani and Thornalley 2011). Sulbutiamine, a dimer of two modified thiamine molecules, is widely used clinically as a treatment for brain function including memory disorders and asthenia (Van Reeth 1999, Trovero, Gobbi et al. 2000, Douzenis, Michopoulos et al. 2006, Volvert, Seyen et al. 2008).

Previously, HPLC methods for the analysis of benfotiamine bulk drug and in tablet dosage forms have been reported (Adithya and Vijayalakshmi 2012, Nanaware, Bhusari et al. 2013). Adithya et al. developed an HPLC method with a range from 5-35 μg ml^{-1}, with a 0.1448 μg ml^{-1} of limit of detection (LOD) and a 0.4388 μg ml^{-1} of limit of quantification (LOQ) (Adithya and Vijayalakshmi 2012). In the literature, an HPLC method for analysis of sulbutiamine was reported with a range from 2-40 μg ml^{-1}, a 0.5 μg ml^{-1} LOD and a 1.51 μg ml^{-1} LOQ from a tablet dosage form (Abdelwahab and Farid 2014). However, no methods have been reported for the determination benfotiamine and sulbutiamine from biological matrices.

There are many ongoing drug discovery efforts focused on the treatment of cancer, a life threatening and unconquered disease. Due to its central role in many biochemical pathways such as glycolysis, thiamine has been drawing attention as a potential therapeutic adjuvant. This has led to the development of the lipophilic thiamine derivatives, benfotiamine and sulbutiamine, which

have improved therapeutic properties including higher bioavailability. However, it is necessary to determine the effects of these two thiamine analogs on cancer cell proliferation.

In this study, we have developed and validated a bioanalytical method for the analysis of benfotiamine and sulbutiamine from cells and cell media. We have applied this method to the determination of both intracellular and extracellular levels of these compounds in order to identify their effect on cancer cell proliferation. Based on these preliminary results, we expect that the developed HPLC method will be vital toward the development of thiamine analogs as potential nutraceutical therapeutics.

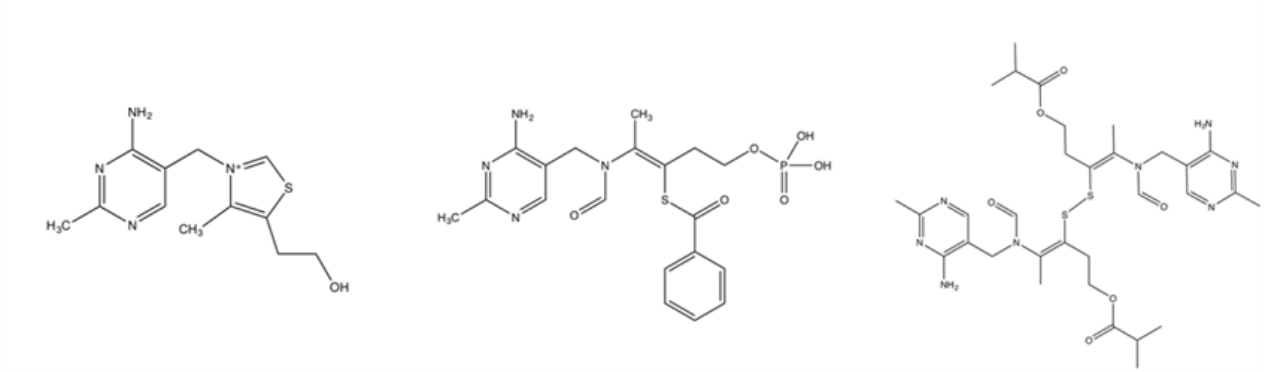

Fig. 1 Structures of thiamine, benfotiamine, and sulbutiamine

2. Materials and methods

2.1 Chemicals and reagents

The reference standards for benfotiamine and sulbutiamine were purchased from MP Biomedicals (Santa Ana, CA, USA) and Toronto Research Chemicals (Toronto, Ontario, Canada), respectively. Water and acetonitrile (chromatographic grade), hydrochloric acid, di-isopropyl ether and trichloroacetic acid (TCA) were obtained from Sigma-Aldrich (St Louis, MO, USA). Dibasic sodium phosphate was supplied by J. T. Baker (Phillipsburg, NJ, USA). All standards were analytical grade with more than 90% chemical purity. Custom-formulated thiamine-deficient RPMI 1640 media and fetal bovine serum (FBS) were purchased by Mediatech (Manassas, VA, USA) and Seradigm (Radnor, PA, USA), respectively.

2.2 Preparation of the stock solutions, calibration standards and quality control (QC) samples

Stock solutions of benfotiamine (1.0 mM) and sulbutiamine (2.0 mM) were prepared in methanol. The aliquots of stock solutions were stored at -80°C. 2 μM of benfotiamine and 4 μM of sulbutiamine were used as internal standards (ISTD) for the determination of the other analyte. Each stock solution was serially diluted with water to prepare the working solutions at appropriate concentrations. For preparation of benfotiamine and sulbutiamine (cells and cell media) calibration curves, the working solutions of benfotiamine were diluted to calibration standards over the range from 100-50000 nM. The range of concentrations of sulbutiamine in cells and media for the calibration standards was 500-30000 nM. Quality control (QC) samples were prepared at concentrations of 300, 1500 and 40000 nM for benfotiamine and 1500, 4000 and 24000 nM for sulbutiamine.

2.3 Instrumentation and chromatographic conditions

HPLC analysis was performed by using an Agilent 1100 quaternary pump HPLC system (Santa Clara, CA). HPLC separation was achieved at 25°C using a Shim-pack MAqC-ODS I column (4.6×150 mm, 5 μm, Shimadzu Corp.). A mobile phase system containing of 15 mM sodium phosphate buffer (pH 3.6) and 100 % acetonitrile were used. The injection volume of each sample was 50 μl and the mobile phase flow rate was set at 0.8 ml min^{-1}. Gradient conditions for benfotiamine analysis were as follows (time (in minutes), % mobile phase B): (0, 10), (8, 30), (10, 70), (15, 80), (16, 80), (16.01, 10), (21, 10). Gradient conditions for sulbutiamine analysis were as follows (time (in minutes), % mobile phase B): (0, 10), (8, 30), (10, 70), (16, 80), (17, 70), (17.01, 10), (22, 10). Benfotiamine and sulbutiamine were detected at wavelengths of 235 nm and 239 nm, respectively. Chemstation (Rev. B.01.03, Agilent) was used for instrument control, data collecting and processing. After each injection, the injection needle was washed with water.

2.4 Cell culture conditions

Human glioblastoma astrocytoma cells (U-87MG) were purchased from ATCC (Manassas, VA, USA). Custom-formulated thiamine-deficient RPMI 1640 media supplemented with 10% heat-inactivated FBS was used for cell culture. Cells were incubated at 37 °C in a humidified atmosphere of 5% CO_2. Cultured cells in T-175 flasks were treated with trypsin/EDTA to be harvested, followed by washing three times using ice-cold phosphate-buffered saline (1xPBS). Cells were counted using a TC20 Automated Cell Counter (Bio-Rad, Hercules, CA, USA) and divided into aliquots of 1×10^6 cells by centrifugation at 4 °C for 5 min at 500g.

2.5 Sample preparation

Sample preparation was done as outlined in the procedure by Basiri *et al.* for thiamine (Basiri, Sutton et al. 2016). Cell pellets were treated with 500 µl of 15% trichloroacetic acid (TCA) solution to precipitate proteins in the samples. Likewise, 500 µl of media was treated with 100 µL of 72% TCA solution. Afterwards, different concentrations of benfotiamine and sulbutiamine were spiked into both cells and media. Internal standards were added to each sample to a final concentration of 2 µM and 4 µM for benfotiamine and sulbutiamine, respectively. Benfotiamine and sulbutiamine were used as an internal standard for each other. Following a 2 min vortex, the mixture was kept on ice for 30 min. The mixture was treated with 6 volumes of di-isopropyl ether to remove the TCA and mixed for another 1 min. After centrifugation at 13,000 g at 10 °C for 6 min, the supernatant (organic layer) of the mixture was discarded. Evaporation of the remaining ether was done in the hood and the mixture was filtered through 0.22 µm hydrophilic nylon membrane syringe filters, prior to analysis by HPLC.

2.6 Method development and validation

This method was validated in accordance with the current U.S. FDA guidance for bioanalytical method validation. Selectivity, linearity, sensitivity, reproducibility, and stability tests were carried out to validate the method.

3. Results and discussion

3.1 Method development

Factors that establish a selectivity and sensitivity were optimized in HPLC with UV detector for quantification of benfotiamine and sulbutiamine. The gradients that provided good separation

of these compounds were step-by-step established. Detection wavelengths for each compound were found to improve sensitivity using the variable wavelength detector. Fluorescence detection was also applied to these compounds in an effort to achieve higher sensitivity because detection based on fluorescence is generally more sensitive than UV absorption. However, it did not improve the detection ability for these compounds. The potential risk that this inorganic salt may precipitate in higher levels of organic solvents was avoided by using a 15 mM sodium phosphate buffer. Both methanol and acetonitrile were tested as organic solvents and acetonitrile provided a more stable baseline for the chromatogram at both 235 nm and 239 nm.

3.2. Sensitivity and selectivity

In Fig. 2 and 3, the representative chromatograms demonstrate the selectivity and sensitivity of the method from cells and media. Fig. 2 shows the chromatograms for benfotiamine and sulbutiamine at the LLOQ levels in both cells and media. Limit of detection (LOD) and lower limit of quantification (LLOQ) that define the sensitivity of the method were determined for each analyte at signal-to-noise (S/N) ratios of greater than 3 and 10, respectively. The LOD was 50 nM (22.3 ng/mL) and LLOQ was 100 nM (210.9 ng/mL) for benfotiamine in both cells and cell media. The LOD was 300 nM and LLOQ was 500 nM for sulbutiamine in these biological matrices. As shown in Table 2, the precision and accuracy of the method at the LLOQ level was validated within 20% of the relative standard deviation (RSD) and relative error (RE). Selectivity of the method helps to differentiate and quantify the analytes of interest in samples that include other compounds. The chromatograms were acquired following sample extraction to investigate any interference. Fig. 3A and 3B shows the chromatograms for benfotiamine and sulbutiamine in media at 0 h and

after 24 h treatment with 0.01 mM of each compound. Fig. 3C and 3D shows the chromatograms for benfotiamine and sulbutiamine in cells after 24 h treatment with 0.01 mM of each compound.

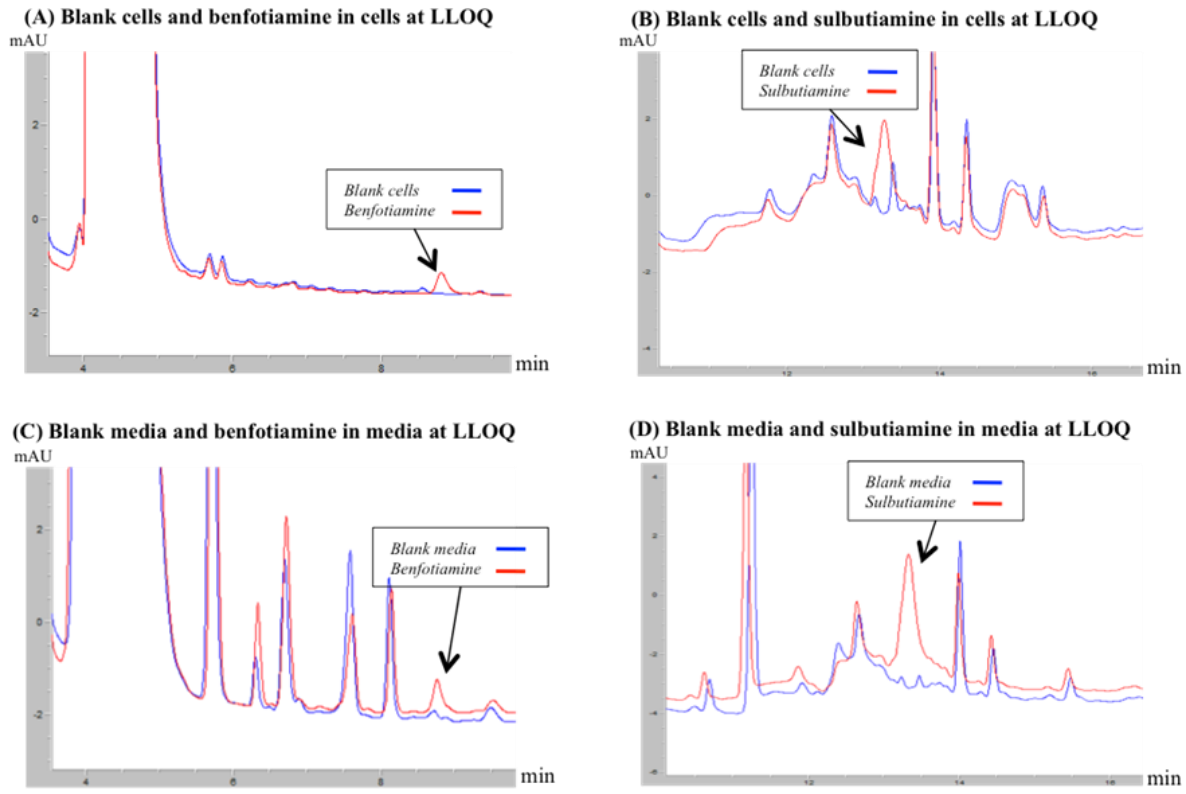

Fig. 2 Representative chromatograms of benfotiamine (A and C, red) and sulbutiamine (B and D, red) at LLOQ levels in cells and media. The chromatograms are overlaid with chromatograms of blank cells (A and B, blue) and blank media (C and D, blue).

3.3. Linearity and calibration curve

Nine increasing concentrations of benfotiamine with 4 μM of sulbutiamine as an internal standard were added to the cells and thiamine-deficient RPMI 1640 media to generate calibration curves. The spiked concentrations were 100, 200, 500, 1000, 2000, 5000, 10000, 50000 nM. Likewise, calibration curves for sulbutiamine quantification with 2 μM of benfotiamine were

plotted with the range of 500, 700, 1000, 3000, 5000, 7000, 10000, 30000 nM. Calibration curves with 1/*x* weighted linear regression were obtained using the peak area ratios between the analyte and the ISTD *versus* the analyte concentration. Slopes, *y*-intercepts and *R*-squared values of the regression lines are shown in Table 1. As shown in Table 1, the method showed good linearity with the values for the correlation coefficients (R^2) > 0.995 for each analyte.

Table 1 Calibration curves for benfotiamine and sulbutiamine in cells and cell media (n=3).

Analyte	Cells			Cell media		
	Slope	Intercept	R^2	Slope	Intercept	R^2
Benfotiamine	0.8686±0.0251	-0.0074±1.7968	0.9972±0.0011	0.8801±0.0268	0.0064±0.6024	0.9958±0.0045
Sulbutiamine	1.0921±0.0499	0.0330±2.9314	0.9975±0.0004	1.0362±0.0464	0.0886±1.9746	0.9966±0.0021

Table 2 The intra-day (n=5) and inter-day (n=15) precision (RSD) and accuracy (RE) for the LC–UV method used to quantitate benfotiamine in cells and cell media.

Matrix	Analyte	Nominal conc. (nM)	Intra-day (n=5)			Inter-day (n=15)		
			Measured conc.	RSD (%)	RE (%)	Measured conc.	RSD (%)	RE (%)
Media	Benfotiamine	100 (LLOQ)	111	5.51	10.50	101	12.21	1.18
		300 (LQC)	274	4.67	-8.80	282	7.28	-5.93
		1500 (MQC)	1443	9.73	-3.82	1443	6.94	-3.79
		40000 (HQC)	41003	7.96	2.51	41832	6.43	4.58
Cells		100 (LLOQ)	107	3.30	6.73	103	7.11	2.60
		300 (LQC)	272	2.99	-9.37	284	5.19	-5.44
		1500 (MQC)	1372	1.21	-8.56	1437	5.82	-4.20
		40000 (HQC)	41977	5.02	4.94	41819	5.44	4.55

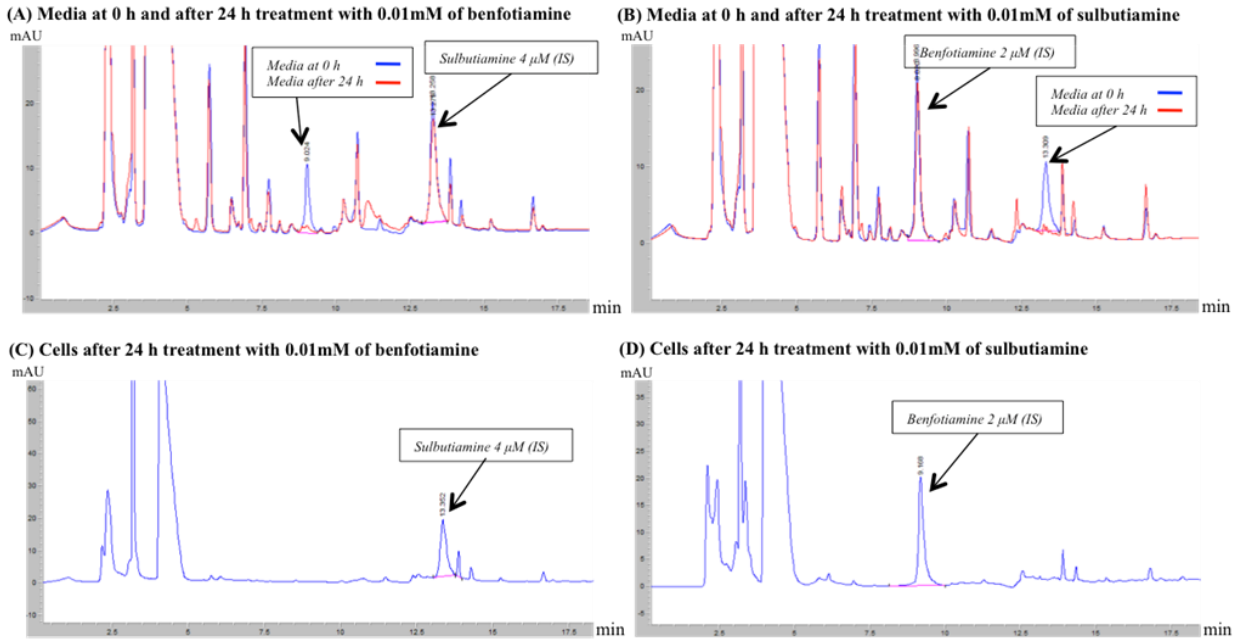

Fig. 3 Representative chromatograms of benfotiamine (A and C) and sulbutiamine (B and D) in media and cells. Media at 0 h and after 24 h treatment with 0.01 mM of benfotiamine and sulbutiamine (A and B). The chromatograms are overlaid with chromatograms of media at 0 h (blue) and media after 24 h (red). Cells are shown after 24 h treatment with 0.01 mM of benfotiamine and sulbutiamine (C and D).

3.4. Precision and accuracy

Precision and accuracy of the method were validated at the LLOQ, LQC, MQC and HQC levels of benfotiamine and sulbutiamine in both cells and cell media. The precision, defined as the closeness of measurements acquired from multiple sampling at the same concentration, was calculated by assessing the % RSD for repeatability (intra-day precision) and reproducibility (inter-day precision) of the method. The accuracy, determined as the closeness between measured concentrations and nominal concentrations was acquired by assessing the % RE. According to the FDA requirements, the % RSD and % RE values should be less than 15% for all QC samples and

less than 20% for the LLOQ (FDA 2001, FDA 2013)**.** RSD and RE values for benfotiamine and sulbutiamine in cells and cell media are shown in Tables 2 and 3, respectively. The intra-day (n=5) and inter-day (n=15) precision and accuracy for benfotiamine were determined at three different concentrations: 300 nM (low quality control, QC), 1500 nM (mid-QC) and 40000 nM (high-QC). The intra-day (n=5) and inter-day (n=15) precision and accuracy for sulbutiamine were evaluated at 1500 nM (LQC), 4000 nM (MQC) and 24000 nM (HQC). All values met the requirements found in the U.S. FDA Guidance.

Table 3 The intra-day (n=5) and inter-day (n=15) precision (RSD) and accuracy (RE) of the LC–UV method used to quantitate sulbutiamine in cells and cell media.

Matrix	Analyte	Nominal conc. (nM)	Intra-day (n=5)			Inter-day (n=15)		
			Measured conc.	RSD (%)	RE (%)	Measured conc.	RSD (%)	RE (%)
Media	Sulbutiamine	500 (LLOQ)	444	8.89	-11.15	456	6.92	-8.87
		1500 (LQC)	1497	7.73	-0.21	1492	6.10	-0.56
		4000 (MQC)	4319	2.46	7.98	4032	6.77	0.79
		24000 (HQC)	22585	2.71	-5.90	23042	3.55	-3.99
Cells		500 (LLOQ)	515	8.96	3.10	506	9.66	1.16
		1500 (LQC)	1400	1.69	-6.65	1410	8.22	-6.02
		4000 (MQC)	4125	3.06	3.13	3990	5.85	-0.25
		24000 (HQC)	24701	1.16	2.92	23384	6.38	-2.57

3.5. Stability

Table 4 shows the autosampler stability (25 °C, 24 h), bench-top stability (4 °C, 8 h) and freeze-thaw stability (three freeze–thaw cycles, −80 °C, 72 h) data for benfotiamine and sulbutiamine in both cells and cell media. All samples were stable on the autosampler for 24 h at the LQC and HQC levels. The samples were kept in the 4 °C refrigerator for 8 h to test bench-top stability. This

simulated the all sample preparation processes which were conducted on ice. After 8 h, the compounds were extracted and analyzed. For freeze-thaw stability testing, the samples were frozen at -80 °C overnight and thawed at room temperature. Subsequently, samples were taken through two more freeze-thaw cycles before being analyzed. In media, both benfotiamine and sulbutiamine at the LQC and HQC levels were stable for 8 h at 4 °C and during all three freeze-thaw cycles. On the other hand, both compounds were degraded at the LQC concentration when incubated with cells for the evaluation of bench-top stability (4 °C) and freeze-thaw stability even though they were stable at the HQC. Additionally, it appears as though sulbutiamine under such conditions was degraded to a derivative compound as shown by the chromatograms (data not shown).

Table 4 Autosampler stability (n = 4), bench-top stability (n = 4), and freeze-thaw stability (n=4) of benfotiamine and sulbutiamine at LQC and HQC in cells and cell media.

Matrix	Analyte	Conc. (uM)	Autosampler stability (%±SD)	Bench-top stability (%±SD)	Freeze-thaw stability (%±SD)
Media	Benfotiamine	300 (LQC)	112±6.76	106±1.66	106±1.91
		40000 (HQC)	102±0.43	101±0.62	101±2.27
	Sulbutiamine	1500 (LQC)	108±9.83	92.4±13.70	110±11.98
		24000 (HQC)	100±5.81	101±1.03	94.0±1.99
Cells	Benfotiamine	300 (LQC)	114±7.07	-	-
		40000 (HQC)	103±2.50	94.6±0.72	101±2.12
	Sulbutiamine	1500 (LQC)	101±5.78	-	58.8±5.36
		24000 (HQC)	99.8±7.83	93.0±0.22	94.2±1.21

3.6. Recovery

Recovery reported as a percentage (%) indicates the extraction efficiency of the analytical process (FDA 2001, FDA 2013). Absolute recovery (AR) and relative recovery (RR) from cells and cell media were evaluated by comparing the peak areas between standard solutions and spiked samples or spiked samples and post-preparation spiked samples at the LQC, MQC and HQC levels. Spiked samples were prepared by adding standard solutions to the biological matrix prior to sample preparation; the post-preparation samples were made by spiking them with standard solutions following sample extraction. Both spiked samples (n=3) in biological matrices and standard solutions (n=3) with equivalent concentrations were prepared at the LQC, MQC, and HQC for benfotiamine and sulbutiamine to evaluate the absolute recovery. Likewise, spiked samples (n=3) in the biological matrices and post-preparation spiked samples (n=3) at same concentrations were prepared for the evaluation of relative recovery.

Table 5 shows the absolute recovery and relative recovery for the two thiamine analogs from biological matrices at the LQC, MQC, and HQC points. Acquired data for benfotiamine was within the range from 91.95% to 113.62% with an average of 101.93% in cells and cell media. The recovery for sulbutiamine was within the range from 88.04% to 115.05% with an average of 101.84% at three concentration levels in both matrices. These results show the complete recovery of all analytes with excellent efficiency.

Table 5 Absolute recovery (n = 3) and relative recovery (n = 3) of the method.

Matrix	Analyte	Conc. (nM)	AR (%)	RR (%)
Media	Benfotiamine	300 (LQC)	113±1.01	100±0.34
		1500 (MQC)	104±8.56	92.1±0.14
		40000 (HQC)	103±0.24	96.1±0.48
	Sulbutiamine	1500 (LQC)	110±3.90	98.2±9.20
		4000 (MQC)	101±1.58	101±3.34
		24000 (HQC)	97.6±1.42	102±0.34
Cells	Benfotiamine	300 (LQC)	106±4.71	103±2.11
		1500 (MQC)	106±1.08	97.3±0.87
		40000 (HQC)	106±0.03	96.3±0.33
	Sulbutiamine	1500 (LQC)	111±3.96	98.1±0.64
		4000 (MQC)	106±1.87	99.6±1.26
		24000 (HQC)	99.8±1.29	98.3±0.59

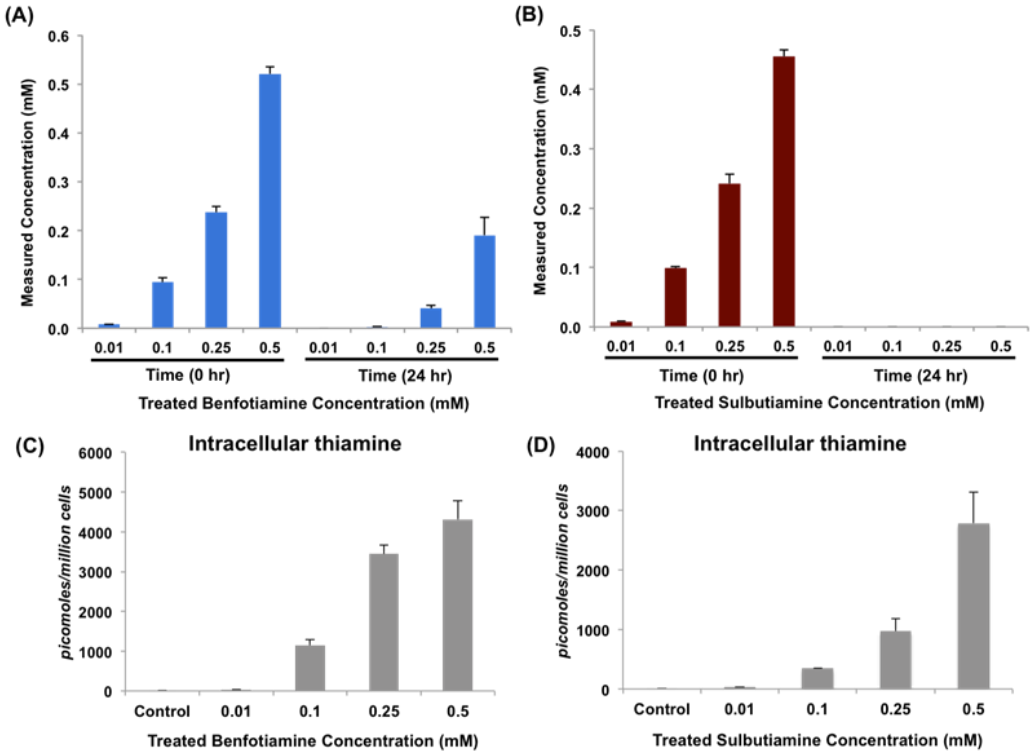

Fig. 4 Determination of benfotiamine (A) and sulbutiamine (B) in media after 24 h treatment with 0.01, 0.1, 0.25 and 0.5 mM of compounds in human colon carcinoma cells (HCT 116).

HCT 116 cells were treated with RPMI 1640 containing different concentrations of benfotiamine and sulbutiamine, and the experiment was done in duplicate. After 24 h, fresh cell media (before cell treatment) treated with compounds and the spent media (after cell culture) were prepared and analyzed. The samples were injected into the HPLC and the concentrations of benfotiamine in both media 0 h and 24 h were determined as shown in Fig. 4A. The results for sulbutiamine are depicted in Fig. 4B. After 24 h treatment with each compound, intracellular thiamine levels were determined in cells (Fig. 4C and 4D). The concentrations shown in the graphs are mean±S.E.M (standard error of mean) values.

3.7. Application of the method

The validated method was applied to biological samples to examine the impact of the two thiamine analogs on intracellular thiamine levels in cancer cells. After treating the cell media with each compound at different concentrations, the levels of benfotiamine and sulbutiamine were determined by harvesting 5 million cells per sample, respectively. The results showed that benfotiamine and sulbutiamine were not detected in the cell samples after 24 h treatment with each compound (Fig 3C and 3D). As shown in many studies (Bettendorff, Weekers et al. 1990, Bettendorff 1994, Volvert, Seyen et al. 2008, Varadi, Zhu et al. 2015), these analogs easily diffuse across plasma membranes leading to increases in intracellular thiamine levels. Therefore, this result suggested that the thiamine analogs were converted into thiamine after crossing the cell membrane. This conclusion was supported by this work which measured intracellular thiamine levels (Fig 4C and 4D) using a previous developed and validated method by Basiri et al. (Basiri, Sutton et al. 2016) in order to confirm the utilization of benfotiamine and sulbutiamine. The cells dosed with higher concentrations of the thiamine analogs contained correspondingly higher

amounts of intracellular thiamine (Fig. 4C and 4D). These results provide valuable insight regarding the behavior of these thiamine analogs in cells. Interestingly, while the levels of benfotiamine decreased in cell media after 24 h following cell treatment (Fig. 4A), Fig. 4B shows that sulbutiamine was not detected in cell media after 24 h. Sulbutiamine, which consists of two modified thiamine molecules (Fig. 1) appears to be transformed into two modified molecules of thiamine. This was confirmed by the fact that these thiamine derivative peaks were detected in both media and cell samples after 24 h treatment with sulbutiamine derivatives that were generated by reducing the disulfide bond in sulbutiamine with dithiothreitol (DTT) (data not shown). Taken together these experiments show that sulbutiamine is reduced under cell culture conditions and the derivatives are further converted into thiamine.

4. Conclusions

A new robust and sensitive HPLC-UV method to determine benfotiamine and sulbutiamine has been developed and fully validated for the first time using cells and cell media as biological matrices in following regulatory guidance. The developed method has good precision, accuracy, and linearity for the determination of benfotiamine within the range from 100-50000 nM and for sulbutiamine within the range from 500-30000 nM in cells and cell media. The LLOQ is 100 nM and 500 nM for benfotiamine and sulbutiamine, respectively. Benfotiamine and sulbutiamine performed well as internal standards for each other. The sample preparation method provided for the complete recovery of these compounds. As a result, this method was successfully applied to in vitro studies of benfotiamine and sulbutiamine in cancer cells, to determine the impact of these thiamine analogs. This study has established a new bioanalytical method to identify the effect of thiamine analogs on cancer cell proliferation.

Acknowledgments

This work was supported by the American Cancer Society through a Research Scholar Grant (RSG-14-026-01-CNE) awarded to Jason Zastre, PhD.

CHAPTER 3

DEVELOPMENT OF AN IPRP-LC-MS/MS METHOD TO DETERMINE THE FATE OF INTRACELLULAR THIAMINE IN CANCER CELLS [2]

[2] Jaeah Kim, Hunter C. Jonus, Jason A. Zastre and Michael G. Bartlett.
In Revision by *Journal of Chromatography B*.

Abstract

Understanding the mechanisms underlying cancer cell survival is critical toward advancing drug discovery efforts in this field. Supplemental vitamins have been proposed to play a role in cancer cell metabolism because the increased supply of nutrients is thought to provide cofactors supporting the higher metabolic rate of cancer cells. Particularly, the role of thiamine (vitamin B1) in many biochemical pathways that supports cancer cell metabolism has been investigated. Consequently, the analysis of thiamine and its derivatives in a manner that reflects its dynamic response to genetic modification and pathophysiological stimuli is essential. In this work, we developed a mass spectrometry based-analytical method to track metabolites derived from stable isotope tracers for a better understanding of the metabolic fate of thiamine in cancer cells. This method used ion-pair reversed phase liquid chromatography to simultaneously quantify underivatized thiamine, thiamine monophosphate (TMP) and thiamine pyrophosphate (TPP) in cells. Hexylamine was used as an ion-pairing agent. The method was successfully validated for accuracy, precision and specificity in accordance with U.S. FDA guidance. Furthermore, the method was then applied for the determination of thiamine and its derivatives with stable isotope labeling to explore the metabolic fate of intracellular thiamine in cancer cells. The finding show that thiamine is rapidly converted to TPP however, the TPP does not return to thiamine. It appears that TPP may be utilized for other purposes rather than simply being an enzyme cofactor, suggesting unexplored roles for thiamine in cancer.

1. Introduction

Thiamine is an important water-soluble vitamin, which is converted to the active coenzyme thiamine pyrophosphate (TPP) (also known as thiamine diphosphate (TDP)) by the enzyme thiamine pyrophosphokinase-1 (TPK-1) (Nosaka, Onozuka et al. 2001, Ganapathy, Smith et al. 2004, Zastre, Sweet et al. 2013). TPP works as a coenzyme in many enzymatic reactions, especially those involved in intracellular glucose metabolism as shown in Fig. 1 (LU'O'NG and NGUYỄN 2013, Zastre, Hanberry et al. 2013, Zastre, Sweet et al. 2013). TPP acts as a cofactor for pyruvate dehydrogenase (PDH), alpha-ketoglutarate dehydrogenase (α-KGDH), and transketolase (TKT). PDH converts pyruvate into acetyl-CoA which is required for the synthesis of the neurotransmitter acetylcholine among other possibilities (Eram and Ma 2013). α-KGDH catalyzes the conversion of alpha-ketoglutarate to succinyl-CoA in the tricarboxylic acid cycle (TCA) that is the central metabolic pathway to generate energy in most aerobic organisms (Tretter and Adam-Vizi 2005). TKT plays a role in the pentose phosphate pathway that generates NADPH and ribose 5-phosphate for the synthesis of nucleotides (Pácal, Tomandl et al. 2010).

In cancer cells, the expression of glycolytic enzymes and nutrient transporters are adaptively regulated for cancer cell survival (Zastre, Hanberry et al. 2013, Zastre, Sweet et al. 2013). Owing to the pivotal role of TPP as an essential coenzyme in many enzyme reactions, many studies have reported the existence of a relationship between thiamine supplementation and cancer (Comín-Anduix, Boren et al. 2001, Shin, Choi et al. 2004). Numerous studies with the goal of understanding the role of thiamine in cancer metabolism have been pursued. However, there is a gap in our knowledge regarding the physiological functions of thiamine itself and its phosphorylated forms, as well as whether the intracellular thiamine concentrations that regulate the cofactor and non-cofactor roles of these metabolites are controlled (Zastre, Sweet et al. 2013).

The need to understand the role of thiamine necessitates a better mechanistic understanding of the metabolic fate of thiamine in cancer cells.

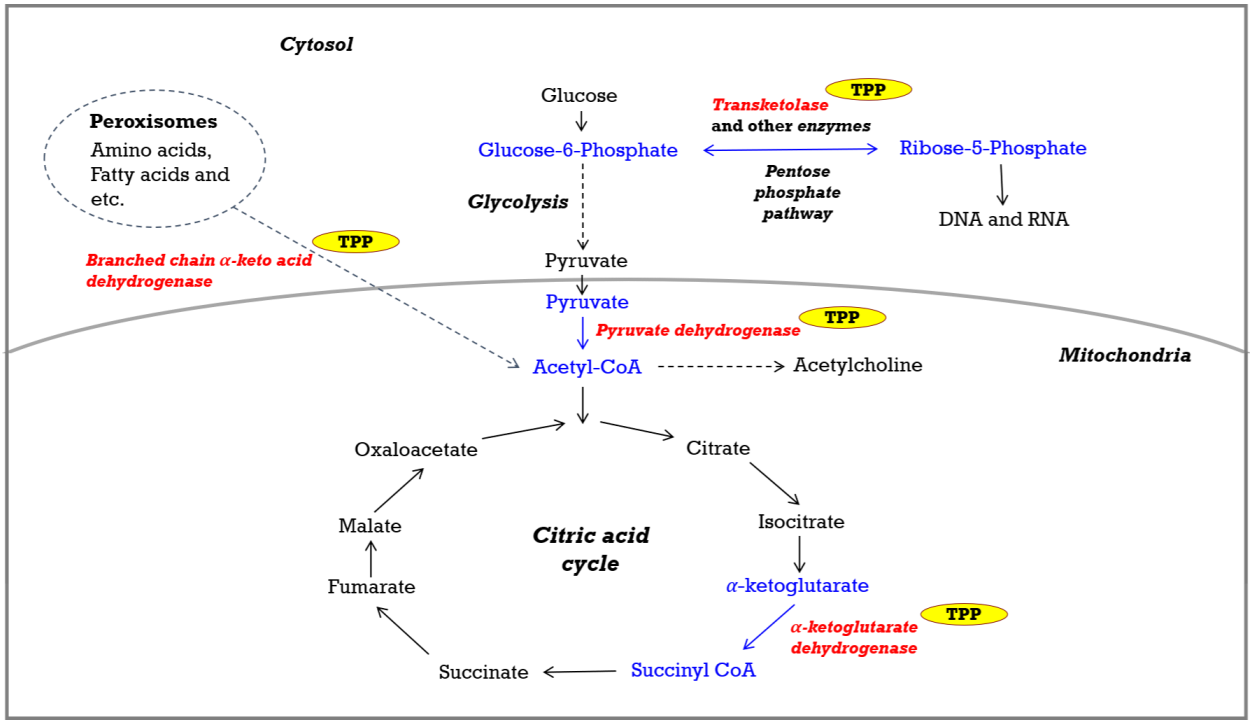

Fig. 1. Summarized schematic of glucose metabolism associated with thiamine-dependent enzymes.

To study how cancer cells adaptively regulate these molecules, a sensitive and accurate bioanalytical method is required to explore the metabolic flux of thiamine using specific isotope-labeled tracers. Liquid chromatography–mass spectrometry (LC-MS/MS) has been widely used for ^{13}C-metabolic flux analysis (Chokkathukalam, Kim et al. 2014, Guo, Sheng et al. 2015, Jang, Chen et al. 2018). However, there are no current validated bioanalytical methods available for the simultaneous quantification of both unlabeled and stable-isotope labeled thiamine, TMP and TPP. Conventional methods to detect thiamine, TMP and TPP have relied on ion-pairing reversed phase high-performance liquid chromatography (IPRP-HPLC) with fluorescence (FL) detection

requiring pre- or post-column derivatization using the thiochrome reaction (van Landeghem, Puts et al. 2005, Lu and Frank 2008, Basiri, Sutton et al. 2016). Improved fluorescence properties of these molecules through derivatization and using ion-pairing reagents contributes to providing better fluorescence sensitivity and separation ability via hydrophobic interaction by compensating for the high polarity of the compounds. However, the sodium phosphate buffer and ion-pairing reagents (e.g., tetrabutyl ammonium hydroxide) generally used in these methods are not compatible with mass spectrometry due to their lack of volatility, resulting in ion suppression. Additionally, the trichloroacetic acid (TCA) solution used for protein precipitation of biological samples and to stabilize the positively charged thiazole ring in thiamine causes salt formation that is unfavorable for mass spectrometry. Moreover, the additional steps in the sample preparation (derivatization) may increase method error and can be laborious (Puts, de Groot et al. 2015). Finally, the potassium ferricyanide used to derivatize thiamine and its metabolites also causes ion suppression through salt formation.

To circumvent these technical challenges, we developed and validated a novel IPRP-LC-MS/MS method that does not rely on derivatization. However without derivatization, these molecules are highly polar and show only differences in their phosphate groups, thereby providing a variety of challenges during method development. Due to these challenges, some published reports have attempted to determine either one or two molecules among these three molecules using LC-MS/MS (Puts, de Groot et al. 2015). Although Cheng et al. proposed an LC-MS/MS method to simultaneously determine the levels of underivatized thiamine, TMP, and TPP in human whole blood using thiamine-d3 and TPP-d3 as internal standards, the method seems to have low separation α values using a C18 column without any ion-pairing agents (Cheng, Ma et al. 2018).

Perchloric acid used for sample preparations in the study, is deleterious for a capillary and sampling cone, and dangerous (Ashcroft 2007).

In this study, with efficient separation using hexylamine and a user-friendly sample preparation method, we have successfully developed an IPRP-LC-MS/MS method for the simultaneous detection of the underivatized versions of both unlabeled and labeled thiamine, TMP and TPP, which allows for the exploration of the metabolic changes within these molecules in cancer cells.

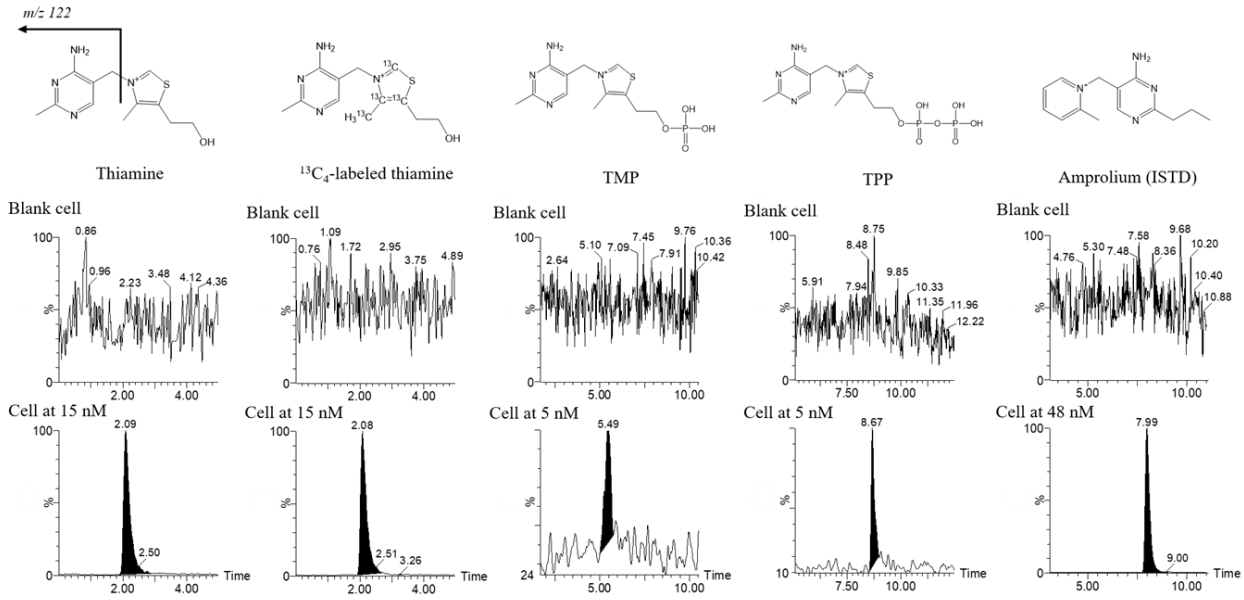

Fig. 2. Typical chromatogram of blank cell spiked with thiamine, labeled thiamine, TMP and TPP at their respective LLOQ.

2. Experimental

2.1. Chemicals and materials

The reference standards for unlabeled thiamine, TMP, TPP, $^{13}C_4$-labeled thiamine (LT) and amprolium (internal standard) were purchased from Sigma-Aldrich (St Louis, MO, USA). The chemical structures of these molecules are shown in Fig. 2. LC-MS grade water, methanol,

acetonitrile, ammonium acetate, ammonium bicarbonate, ammonium formate and formic acid were obtained from Sigma-Aldrich (St Louis, MO, USA). Various alkylamines including triethylamine, N,N-dimethylhexylamine, N-methyldibutylamine, N,N-dimethylbutylamine, tributylamine, N,N-diisopropylethylamine and hexylamine were supplied by Sigma-Aldrich (St Louis, MO, USA). Custom-formulated thiamine-deficient RPMI 1640 media and fetal bovine serum (FBS) were acquired by Mediatech (Manassas, VA, USA) and Seradigm (Radnor, PA, USA), respectively.

2.2. Preparation of standards, quality control samples and internal standard

1.0 mM stock solutions of thiamine, LT, TMP and TPP were prepared in 0.1 M HCl and their aliquots were stored at -80 °C. 48 nM of amprolium hydrochloride was used as an internal standard (ISTD) for the determination of thiamine and its metabolites. Working solutions were prepared at appropriate concentrations through serial dilution with water. The human colon cancer cell line (HCT 116) was used as the biological matrix for calibration standards and quality control samples. Calibration standards were spiked in blank cells for the following calibration ranges of analytes: thiamine (15-500 nM); LT (15-500 nM); TMP (5-1400 nM); TPP (5-1400 nM). The quality control (QC) samples were prepared in blank cells at concentrations of 45, 100, and 400 nM for thiamine and LT, and 15, 120 and 1000 nM for TMP and TPP.

2.3 Sample preparation

Cell pellets were treated with a 500 µL mixture of water, methanol and acetonitrile (1:1:1) with 5% acetic acid to precipitate proteins. 4 µL of ISTD solution (6 µM) was added to each sample. The samples were placed on ice 15 min after being vortexed for 2 min. The samples were

centrifuged at 13,000 g at 10 °C for 10 min before filtration of the supernatants with 0.22 µm hydrophilic nylon membrane syringe filters. Samples were evaporated under a stream of nitrogen and then reconstituted with 120 µL of the initial mobile phase prior to analysis by LC-MS/MS.

Table 1 Optimized ESI (+) mass spectrometric parameters for multiple reaction monitoring (MRM).

Compound	Precursor ion (m/z)	Product ion (m/z)	Cone energy (eV)	Collision voltage (V)
Thiamine	265	122	15	20
$^{13}C_4$-labeled thiamine	269	122	15	20
Thiamine monophosphate	345	122	20	10
$^{13}C_4$-thiamine monophosphate	349	122	20	10
Thiamine pyrophosphate	425	122	30	30
$^{13}C_4$-thiamine pyrophosphate	429	122	30	30
Amprolium	243	150	10	10

2.4. Instrumentation and LC-MS/MS conditions

The samples were analyzed using an Agilent 1100 binary pump HPLC system (Santa Clara, CA, USA) connected to a Waters Micromass Quattro Micro triple quadrupole mass spectrometer with an electrospray source (Milford, MA, USA). The HPLC was equipped with a thermostated autosampler for effective temperature control. Waters Masslynx software (version 4.1) was used to process mass spectral data and control all systems. A Waters Atlantis T3 (2.1 × 50 mm, 3 µm) column with a Phenomenex SecurityGuard C18 guard cartridge (4.0 mm × 2.0 mm) was used to

achieve a chromatographic separation of the highly polar analytes at 25 °C. Mobile phase A consisted of 10 mM ammonium formate and 1.5 mM hexylamine in water at pH 7 adjusted with MS grade formic acid. Mobile phase B was acetonitrile. The gradient condition was (time/minute, % mobile phase B): (0.00, 1), (3.50, 1), (4.50, 15), (10.00, 15), (10.01, 1), (15.00, 1) with a 0.3 mL/min flow rate and the injection volume was 50 µL. The injection needle was washed with water followed by each injection. Samples were analyzed by mass spectrometry under positive ionization mode and using multiple reaction monitoring (MRM). The mass spectrometry parameters were optimized to achieve high sensitivity for the analytes. The source temperature, desolvation temperature, desolvation gas (N_2) flow rate and cone gas flow rate were set at 150 °C, 400 °C, 400 L/h and 0 L/h, respectively. The capillary voltage was 3 kV and the cone voltages, collision energies, precursor ions and product ions used for detection of the analytes are presented in Table 1.

2.5. Method validation

Validation of bioanalytical method followed the current FDA guidance (FDA 2013, FDA 2018). Selectivity, linearity, sensitivity, precision, accuracy, stability and recovery were conducted to evaluate the method.

The limit of detection (LOD) and the lower limit of quantitation (LLOQ) of analytes were determined to evaluate the sensitivity of the method. LODs and LLOQs of all analytes in cells were determined using a S/N ratio greater than 3 and 10, respectively. Calibration curves were plotted from each analyte response ratio between analytes and ISTD with *1/x* weighted linear regressions.

The precision was calculated by assessing the % relative standard deviation (RSD) for repeatability and reproducibility and the accuracy (% relative error (RE)) was determined by comparing measured concentrations to nominal concentrations according to equations (1) and (2).

$$\text{RSD (\%)} = \frac{\text{Sample standard deviation}}{\text{Sample mean}} \text{ x } 100\ \% \quad (1)$$

$$\text{RE (\%)} = \frac{(\text{Nominal conc.} - \text{measured conc.})}{\text{Nominal conc.}} \text{ x } 100\ \% \quad (2)$$

The absolute recovery (AR, n=3), relative recovery (RR, n=3), and matrix effects (ME, n=3) in cells were calculated as following equations (3), (4), and (5).

$$\text{AR (\%)} = \frac{\text{The peak area of spiked cell samples}}{\text{The peak area of standard solutions}} \text{ x } 100\ \% \quad (3)$$

$$\text{RR (\%)} = \frac{\text{The peak area of spiked cell samples}}{\text{The peak area of post-preparation spiked cell samples}} \text{ x } 100\ \% \quad (4)$$

$$\text{ME (\%)} = \frac{\text{The peak area of post-preparation spiked cell samples}}{\text{The peak area of standard solutions}} \text{ x } 100\ \% \quad (5)$$

2.6. Cell culture

Human colon cancer cells (HCT 116) were purchased from American Type Culture Collection (ATCC) (Manassas, VA, USA). The cells were incubated in a humidified atmosphere of 5% CO_2 at 37 °C. HCT 116 cells for the method validation were cultured in a thiamine-deficient RPMI 1640 media supplemented with 10% FBS. After treatment with trypsin/EDTA to be harvested, the samples were washed with cold phosphate-buffered saline three times, then aliquots of 1 x 10^6 cells were prepared for method validation. To eliminate endogenous thiamine and its metabolites, samples were further incubated at 60 °C for more than 96 hrs to generate analyte-free samples since they are thermally labile compounds (Puts, de Groot et al. 2015).

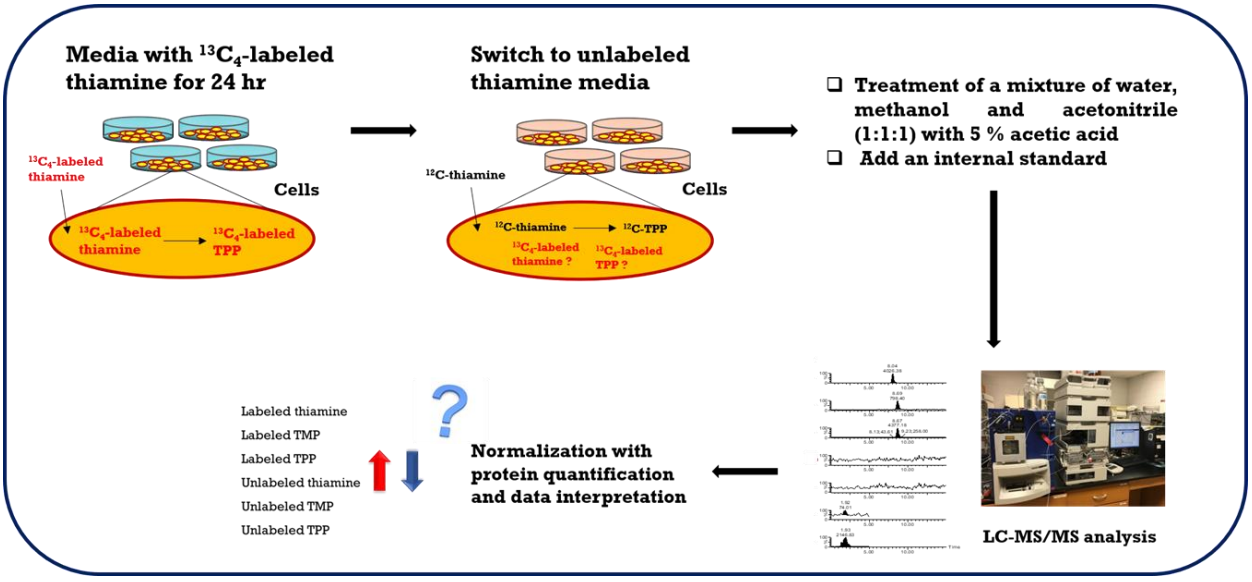

Fig. S1. A schematic of the workflow for the experiments to explore the metabolic fate of thiamine in cancer cells.

2.7. Method application: exploration of the metabolic fate of intracellular thiamine in cancer cells

A schematic of the workflow for the experiments to explore the fate of thiamine in cancer cells is shown in Fig. S1. The HCT 116 cells were seeded with normal media containing 3 µM of unlabeled thiamine on 100 x 15 mm petri dishes and then stabilized for 48 hr. When confluency was reached approximately ~90%, the media was switched to media containing 3 µM of 100% $^{13}C_4$-labeled thiamine. Twenty-four hours after treatment with labeled thiamine, the media was changed to media composed of unlabeled thiamine with (n=3)/without (n=3) sodium fluoride (NaF), which is widely used as a phosphatase inhibitor. Control samples (n=3) were harvested before loading with unlabeled thiamine as a control sample (time 0 or T=0). The cells were harvested at 12 hr and 24 hr after treatment with 3 µM of unlabeled thiamine.

2.8. Determination of total cellular protein

Precipitated cell pellets were solubilized using a 0.01N NaOH buffer. The protein concentration was determined using a Thermo Scientific Pierce BCA protein assay kit. The MS data were normalized to the protein concentration of each sample for the determination of thiamine kinetics.

3. Results

3.1. Method development

Conventional HPLC columns were tested to retain and separate thiamine and its metabolites, but there were several challenges to successfully analyze these highly polar compounds using C18 columns. Additionally, we tried hydrophilic interaction chromatography (HILIC) or normal phase columns which have been successful for the analysis of highly polar compounds, but these did not facilitate separation of these analytes which have highly similar physio-chemical properties, especially between TMP and TPP. On conventional C18 reversed phase columns, TMP and TPP could be retained by using IP agents and adequately separated depending on the identity of the IP agent. However under these conditions, thiamine was too polar to retain on the C18 column. To circumvent phase collapse in the reversed phase column, a Waters Atlantis T3 column designed for polar compounds was therefore applied for analysis of thiamine and its metabolites. The strength of the column is compatibility with 100% aqueous mobile phases despite having a C18 stationary phase. At pH 7, highly polar thiamine can be retained on this column and thereby separated from unretained endogenous compounds in this column. Consequently, TMP and TPP containing negatively charged phosphate groups have ionic interactions with IPs composed of

positively charged nitrogen and then their hydrophobic chains facilitate retention of the analytes on the column.

Alkylamines are commonly used as IP agents for retention and separation for ionic compounds by reversed phase liquid chromatography (Coulier, Bas et al. 2006, Doneanu, Chen et al. 2009, Yang, Li et al. 2010, Basiri, Sutton et al. 2016, Elzahar, Magdy et al. 2018). Several MS compatible alkylamines including hexylamine, triethylamine, tripropylamine, dibutylamine and N,N-dimethylbutylamine, have been tested to separate TMP and TPP. As a result, 1.5 mM hexylamine provided a reasonable separation of TMP and TPP and was utilized for these ionic analytes after optimization of pH considering their pKa properties. Less than 25 mM of ammonium salt buffer systems are typically used for MS friendly methods. A combination of 10 mM ammonium formate and formic acid provided good chromatographic resolution and peak shapes when compared with ammonium acetate and ammonium bicarbonate.

Another challenge during the method development resulted from the lack of proper internal standards. Amprolium hydrochloride was used as an internal standard since it has a similar structure to thiamine whereas pyrithiamine has been previously used for thiamine HPLC analysis (Basiri, Sutton et al. 2016) for which derivatization methods are required. However, pyrithiamine was even more hydrophilic than thiamine and hence was not retained on the column. Additionally, since strongly aqueous mobile phases were used in the initial buffer system, efficient electrospray ionization required a low flow rate of 0.3 mL/min.

In this study, underivatized thiamine and its derivatives were analyzed using the developed LC-MS/MS method instead of a conventional HPLC method with pre- or post-derivatized molecules. In fact, derivatization of these analytes improved their stability by oxidation with potassium hexacyanoferrate (III) in an alkaline solution that is not MS-compatible to form

fluorescent thiochrome derivatives. Without derivatization, the stability of these thermolabile molecules was significantly reduced, but we found that this could be compensated by maintaining the temperature of samples at 6 °C using a refrigerated autosampler during injection and analysis.

3.2. Optimization of sample preparation

Conventional sample preparation techniques for thiamine, its metabolites and derivatives were described in several previous studies (Basiri, Sutton et al. 2016, Kim, Hopper et al. 2016). In these methods, a 15% TCA solution was widely used to precipitate the protein in biological samples, but this high concentration of TCA causes ion suppression due to its low volatility in mass spectrometry. Therefore, other protein precipitation methods using organic solvents were considered to extract the analytes from cell samples. Cold organic solvents (-40°C) are generally used to quench cellular metabolism by dropping the temperature and denaturing the enzymes involved in metabolism (de Koning and van Dam 1992). Metabolites can be extracted from the cells due to the disintegration of the cell membrane. An optimal mixture of organic solvents was water, methanol and acetonitrile with 1:1:1 ratio, which provided the highest recovery of the analytes. The pH of the mixture of organic solvents was optimized since thiamine and its metabolites were stable at acidic pH and hence was the advantage of using TCA solutions for thiamine. Several MS-compatible acids, such as acetic acid and formic acid for positive ionization mode, were tested to increase the stability of the analytes during sample preparation. Finally, a 5% acetic acid solution was used instead of 15% TCA solution to adjust pH and improve the stability of thiamine, TMP and TPP.

3.3. Specificity: chromatographic separation of thiamine, LT, TMP and TPP

The unwanted ionization competition of co-eluting analytes and unknown endogenous species can cause ion suppression or enhancement in LC-MS/MS methods (Remane, Meyer et al. 2010). Hence, a good chromatographic separation of analytes is essential to circumvent these effects. As shown in Fig. 2, the representative chromatogram for each analyte demonstrates the achievement of a good separation with the LC method and a good selectivity of the LC-MS/MS method was determined with no significant interference in blank cells.

Table 2 Calibration curves for thiamine, labeled thiamine, TMP and TPP in cells (n=3).

Analyte	Cells		
	Slope	**Intercept**	**R^2**
Thiamine	0.8441±0.3209	13.1246±0.5206	0.9917±0.0015
$^{13}C_4$-labeled thiamine	0.6338±0.2913	10.2900±0.3397	0.9911±0.0040
TMP	0.0955±0.3662	0.2985±0.1431	0.9967±0.0015
TPP	0.5198±1.0771	0.6947±0.9241	0.9972±0.0027

3.4. Linearity, LOD and LOQ of thiamine, LT, TMP, and TPP

The LODs were 1 nM for thiamine and LT, and 1 nM for TMP and TPP. The LLOQs were 15 nM for thiamine and labeled thiamine, and 5 nM for TMP and TPP. The range of calibration curves for thiamine and LT was 15-500 nM and the range of them for TMP and TPP was 5-1400 nM. As shown in Table 2, slopes, y-intercepts and correlation coefficients (R^2) values were determined from the calibration curves. Over 0.99 of R^2 values for each analyte demonstrated the good linearity of the developed method for the determination of thiamine, LT, TMP and TPP in cell samples.

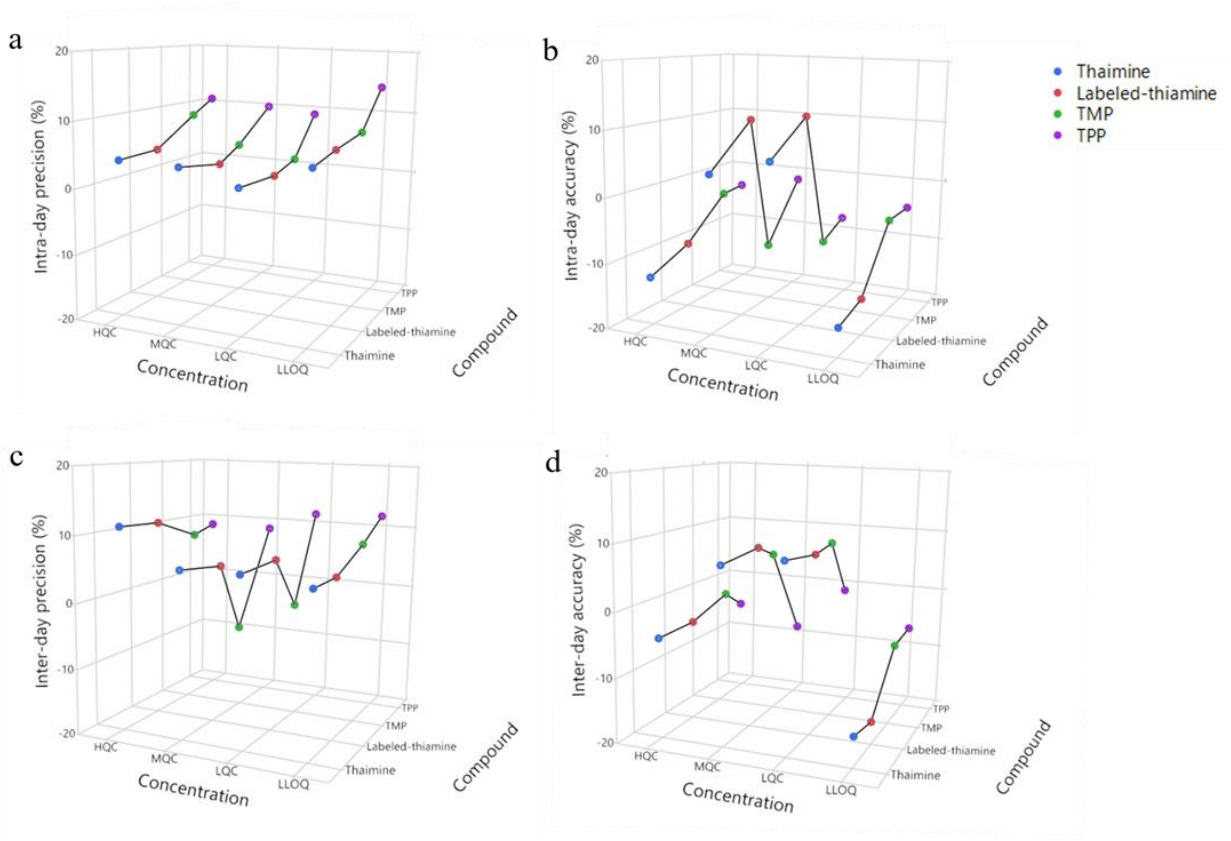

Fig. 3. The intra-day (n=5) and inter-day (n=15) precision (RSD) and accuracy (RE) for the LC-MS/MS method used to determine thiamine, labeled thiamine, TMP and TPP in cells. The LLOQ, LQC, MQC, and HQC samples were prepared in blank cells at 15, 45, 100 and 400 nM for thiamine and LT, and 5, 15, 120 and 1000 nM for TMP and TPP. (a) The intra-day precision. (b) The intra-day accuracy. (c) The inter-day precision. (d) The inter-day accuracy.

Table S1

The intra-day (n=5) and inter-day (n=15) precision (RSD) and accuracy (RE) for the LC-MS/MS method used to determine thiamine, labeled thiamine, TMP and TPP in cells.

Matrix	Analyte	Nominal conc. (nM)	Intra-day (n=5)			Inter-day (n=15)		
			Measured conc. (nM)	Precision RSD (%)	Accuracy RE (%)	Measured conc. (nM)	Precision RSD (%)	Accuracy RE (%)
Cells	Thiamine	15 (LLOQ)	12.65±0.06	5.58	-15.67	12.70±0.05	4.72	-15.32
		45 (LQC)	48.06±0.02	1.83	6.80	48.97±0.06	5.76	8.81
		100 (MQC)	103.97±0.04	3.70	3.97	107.12±0.05	5.40	7.21
		400 (HQC)	349.22±0.04	4.00	-12.69	382.04±0.11	11.15	-4.49
	$^{13}C_4$-labeled thiamine	15 (LLOQ)	12.84±0.07	6.69	-14.38	12.54±0.05	4.79	-16.43
		45 (LQC)	50.49±0.02	1.93	12.19	48.72±0.07	6.53	8.26
		100 (MQC)	111.06±0.03	2.81	11.06	108.55±0.05	4.79	8.55
		400 (HQC)	360.56±0.04	4.16	-9.86	382.78±0.11	10.77	-4.30
	TMP	15 (LLOQ)	4.78±0.08	8.12	-4.35	4.65±0.09	8.51	-6.91
		45 (LQC)	13.67±0.03	3.16	-8.87	14.72±0.09	-1.88	8.86
		100 (MQC)	106.53±0.04	4.37	-11.22	111.42±0.06	-7.15	5.97
		400 (HQC)	968.70±0.09	8.86	-3.13	986.03±0.08	7.96	-1.40
	TPP	5 (LLOQ)	4.80±0.14	14.41	-4.06	4.69±0.12	12.08	-6.16
		15 (LQC)	13.93±0.09	9.27	-7.13	14.90±0.12	11.74	-0.68
		120 (MQC)	118.34±0.10	9.93	-1.38	110.00±0.09	8.64	-8.33
		1000 (HQC)	968.33±0.11	10.85	-3.17	950.91±0.09	8.88	-4.91

3.5. Precision and accuracy

The low-, mid- and high-QC samples were prepared in blank cells at 45, 100 and 400 nM for thiamine and LT, and 15, 120 and 1000 nM for TMP and TPP. The intra-day (n=5) and inter-day (n=15) precision and accuracy were established using these QC samples in the cells as shown in Fig. 3 and Table S1. The precision and accuracy of the method for all analytes at the LQC, MQC and HQC levels were validated within 15% of the RSD and RE. The precision and accuracy at LLOQ levels were also determined within 20% RSD and RE. These values met U.S. FDA guidance.

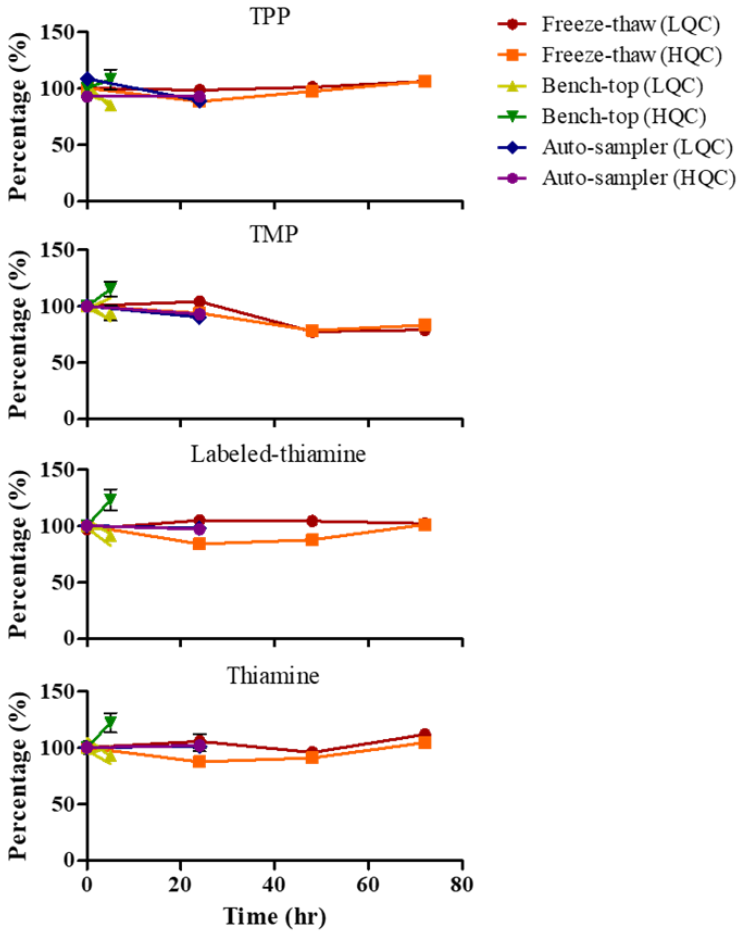

Fig. 4. Freeze-thaw stability (n=4), autosampler stability (n = 3), and bench-top stability (n = 3) of thiamine, LT, TMP, and TPP at LQC and HQC in cells. The LQC and HQC samples were prepared at 45 and 400 nM for thiamine and LT, and 15 and 1000 nM for TMP and TPP.

Table S2

Freeze-thaw stability (n=4), autosampler stability (n = 3), and bench-top stability (n = 3) of thiamine, LT, TMP, and TPP at LQC and HQC in cells.

Matrix	Analyte	Conc. (nM)	Freeze-thaw stability				Bench-top (4-10 °C, 5 hr)	Auto-sampler (6 °C, 24 hr)
			Day 0	Day 1	Day 2	Day 3		
Cell	Thiamine	45	100.00±3.89	105.61±15.64	95.64±5.93	111.66±6.74	92.81±7.41	101.20±6.57
		400	100.00±13.74	87.39±2.05	91.04±3.56	104.42±3.08	121.99±14.78	101.79±8.96
	$^{13}C_4$-labeled thiamine	45	100.00±5.87	101.09±9.73	95.35±2.83	112.22±2.81	91.38±8.12	97.97±4.00
		400	100.00±12.01	83.93±7.21	87.76±4.14	101.20±1.77	123.03±16.37	97.11±5.46
	TMP	15	100.00±3.60	104.13±3.77	77.44±10.54	78.90±6.01	93.87±11.42	90.02±8.02
		1000	100.00±2.90	93.82±1.64	78.47±3.37	83.06±2.59	115.05±11.63	92.97±5.67
	TPP	15	100.00±8.44	98.28±6.63	101.00±10.41	106.27±11.11	84.77±2.66	89.01±7.56
		1000	100.00±15.32	88.22±2.56	97.24±1.45	106.14±1.35	107.65±15.13	92.64±4.16

3.6. Assessment of the short-term stability

The bench-top stability (4-10 °C on ice, 5 hr), autosampler stability (6 °C, 24 hr) and freeze-thaw stability (3 freeze-thaw cycles, -80 °C, 72 hr) were conducted with spiked cell samples at LQC and HQC levels for each analyte. Three sets (n=3 for each set) of samples were prepared and the first set was used as a control (time 0) by analyzing immediately. Subsequently, the first set was analyzed for the determination of autosampler stability after 24 hr. The second set was used for bench-top stability testing after incubation on ice for 5 hr at the bench and then analyzed. The third set was analyzed after 1-3 freeze-thaw cycles from samples were frozen at -80 °C overnight and thawed at room temperature. The short-term stabilities are summarized in Fig. 4 and Table S2.

Table 3 Absolute recovery (n = 3), relative recovery (n = 3), and matrix effect (n=3) of the method for thiamine, LT, TMP, and TPP.

Matrix	Analyte	Conc. (nM)	AR (%)	RR (%)	ME (%)	Type of effect	
Cell	$^{13}C_4$-labeled thiamine	45	93.79±4.41	110.73±6.99	103.85±6.55	3.85	Enhancement
		100	105.37±11.57	102.54±5.62	108.05±5.92	8.05	Enhancement
		400	87.49±3.57	86.15±4.91	75.37±4.30	24.63	Suppression
	Thiamine	45	90.85±6.58	109.20±10.91	99.20±9.91	0.80	Suppression
		100	94.86±10.07	106.87±7.11	101.38±6.74	1.38	Enhancement
		400	77.88±2.30	86.24±7.19	67.17±5.60	32.83	Suppression
	TMP	15	86.41±2.40	101.92±7.27	88.08±6.28	11.92	Suppression
		120	107.23±1.19	95.19±3.17	102.07±3.40	2.07	Enhancement
		1000	92.18±2.26	87.69±1.66	80.83±1.53	19.17	Suppression
	TPP	15	162.49±12.28	87.42±9.35	142.05±15.20	42.05	Enhancement
		120	152.45±10.75	92.48±4.28	140.98±6.52	40.98	Enhancement
		1000	129.42±4.99	102.06±2.13	132.09±2.76	32.09	Enhancement

3.7. Quantitative estimations of matrix effects and recovery

The AR, RR, and ME in cells were summarized in Table 3. The values were generated from peak areas of standard solutions, spiked cell samples and post-preparation spiked cell samples at three QC levels. The AR and RR were generated by comparing spiked samples to standards solutions and spiked samples to post-preparation spiked samples at each QC point, respectively. Acquired data showed high levels of recovery of all analytes with good efficiency. The ME was determined by comparing post-preparation spiked samples to standard solutions. Both ion suppression and enhancement were determined due to ionization competition arising from other endogenous compounds extracted from cell samples during the liquid-liquid extraction by the organic solvent mixture. Interestingly, the high values of AR and ME for TPP samples suggest that negative charged TPP consisting of two highly reactive phosphate groups can either bind to the DNA lobind tubes more than other molecules or was stabilized more in the presence of sodium chloride in cell samples.

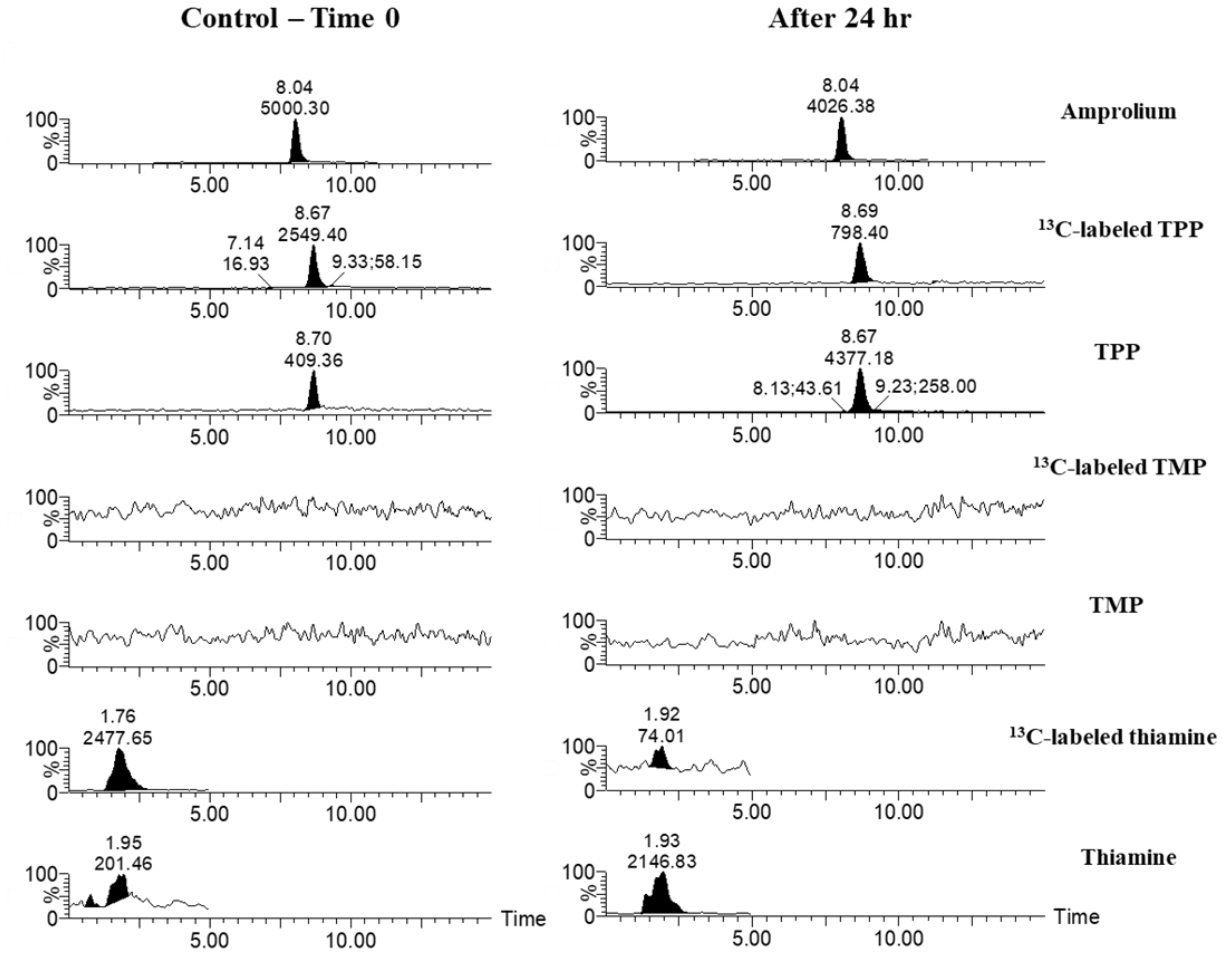

Fig. 5. The representative chromatograms to simultaneously determine unlabeled and labeled thiamine, TMP, and TPP in the cell samples for the empirical study of method application.

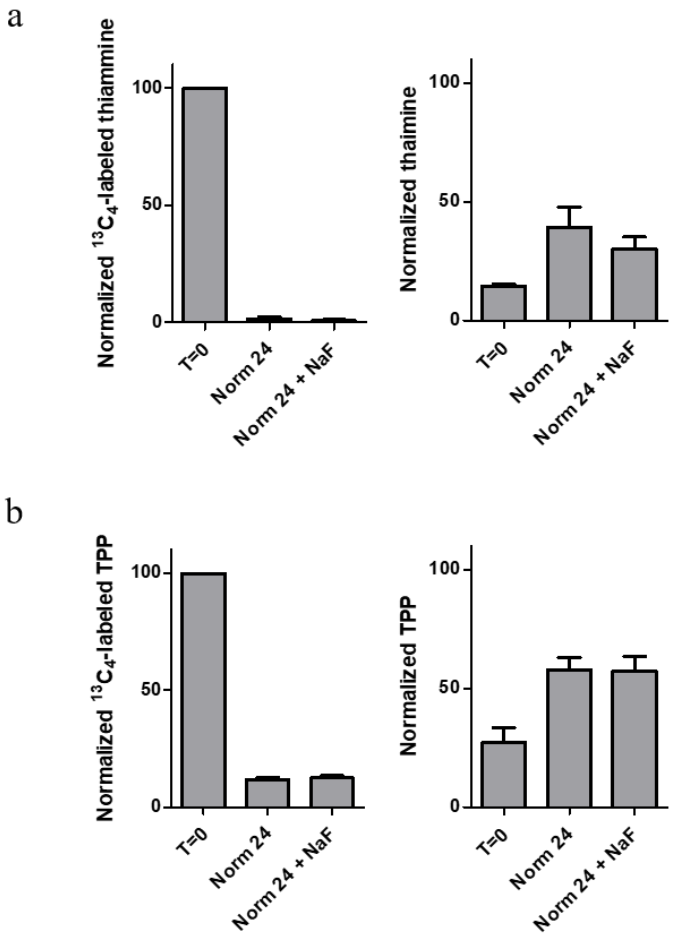

Fig. 6. Determination of thiamine kinetics on HCT 116 cell (n=3) metabolism. (a) Normalized intracellular concentration of $^{13}C_4$-labeled thiamine and unlabeled thiamine after 24 hr with unlabeled thiamine supplementation switched from the media containing labeled thiamine. Sodium fluoride was treated to inhibit TMPase and TPPase. (b) Normalized intracellular concentration of $^{13}C_4$-labeled TPP and unlabeled TPP after 24 hr with unlabeled thiamine supplementation switched from the media containing labeled thiamine. Sodium fluoride was treated to inhibit TMPase and TPPase. The normalized concentrations are mean±S.E.M (standard error of mean) values.

3.8. Application of the method: exploration of the metabolic fate of intracellular thiamine in cancer cells

To demonstrate the applicability of the developed method for the exploration of the metabolic fate of intracellular thiamine in cancer cells, $^{13}C_4$-labeled thiamine was built up in the cells for 24 hr to allow cells to simultaneously produce $^{13}C_4$-labeled TPP from the freshly supplied labeled thiamine. Fig. 5 shows the representative chromatograms to simultaneously determine unlabeled and labeled thiamine, TMP and TPP in the cell samples for the application of this method.

Compared to control samples harvested at time 0, $^{13}C_4$-labeled thiamine was almost consumed in cells 24 hr after switched to media with unlabeled thiamine and $^{13}C_4$-labeled TPP was reduced to 10-14% in the cells (Fig. 6). After changing the media with unlabeled thiamine, increased unlabeled thiamine and TPP was observed in the cells. These findings suggest that the cells kept using the freshly supplemented thiamine to produce new TPP and that TPP was being consumed into other molecules or degraded. Additionally, the result of the intervention of NaF—a phosphatase inhibitor used to offset the effect of thiamine monophosphatase (TMPase) and thiamine pyrophosphatase (TPPase)—when compared to that of samples without NaF intervention, showed that there was no significant difference as shown in Fig. 6. This result implies that TPP was being consumed for other purposes and not just being converted to thiamine or TMP. Furthermore, it was confirmed that there was no effect by methotrexate treatment, which implies that TPP consumption was not caused by its efflux from cells (Jonus, Hanberry et al. 2018).

4. Discussion

We have introduced a new mobile phase system with an IP agent and sample preparation method for the determination of the underivatized versions of both unlabeled and labeled thiamine, TMP, and TPP. The mobile phase containing hexylamine provides an increased retention of polar compounds on a C18 column to achieve a good separation which occurs through electrostatic interactions between the negatively charged phosphorylated forms and the positively charged alkylamines. This sample preparation method without a derivatization step allows simple and fast utilization for the exploration of the metabolic fate of thiamine and its two phosphorylated forms.

Our preliminary study suggested that the production of intracellular $^{13}C_4$-labeled TPP was started within 1-4 hr in HCT 116 cells after the treatment with $^{13}C_4$-labeled thiamine. Additionally, newly introduced thiamine was almost consumed in cells after 24 hr as shown in Fig. 6. Once inside the cells, thiamine can be absorbed by thiamine transporters and converted to TPP by TPK1 (Zastre, Sweet et al. 2013). The uptake of thiamine occurs within 5-7 min in several breast cancer cell lines including MCF 7 (human breast adenocarcinoma cell line) (Zastre, Hanberry et al. 2013) and MDTF (Mus dunni tail fibroblasts) cells (Mendoza, Miller et al. 2013). It has been demonstrated that the turnover time of TPP is about 17 hr in cultured mouse neuro-2a cells (Bettendorff 1994) and the levels intracellular thiamine, TMP and TPP was determined after 24 hr treatment with fresh thiamine in the study of thiamine homeostasis genes (Zastre, Hanberry et al. 2013). Hence, in this study, a 24 hr thiamine incubation time was used to capture the pool change of unlabeled and labeled TPP in the cells without additional introduction of new thiamine.

In a previous study, our group demonstrated that intracellular thiamine levels increased approximately 40-fold in a dose-dependent manner after 10 nM and 3 μM of thiamine supplementation in cancer cells under normoxic conditions (Jonus, Hanberry et al. 2018).

However, intracellular TPP levels increased approximately 2-fold which was not comparable to that of thiamine (Jonus, Hanberry et al. 2018). These results could lead to possible explanations for the phenomena such as the functionality of TPK1 for the conversions of thiamine into TPP being suppressed through negative feedback at certain levels of thiamine, TPP or unknown factors. Otherwise, while TPP was steadily generated by TPK1, TPP can be rapidly converted back to TMP, thiamine or other molecules with control of TPP levels in cancer cells.

The role of TPP is prominently known as a cofactor that catalyzes a reversible decarboxylation reaction in several reactions, especially PDH and α-KGDH (Schellenberger and Hübner 1985, Berg, Tymoczko et al. 2002, Malandrinos, Louloudi et al. 2006, Ranoux and Hanefeld 2013). Like most cofactors, TPP also can be recycled by being reformed to TPP in the last step of the reaction mechanisms (Schellenberger and Hübner 1985, Berg, Tymoczko et al. 2002, Malandrinos, Louloudi et al. 2006, Ranoux and Hanefeld 2013), which implies that certain levels of TPP are sufficient in cells. In other words, intracellular consumption of TPP may not significantly occur if TPP acts as only a cofactor. Additionally, it has been known that TPP can be converted to thiamine and/or TMP during intracellular thiamine homeostasis (Zastre, Sweet et al. 2013). However, there is a lack of knowledge about how thiamine homeostasis changes in cancer cells and which factors are involved in these changes.

Using conventional LC methods only the levels of total thiamine, TMP and TPP in cells can be captured. Hence, we have developed this method to reveal the dynamic change of thiamine kinetics using a stable-isotope labeled thiamine as a metabolic tracer to provide important insights into how the thiamine conversion pathways change in cancer cells. As a result of exploration of the metabolic fate of thiamine using the method, we have demonstrated continuous intracellular consumption of TPP which implies its potential non-cofactor roles.

We believe that this method could be applied for more studies on the alteration of thiamine homeostasis in cancer metabolism by specific interventions or certain conditions for further comprehensive investigations, resulting in a mechanistic understanding of the role and fate of thiamine in cancer metabolism. Ultimately, the studies would provide a basis for nutraceutical approaches for cancer treatment related to thiamine.

5. Conclusion

In conclusion, a new robust and sensitive IPRP-LC-MS/MS method without derivatization to simultaneously determine both unlabeled and labeled thiamine, TMP and TPP has been developed and fully validated following current regulatory guidance. In addition, a rapid, reliable and effective sample preparation method was designed for efficient extraction of analytes from cells and stability of these compounds. The developed method has good linearity, precision and accuracy for the determination of the unlabeled and labeled thiamine within the range from 15-500 nM, and for TMP and TPP within the range from 5-1400 nM in cells. The new sample preparation method that does not require derivatization was successfully applied for efficient extraction, while amprolium performed well as an internal standard. Hexylamine as an ion-pairing agent resulted in an effective separation of analytes. As a result, the method was successfully applied to *in vitro* studies to provide valuable insights for the fate of thiamine in cancer cells by tracking stable-isotope labeled molecules. In the application of the method, we observed thiamine pool changes during cancer, as well as continuous intracellular consumption of TPP which proposes its potential non-cofactor roles.

Acknowledgments

This work was supported by the American Cancer Society through a Research Scholar Grant (RSG-14-026-01-CNE) awarded to Jason Zastre, PhD.

CHAPTER 4

METABOLITE PROFILING OF THE ANTISENSE OLIGONUCLEOTIDE ELUFORSEN USING LIQUID CHROMATOGRAPHY-MASS SPECTROMETRY [3]

[3] Jaeah Kim, Babak Basiri, Chopie Hassan, Carine Punt, Erik van der Hage, Cathaline den Besten, and Michael G. Bartlett. In Revision by *Molecular Therapy-Nucleic Acid*

Abstract

Eluforsen (previously known as QR-010) is a 33-mer 2'-*O*-methyl modified phosphorothioate antisense oligonucleotide targeting the F508del mutation in the gene encoding CFTR protein of cystic fibrosis patients. In this study, eluforsen was incubated with endo- and exonucleases, and mouse liver homogenates to elucidate it's *in vitro* metabolism. Mice and monkeys were used to determine *in vivo* liver and lung metabolism of eluforsen following inhalation. We developed a liquid chromatography-mass spectrometry method for the identification and semi-quantitation of the metabolites of eluforsen, and then applied the method for *in vitro* and *in vivo* metabolism studies. Solid-phase extraction was used following proteinase K digestion for sample preparation. Chain-shortened metabolites of eluforsen by 3'-exonuclease were observed in mouse liver in an *in vitro* incubation system and by either 3'-exonuclease or 5'-exonuclease in liver and lung samples from an *in vivo* mouse and monkey study. This study provides approaches for further metabolite characterization of 2'-ribose-modified phosphorothioate oligonucleotides in *in vitro* and *in vivo* studies to support the development of oligonucleotide therapeutics.

Introduction

Nonclinical evaluation of drug safety usually consists of standard animal toxicology studies, which includes assessment of drug exposure and primarily parent drug plasma concentrations. This information is used to predict and assess potential risks in clinical trials. The U.S. Food and Drug Administration (FDA) Guidance for Industry about Safety Testing of Drug Metabolites has reported, "We encourage the identification of differences in drug metabolism between animals used in nonclinical safety assessments and humans as early as possible during the drug development process" (2008). Therefore, metabolite profiling of the investigational drug in different species, which are used in nonclinical toxicity studies, is essential since this information provides comprehensive insight into the potential risk during clinical trials. In human studies, measurement of only the parent compound is usually sufficient when the metabolite profiles in humans are similar to those in at least one of animal species used in the nonclinical safety assessment.

Eluforsen is a 33-mer antisense oligonucleotide (ASO) product that is being developed for the chronic inhalation treatment of patients with cystic fibrosis (CF) that have the F508del mutation. It has been granted orphan drug designation in the United States (09/23/2013) (2013) and the European Union (07/10/2013) (2013), and received FDA Fast-Track designation (07/18/2016). Two clinical studies, an exploratory proof of concept trial and a phase 1b safety study (NCT02564354), have been completed. More than 85% of all CF patients are affected by ΔF508 (p.Phe508del) mutations in the gene responsible for the expression of the CF transmembrane conductance regulator (CFTR). The lack of CFTR function leads to a reduction of chloride transport, resulting in thick and sticky mucus in the lungs, pancreas, and other organs (Van Goor, Hadida et al. 2011). Specifically, the mucus clogs the airways in the lungs resulting in extensive

damage. All of the eluforsen nucleotides are modified with phosphorothioate (PS) and 2'-*O*-methyl ribose modifications. These modifications result in resistance to nuclease-mediated degradation, thereby greatly reducing its metabolic rate and increasing plasma and tissue half-life times for eluforsen (Patil, Rhodes et al. 2005, Seth, Siwkowski et al. 2009, Seth, Vasquez et al. 2010, Chen and Bartlett 2012, McGinnis, Chen et al. 2012, Pallan, Allerson et al. 2012).

Unlike the metabolism of small molecules which is largely accomplished through CYP-mediated oxidative metabolic and/or conjugation pathways, oligonucleotides undergo different routes of metabolism (Geary 2009, Geary, Norris et al. 2015). Oligonucleotide metabolites are mainly formed by endo/exonucleases that degrade nucleic acids by hydrolyzing phosphodiester bonds (Schildkraut 2001), which are ubiquitously present in many different cell types (McGinnis, Chen et al. 2012). Studies on the various FDA-approved oligonucleotides (e.g., Kynamro®, Macugen®, and Spinraza®) have shown that oligonucleotides are primarily metabolized by intracellular endo/exonucleases to produce chain-shortened oligonucleotide metabolites (Geary, Baker et al. 2015). The modifications present on the backbone of oligonucleotides determine the enzymatic activities leading to the generation of metabolites. Kynamro® is a 20-nucleotide gapmer with 2'-*O*-methoxyethyl (MOE)-modified bases at the 5'- and 3'-ends with ten internal nucleotides placed between the modified ends. All 20 nucleotides are modified by a PS backbone. Kynamro® chain-shortened metabolites within tissues occur initially by endonucleases that cleave the molecule in the gap, resulting in the production of short oligonucleotides which are further digested by exonucleases to produce a cascade of shorter oligonucleotides (Rosie, Kim et al. 2006, Crooke and Geary 2013, Geary, Baker et al. 2015). However, Spinraza® which has a fully 2'-*O*-methoxyethyl ribose and PS backbones modifications, is metabolized more slowly and

predominantly via exonuclease (3'- and 5') -mediated hydrolysis producing chain-shortened metabolites in different tissues (2016).

Different techniques (e.g. hELISA, radiolabeling or liquid chromatography-mass spectrometry) have been used for identification of ASO and its metabolites. Each technique has its own limitations. For preclinical development, bioanalytical methods are required to perform bioanalysis of eluforsen in various biological fluids (e.g. plasma, urine, tissue, etc.) in order to generate toxicokinetic (TK), pharmacokinetic (PK), bioavailability, and metabolic stability data of the parent molecule. Because of its unmatched sensitivity, hELISA methods are in place to determine the concentration of eluforsen in preclinical species and humans. However, the major limitation of hELISA is that this method generally does not distinguish between full length oligonucleotides and its truncated metabolites (Zhang, Lin et al. 2007, Basiri and Bartlett 2014). Currently, mass spectrometry (MS) plays a key role in studies for the determination of metabolic stability of oligonucleotides in biological matrices, which is an important part of the drug development process (Lin, Li et al. 2007, Zhang, Lin et al. 2007, McGinnis, Chen et al. 2012, Basiri and Bartlett 2014). LC-MS technology, on one hand, has the capability to perform metabolite identification and on the other hand has the inherent ability to monitor individual target oligonucleotides, as well as their metabolites. Our group has developed LC-MS/MS methods for the detection of oligonucleotides (Chen and Bartlett 2012, Chen and Bartlett 2013). In this study, we have developed an LC-MS approach for the metabolite identification of eluforsen and applied this method to the characterization and semi-quantification of metabolites in *in vitro* incubations and in tissues obtained from *in vivo* animal studies.

Materials and methods

Chemicals and reagents. Eluforsen, a 33-mer phosphorothioate (PS) oligonucleotides with 2'-*O*-methyl modified 2'-ribose sites, was provided by ProQR Therapeutics (Leiden, Netherlands). Its sequence was 5'-AUC AUA GGA AAC ACC AAA GAU GAU AUU UUC UUU-3'. All alkylamines including N, N-dimethylcyclohexylamine (DMCHA), N, N-diisopropylethylamine (DIEA), as well as 1,1,1,3,3,3-hexafluoro-2-propanol (HFIP), and LC-MS grade methanol, acetonitrile and water were purchased from Sigma Aldrich (St. Louis, MO, USA). 1,1,1,3,3,3-hexafluoro-2-methyl-2-propanol (HFMIP) was supplied from Fisher Scientific (Toronto, ON, Canada). RNase A was acquired from Thermo Fisher Scientific (Waltham, MA, USA), and Exo T, their reaction buffer (10X NE buffer 4) and streptavidin magnetic beads were purchased from New England Biolabs (Ipswich, MA, USA). Magnesium acetate, ethylenediaminetetraacetic acid (EDTA), dithiothreitol (DTT), guanidine hydrochloride, Triton X-100, tetrahydrofuran (THF), ammonium bicarbonate (NH_4HCO_3), tris (2-carboxyethyl) phosphine (TCEP), and sodium chloride (NaCl) were obtained from Sigma Aldrich (St. Louis, MO, USA) as well. Proteinase K was purchased from Gold Biotechnology (St. Louis, MO, USA). Mouse liver homogenates and mouse lung tissue used as blanks to generate calibration curves were acquired from BioIVT (Westbury, NY, USA).

***In vitro* incubation with purified enzymes: Endo (RNase A) and exonuclease (Exo-T).** 1 µg of eluforsen was incubated with 20 units of either endonuclease (20/0), exonuclease (0/20) or endonuclease and exonuclease (20/20) at 37 °C for 1, 2, and 7 days. Heat inactivation at 65 °C for 20 minutes was used to stop the reaction after the incubation period. Eluforsen was incubated in buffer only without endo/exonuclease for 1, 2, and 7 days as a negative control. An RNA strand with sequence 5'-CGUACUAGUGGUCCUAAUCGUAC-3' was used as a positive control.

***In vitro* incubation with mouse liver homogenates.** The homogenization buffer consisted of 100 mM Tris-HCl (pH 8.0), 1 mM magnesium acetate, and 1X penicillin/streptomycin mixture. 5 grams of untreated mouse liver (BioIVT, Westbury, NY, USA) was placed in a glass vessel and 10 mL of the homogenization buffer was added. These were homogenized mechanically with a Polytron (Kinematica AG, Lucerne, Switzerland). The resulting homogenate was further diluted with the homogenization buffer to make several 400 µL aliquots of liver homogenate. Based on the optimized ratio, 10 µL of liver homogenate was added to 390 µL of buffer solution. 50 µg/mL of eluforsen was added to each tube and then the samples were incubated for 0, 24, 48, 72, 96, and 120 hr for the determination of the rate of formation of shortmers of eluforsen.

Table 1 *In vivo* samples from the eluforsen 13-week inhalation study in Cynomolgus Monkey (REXM and REXL) and FVB/NCrl mice (REXQ and REXP).

Sample number	Tissue	Gender
REXM 16-19	Liver	M
REXM 36-39	Liver	F
REXL 16-19	Lung	M
REXL 36-39	Lung	F
REXQ 80-84	Liver	F
REXQ 281-285	Liver	M
REXP 281-285	Lung	F

***In vivo* metabolism studies of eluforsen.** The tissue samples were collected from inhalation toxicity studies of eluforsen in mice and in Cynomolgus monkeys. The studies complied with the OECD Principles of Good Laboratory Practice, ENV/MC/CHEM (98)17 (issued January 1998), and FDA Title 21 Code of Federal Regulations Part 58, Good Laboratory Practice for Non-Clinical studies issued 22 December 1978 Federal Register plus subsequent amendments. The studies were conducted in an AAALAC (Association for Assessment and Accreditation of Laboratory Animal

Care) facility. After 13-week inhalation administration of eluforsen (10 mg/kg), FVB/NCrl mice (n=10 (5 male, 5 female)) exposed 1 or 3 times/week and Cynomolgus monkeys (n=8 (4 male, 4 female)) exposed 3 times/week, were euthanized upon completion of the treatment period of the study. Upon sacrifice, lung and liver tissue samples were collected, snap frozen in liquid nitrogen and stored frozen (≤60ºC) until shipment and analysis (**Table 1**).

Tissue homogenization. Liver and lung samples from mice and monkeys were prepared into appropriately sized amounts for processing (10 mg to 300 mg per tube). Beads with the same mass as the tissue were added to the tube. Two volumes of buffer were added to each sample prior to homogenization using a Bullet Blender (Next Advance, Averill Park, NY, USA). After centrifugation, homogenates were separated from the debris and beads. The tissue homogenates were stored at -80 °C ± 10 °C.

Proteinase K digestion. The proteinase K digestion buffer (60 mM Tris, 100 mM EDTA, 400 mM guanidine hydrochloride, and 0.1% Triton X-100 at pH 9) was stored at 4 °C. 20 mM DTT was added to aliquots of the buffer before use. 200 mg/mL of proteinase K solution was prepared in water and was stored at -20 °C. 20 µL of digestion buffer and 15 µL of proteinase K for *in vivo* samples were added into 100 µL of each homogenate sample. All samples were vortexed for at least 1 min, then heated at 55 °C while shaking (250 g) for 3 h. Samples were then processed with either SPE or using streptavidin magnetic beads.

Solid-phase extraction. Solid-phase extraction (SPE) was performed using Phenomenex Clarity OTX cartridges (Phenomenex, Torrance, CA) after the proteinase K digestion. As previously described (Chen and Bartlett 2012), the equilibration buffer (50 mM NH_4OAc) was prepared in water and the pH adjusted with acetic acid to 5.5. The wash buffer was made by mixing the equilibration buffer with acetonitrile in a 1:1 ratio. The elution buffer was made by mixing 50 mL

of solution (100 mM NH_4HCO_3 and 1 mM TCEP in water at pH 9.5) with 40 mL of acetonitrile and 10 mL of THF. The SPE cartridges were conditioned using 1 mL of methanol and then 1 mL of equilibration buffer. Tissue samples were then mixed with 900 µL of Clarity OTX buffer and loaded onto the column. The cartridges were washed using 4 mL of washing buffer, and the analytes were eluted with 0.5 mL × 2 of elution buffer. The collected solutions were evaporated to near dryness under vacuum and reconstituted with deionized water.

Magnetic bead approaches. A proteinase K digestion step was added at the beginning of the extraction protocol. Streptavidin magnetic beads with biotinylated capture strand (5'-Biotin-AAAGAAAATATCATCT-3') were used to selectively capture eluforsen and its metabolites. Elution buffer containing 10 mM Tris-HCl (pH 7.5) and 1 mM EDTA was pre-warmed in a 65 °C bath and a low salt buffer consisting of 0.15 M NaCl, 20 mM Tris-HCl (pH 7.5), and 1 mM EDTA was chilled on ice. 50 µg of biotinylated capture strand was dissolved in 500 µL of wash/binding buffer containing 0.5 M NaCl, 20 mM Tris-HCl (pH 7.5), and 1 mM EDTA. 200 µL (1500 µg) of hydrophilic streptavidin-coated magnetic beads were added into a new *RNase*-free microcentrifuge tube. 200 µL of wash/binding buffer was added to the beads and they were vortexed to create a suspension. The magnet was applied for approximately 30 seconds and the supernatant was discarded. 50 µL of biotinylated capture solution was added to the magnetic beads and the mixture was vortexed. This sample was incubated at room temperature for 10 minutes with occasional agitation. The magnet was then applied and the supernatant was discarded. The beads were washed by adding 200 µL of wash/binding buffer and then vortexing. The magnet was applied and the supernatant was discarded. The wash step was repeated two more times. 150 µL of 2X wash/binding buffer consisting of 1 M NaCl, 40 mM Tris-HCl (pH 7.5), and 2 mM EDTA was added to the samples. They were heated at 65 °C for 5 minutes, and then quickly chilled on ice for

3 minutes. The samples from the previous step were added into the previously prepared biotinylated capture strand that was bound to streptavidin-coated magnetic beads, vortexed to suspend the particles, then incubated at room temperature for 20 minutes with occasional agitation. The magnet was applied and the supernatant was removed. 200 µL of wash/binding buffer was added and the tubes were vortexed to suspend the beads. The magnet was applied and the supernatant was discarded. Washing with fresh wash buffer was repeated two more times. 200 µL of cold low salt buffer was added to the beads and the tubes were vortexed to suspend them. The magnet was applied and the supernatant was discarded. 20 µL of pre-warmed elution buffer was added followed by vortexing to suspend the beads and incubated at 65 °C in a bath for 2 minutes. The magnet was applied and the supernatant was transferred to a new auto-sampler vial. Elution was repeated with 20 µL of fresh elution buffer. The magnet was applied and the supernatant was added to the first oligonucleotide elution.

LC-MS/MS conditions. The samples were analyzed using a Waters Acquity UPLC connected to a Waters Synapt G2 Q-TOF mass spectrometer (Waters, Milford, MA). The LC separation was performed on a Phenomenex Clarity 2.6 µm Oligo-XT 100Å, 2.1 x 100 mm column (Phenomenex, Torrance, CA) at 60 °C. The flow rate and injection volume were 0.5 mL/min and 15 µL, respectively. Mobile phase A consisted of 15 mM DMCHA and 25 mM HFIP in 5% methanol and mobile phase B was 95% methanol. The gradient conditions were as follows (time (in minutes), % mobile phase B): (0.00, 0), (5.00, 0), (25.00, 35), (25.01, 100), (30.00, 100), (30.01, 0), (35.00, 0). The capillary voltage was -2.0 kV, the cone voltage was 25 V, and the extraction cone voltage was 2 V. The source temperature was 125 °C and the desolvation temperature was 450 °C. The flow rate of the desolvation gas (nitrogen) was 1000 L/h. The MS data acquisition was performed using the MS^E sensitivity mode with a 1s scan time. The low collision energy was set to zero and

high collision energy ramping was from 20 to 30 eV. Additionally, the UPLC flow-through was diverted from the mass spectrometer during the initial 1 minute and the final 10 minutes.

Selections of charge states and *m/z* of eluforsen and its potential metabolites. To optimize the metabolite identification, different charge states were selected as precursor ions seen in MS1 to avoid overlapped *m/z* series for each analyte. For this reason, several calibration curves with different charge states corresponding to each analyte were needed to estimate concentrations. **Table 2** shows *m/z* values for eluforsen and its potential metabolites used for identification.

Table 2 Sequences, selected charge states, and *m/z* of eluforsen and its potential metabolites.

Name	Sequence (from 5' to 3')	Selected charge state	The number of phosphorothioate oxidations (*m/z*)					
			0	1	2	3	4	5
Eluforsen	AUC AUA GGA AAC ACC AAA GAU GAU AUU UUC UUU	-15	763.60	762.54	761.47	760.40	759.32	758.25
3' n-1	AUC AUA GGA AAC ACC AAA GAU GAU AUU UUC UU	-15	741.20	740.12	739.05	737.98	736.91	735.84
3' n-2	AUC AUA GGA AAC ACC AAA GAU GAU AUU UUC U	-14	770.19	769.04	767.89	766.74	765.60	764.45
3' n-3	AUC AUA GGA AAC ACC AAA GAU GAU AUU UUC	-15	696.36	695.29	694.21	693.14	692.07	691.00
3' n-4	AUC AUA GGA AAC ACC AAA GAU GAU AUU UU	-16	631.82	630.81	629.81	628.80	627.80	626.80
3' n-5	AUC AUA GGA AAC ACC AAA GAU GAU AUU U	-14	698.20	697.05	695.91	694.76	693.61	692.46
3' n-6	AUC AUA GGA AAC ACC AAA GAU GAU AUU	-13	726.12	724.88	723.65	722.41	721.18	719.94
3' n-7	AUC AUA GGA AAC ACC AAA GAU GAU AU	-14	650.16	649.02	647.87	646.72	645.57	644.43
3' n-8	AUC AUA GGA AAC ACC AAA GAU GAU A	-14	626.15	625.00	623.85	622.70	621.56	620.41
5' n-1	UC AUA GGA AAC ACC AAA GAU GAU AUU UUC UUU	-14	792.56	791.41	790.26	789.12	787.97	786.82
5' n-2	C AUA GGA AAC ACC AAA GAU GAU AUU UUC UUU	-17	632.74	631.79	630.85	629.90	628.96	628.01
5' n-3	AUA GGA AAC ACC AAA GAU GAU AUU UUC UUU	-14	744.59	743.44	742.30	741.15	740.00	738.85
5' n-4	UA GGA AAC ACC AAA GAU GAU AUU UUC UUU	-15	670.93	669.86	668.79	667.72	666.65	665.58
5' n-5	A GGA AAC ACC AAA GAU GAU AUU UUC UUU	-12	810.90	809.56	808.22	806.88	805.54	804.20
5' n-6	GGA AAC ACC AAA GAU GAU AUU UUC UUU	-15	624.56	623.49	622.42	621.35	620.28	619.21
5' n-7	GA AAC ACC AAA GAU GAU AUU UUC UUU	-15	599.54	598.47	597.40	596.33	595.26	594.19
5' n-8	A AAC ACC AAA GAU GAU AUU UUC UUU	-15	574.52	573.45	572.38	571.31	570.24	569.17

Results

LC-MS/MS method development for identification of metabolites

Based on the results of direct infusion experiments, the MS tuning parameters were optimized as described in the LC-MS conditions of the method section. The characterization of the effect of various alkylamine ion-pairing agents and fluorinated alcohols on the MS signal intensity of eluforsen were performed for the development of a sensitive LC-MS method. Initially, a concentration of 20 µg/mL of eluforsen in 50:50 methanol/water was directly infused into a Waters Synapt G2 HDMS quadrupole time-of-flight hybrid mass spectrometer. Subsequently, precise amounts of ion-pairing (IP) agents including N, N-diisopropylethylamine (DIEA) and N, N-dimethylcyclohexylamine (DMCHA), octylamine, tripropylamine, tributylamine, and N, N-dimethylbutylamine were added to the aliquots of the same solution and infused to the mass spectrometer. DIEA and DMCHA generated the highest ESI-MS signal intensities for eluforsen compared to other alkylamine IP agents (Basiri, van Hattum et al. 2017). In order to further optimize the mobile phase composition for higher MS sensitivity, the effect of various perfluorinated alcohols including hexafluoroisopropanol (HFIP) have been investigated as counter ions (Basiri, van Hattum et al. 2017). For these experiments, the concentration of 25 mM perfluorinated alcohols along with 15 mM IP agents were utilized. DIEA and DMCHA still generated the strongest MS signal intensities even after the addition of HFIP. As a result, DMCHA performed well and slightly better than DIEA while maintaining equivalent LC separations. **Figure 1** shows the HPLC chromatogram of eluforsen and its n-1 truncated oligonucleotide using the buffer system with DMCHA. Finally, the LC-MS method with 15 mM DMCHA and 25 mM HFIP was applied to analyze eluforsen and its metabolites for *in vitro* and *in vivo* metabolism studies.

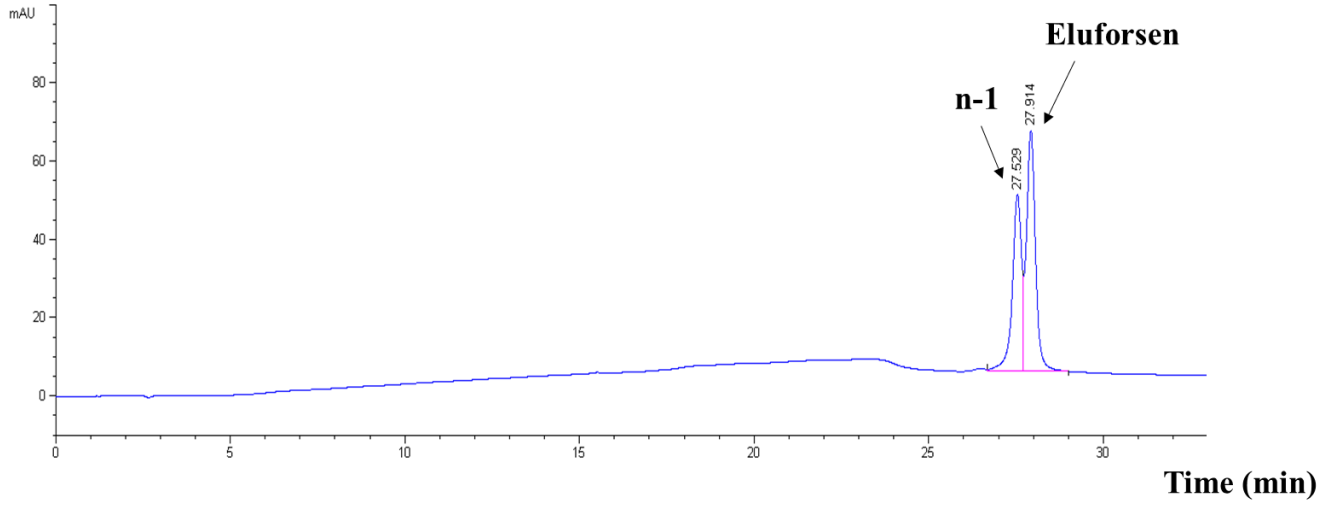

Figure 1 HPLC separation of eluforsen from its 3'n-1 truncated oligonucleotide with ion-pair DMCHA. DMCHA was selected as an ion-pair agent to provide good chromatographic separation after investigation of various alkylamines. 40 µg/mL of oligonucleotides were detected at 260 nm.

Optimization and comparison of sample preparation methods for metabolism studies

Designing proper sample preparation is critical in the MS-based analysis due to the significant impact on the quality and reproducibility of sample preparation (McGinnis, Chen et al. 2012, Basiri and Bartlett 2014). Appropriate sample extraction and preparation methods need to be chosen depending on the analyte of interest, analytical method used, and experimental goals. Biological samples for therapeutic oligonucleotides contain significant amounts of unwanted cellular materials including proteins and lipids that cause signal suppression and non-specific binding of therapeutic oligonucleotides (Annesley 2003, Panuwet, Hunter et al. 2016). Many approaches including liquid-liquid extraction (LLE) (Zhang, Lin et al. 2007, Deng, Chen et al. 2010, Chen and Bartlett 2013), trizol extraction (Chomczynski and Sacchi 1987), proteinase K digestion

(McGinnis, Cummings et al. 2013), solid-phase extraction (SPE) (Dai, Wei et al. 2005, Johnson, Guo et al. 2005, Zhang, Lin et al. 2007, Deng, Chen et al. 2010, Chen and Bartlett 2012), and magnetic bead extraction methods (Ye and Beverly 2011), can be applied successfully to isolate oligonucleotides from biological samples prior to LC-MS analysis.

Proteinase K is a general enzyme used to hydrolyze all proteins with a quick digestion time. It can be easily modified to improve the quality of the approach by adding dithiothreitol to reduce protein disulfide bonds and adding guanidinium chloride to increase the rate of protein degradation (Jeanpierre 1987). Ethylenediamine tetra acetic acid (EDTA) can be used to inhibit nucleases activity during the proteinase K digestion by acting through the sequestration of metal atoms that are essential cofactors for several families of nucleases (Dattagupta, Fujiwara et al. 1975, Hilz, Wiegers et al. 1975). The approach can minimize the loss of oligonucleotides caused by non-specific adsorption during sample preparation by greatly reducing the number of sample transfer steps (McGinnis, Cummings et al. 2013). Additionally, the recovery for oligonucleotides has been determined to be greater than 90% (McGinnis, Cummings et al. 2013). It can be readily used with other methods including solid-phase extraction. Hence, proteinase K digestion was chosen in this study to remove contaminating proteins prior to the extraction of oligonucleotides from biological samples.

To assess the effectiveness of sample preparation methods for metabolic studies of eluforsen, samples were incubated with mouse liver homogenates for 7 days. After proteinase K digestion, the samples were extracted using either anion-exchange SPE or the immunoaffinity capture approach using streptavidin-coated magnetic beads with a biotinylated capture strand. A biotinylated capture strand that was complementary with eluforsen and bound to streptavidin magnetic beads was used to selectively capture eluforsen and its metabolites. As a result, only n-

1, n-2 and n-3 metabolites (3'-end shortmers) of eluforsen were detected using the streptavidin magnetic bead method while more 3'-end shortmers (from n-1 to n-8) were observed using the SPE method. These results indicate that the highly selective capture strand loses affinity from 3' n-4 shortmers onward when using the magnetic bead approach. It should be noted that, in this stage 5'-end shortmers were not observed using either approach. Hence, to recover a wide variety of different types of oligonucleotides, a relatively non-specific solid-phase extraction method rather than a magnetic bead-based approach was used following proteinase K digestion in order to maximize the coverage of metabolites.

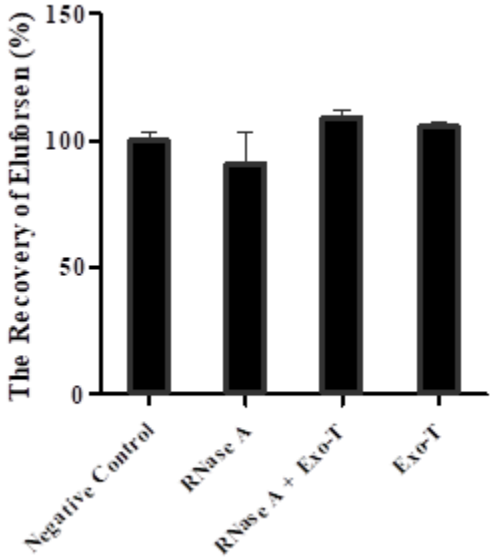

Figure 2 Comparison of the recovery (%) of eluforsen after 2-day incubations with purified nucleases. 1 µg of eluforsen was incubated with either endonuclease (RNase A), exonuclease (Exo-T), or both enzymes (double-digestion) at 37 °C for 2 days. A negative control was prepared by incubation of eluforsen in buffer but without any endo/exonuclease. The recoveries of eluforsen were 100.00 ± 3.35%, 90.84 ± 12.23, 109.17 ± 2.90%, and 105.46 ± 1.73% (mean ± standard error mean) in the buffer only, RNase A, both enzymes, and Exo-T, respectively.

Determination of *in vitro*-generated metabolites by endo/exonucleases

Eluforsen was incubated with purified endo- (*RNase A*) and exonuclease (*Exo-T*) enzymes to identify the possible metabolites that could be formed *in vitro*. An RNA strand was used as a positive control which was totally degraded after 1 hour of incubation with *RNase A*. The samples were analyzed by LC-MS. As shown in **Figure 2**, the recoveries of eluforsen were 100.00 ± 3.35%, 90.84 ± 12.23, 109.17 ± 2.90%, and 105.46 ± 1.73% (mean ± standard error mean) in the buffer only, *RNase A*, both enzymes, and *Exo-T*, respectively. Eluforsen did not show any metabolism after 2 days of incubation with *RNase A* and *Exo-T*. Since eluforsen is fully modified with phosphorothioates and 2'-*O*-methylribonucleosides, it is highly resistant against digestion by endo/exonuclease enzymes. This result is consistent with previous studies involving enzymatic incubations of phosphorothioate-containing oligonucleotides when using purified enzymes (Stein, Subasinghe et al. 1988) and nucleases derived from cells (Hoke, Draper et al. 1991). Because the purified enzymes were not able to digest eluforsen, we proceeded to test mouse liver homogenate to identify metabolites (Baek, Yu et al. 2010).

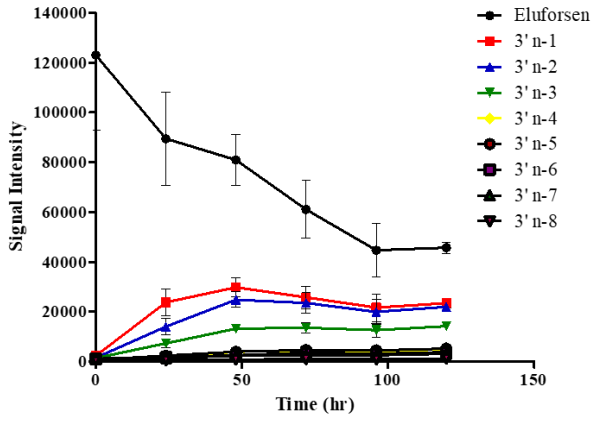

Figure 3 Determination of the rate of formation of 3'-end shortmers of eluforsen with mouse liver homogenates. 50 µg/mL of eluforsen was incubated for 0, 24, 48, 72, 96, and 120 hr with mouse liver homogenates.

Table 3 *In vitro*-generated eluforsen metabolites after incubation with purified nucleases and mouse liver homogenates, and *in vivo*-generated metabolites in liver and lung samples of mice and monkeys. Data reported as the mean percentage.

Metabolites	*In vitro*-generated metabolites		*In vivo*-generated metabolites			
	Incubation with purified nucleases (after 7 days)	Incubation with mouse liver homogenates (after 5 days)	Mouse		Monkey	
			Liver	Lung	Liver	Lung
3' n-1	-	18.97%	13.03%	12.09%	9.97%	6.72%
3' n-2	-	17.80%	7.14%	9.44%	8.07%	5.41%
3' n-3	-	11.48%	5.72%	8.91%	1.75%	3.38%
3' n-4	-	3.94%	4.25%	6.60%	1.01%	2.84%
3' n-5	-	4.21%	3.71%	5.55%	1.12%	3.47%
3' n-6	-	3.03%	4.58%	4.79%	1.97%	4.19%
3' n-7	-	2.53%	3.25%	4.20%	0.97%	3.22%
3' n-8	-	0.98%	1.40%	-	-	2.78%
5' n-1	-	-	15.41%	19.88%	7.48%	7.62%
5' n-2	-	-	7.31%	6.94%	1.24%	3.27%
5' n-3	-	-	8.25%	8.98%	3.18%	4.24%
5' n-4	-	-	4.90%	9.05%	1.68%	4.50%
5' n-5	-	-	10.29%	15.03%	6.77%	7.01%
5' n-6	-	-	-	-	-	2.37%
5' n-7	-	-	-	-	-	2.25%
5' n-8	-	-	-	-	-	-

Determination of the rate of formation of shortmers of eluforsen with mouse liver homogenates

In vitro metabolic studies of eluforsen were performed by incubation with mouse liver homogenates for 0, 24, 48, 72, 96, and 120 hr, to determine the rate of formation of shortmers of eluforsen. Subsequently, the samples were analyzed by LC-MS after sample preparation using a combination of proteinase K digestion and SPE extraction. **Table 3** and **Figure 3** show the results obtained in a series of short time incubations with mouse liver homogenates. **Table 3** shows 3'-end shortmers generated after 120 hours of incubation with mouse liver homogenates; 5'-end shortmers were not observed during incubation with mouse liver homogenates. The results suggest

that 3'-exonucleases are the major enzyme responsible for metabolizing eluforsen in mouse liver homogenates as supported by the high level of formation of 3'-end shortmers. As shown in **Figure 3**, 3'-end shortmers were mainly produced in the order of n-1, n-2 and n-3. The result suggests that the 3'-poly(U) tail appears to be the most metabolically susceptible portion of eluforsen in mouse liver homogenates. We could not observe the presence of any oxidation of the phosphorothioate backbone, conversion of a 2'-*O*-Me to a hydroxyl group, or simple loss of any of the bases (e.g. depurination or depyrimidination).

Determination of *in vivo*-generated metabolites of eluforsen in liver and lung samples of mice and monkeys using LC-MS/MS

Drug metabolism studies usually involve identification of circulating metabolites in plasma or serum, as this enables cross-species comparison between animals and humans. However, following inhalation administration of eluforsen, systemic exposure in serum was too low to serve as a matrix for metabolite profiling investigations (data not shown). Metabolite profiles were therefore characterized in lung and liver obtained from mice and monkeys following 13-weeks of inhalation delivery of eluforsen. Lung is the intended pharmacological target organ of eluforsen and the main organ for disposition following the inhalation delivery of eluforsen, and the liver is a key organ for accumulation of oligonucleotides following systemic exposure (Baek, Yu et al. 2010, Husser, Brink et al. 2017), as well as the main organ for metabolism of xenobiotics including therapeutics (2013).

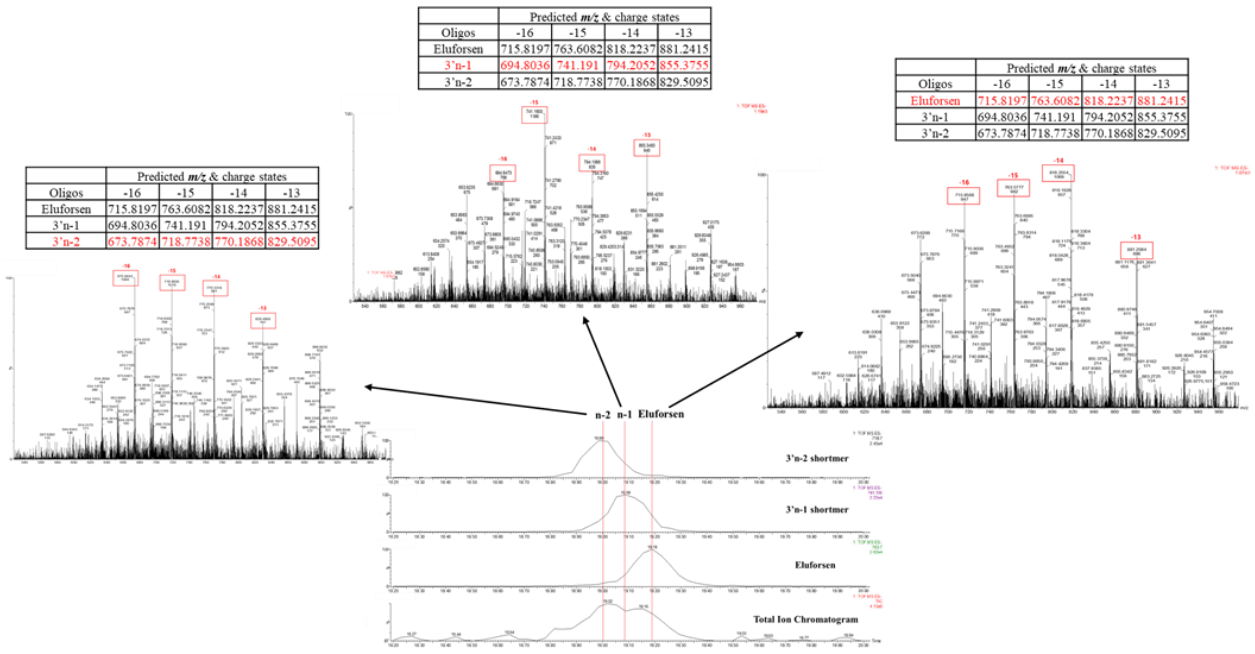

Supplementary Figure 1. Examples of how to identify eluforsen and its metabolites from precursor ion chromatogram and MS spectra.

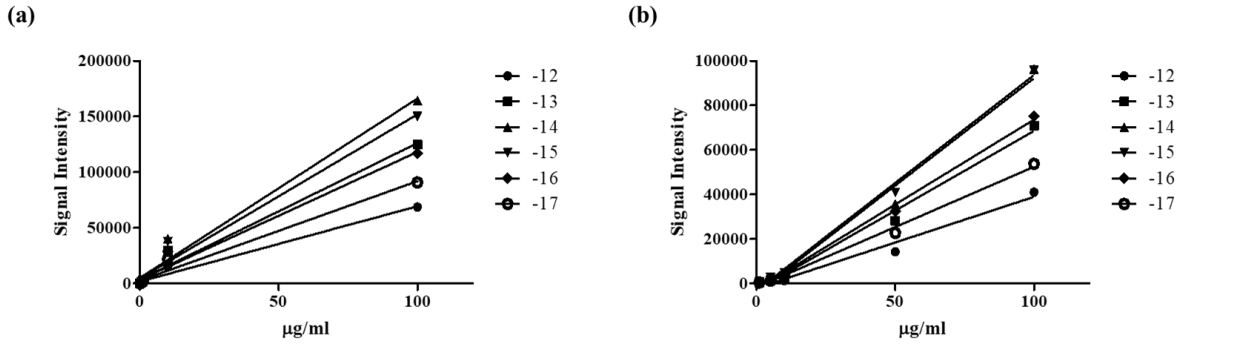

Charge States	-12	-13	-14	-15	-16	-17
R^2 (from 0.1 to 100 µg/ml)	0.9846	0.9807	0.9789	0.9771	0.9790	0.9805
R^2 (from 0.1 to 10 µg/ml)	0.9997	0.9995	0.9997	0.9994	0.9997	0.9996

Charge States	-12	-13	-14	-15	-16	-17
R^2 (from 1 to 100 µg/ml)	0.9782	0.9902	0.9842	0.9947	0.9950	0.9946
R^2 (from 1 to 50 µg/ml)	0.9914	0.9915	0.9922	0.9939	0.9934	0.9968

Supplementary Figure 2. Calibration curves for liver (a) and lung (b) samples.

From the 13-week inhalation studies, 18 liver samples (from 8 monkeys, 10 mice) and 13 lung samples (from 8 monkeys, 5 mice), collected at the end of the 13-week treatment period, were prepared to identify *in vivo*-generated eluforsen metabolites. The liver and lung samples were homogenized by following the protocol as detailed in the methods section. Mouse lung and liver homogenates were pre-incubated with proteinase K followed by SPE for making matrix-matched standard calibration curves to mimic the loss of recovery from the biological matrix. As shown in **Supplementary Figure 1,** eluforsen and its metabolites were identified from the MS1 precursor ion chromatogram and MS^E spectra. The limitations of using MS/MS in qualitative analysis have been previously addressed because major MS/MS fragment ions to fully characterize each metabolite were generally not observed.(Studzińska, Rola et al. 2016). To calculate signal intensities, an ion peak for each analyte was extracted using the *m/z* value of the MS1 precursor ion at a specific charge state and used to determine the area of the peak. As shown in **Table 2**, different charge states were selected as precursor ions as seen in MS1 to avoid overlapped *m/z* series for each analyte. Six calibration curves (**Supplementary Figure 2**) were made separately using signal intensities of eluforsen in different charge states (-12, -13, -14, -15, -16 and -17). The calibration curves of eluforsen were used to estimate the concentrations of its metabolites, which although semi-quantitative, could still be used to approximate the metabolic stability of eluforsen in *in vitro* and *in vivo* systems. The calibration curve with the same charge state as each analyte was used to estimate the concentration of each analyte. PO_2S^- fragment ions (*m/z* 94.9 seen in MS/MS data) were observed to confirm the presence of therapeutic oligonucleotides in *in vivo* samples (Husser, Brink et al. 2017).

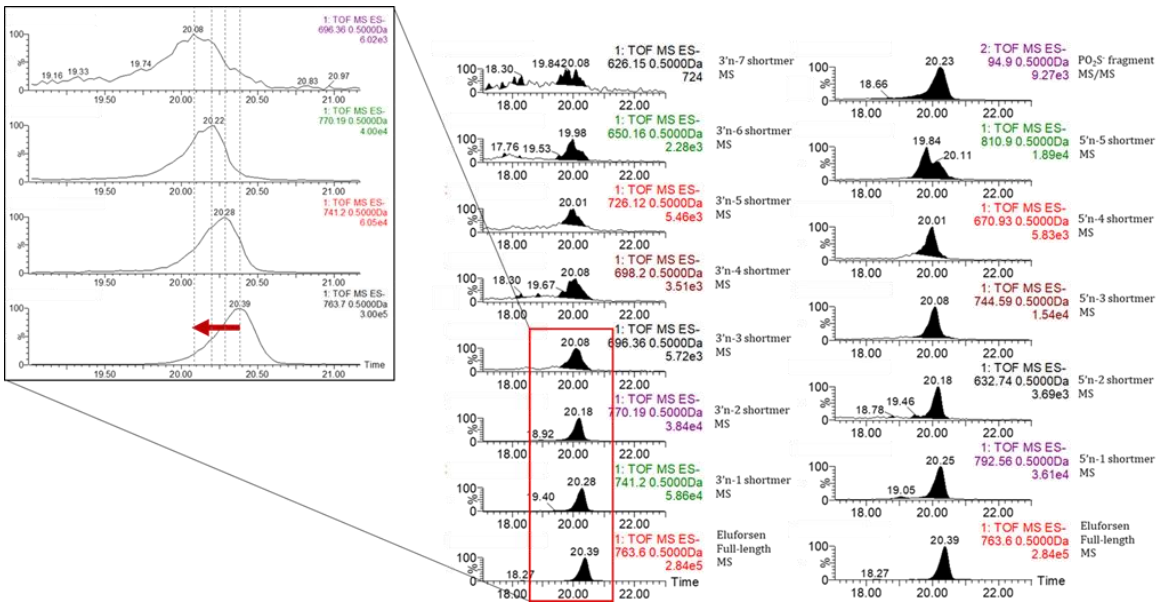

Figure 4 Representative extracted ion chromatograms of eluforsen and its metabolites. *In vivo* samples were analyzed by LC-MS after sample preparation using a combination of proteinase K digestion and SPE extraction. Mobile phase A consisted of 15 mM DMCHA and 25 mM HFIP in 5% methanol, and mobile phase B containing 95% methanol were used as an optimized buffer system.

Figure 4 shows the representative chromatograms of one *in vivo* sample. Eluforsen and its metabolites were observed in both *in vivo* mouse and monkey liver samples. The estimated mean percentages for *in vivo*-generated metabolites in liver and lung samples of mice and monkeys are presented in **Table 3**. 3'-end shortmers (from n-1 to n-8) and 5'-end shortmers (from n-1 to n-5) were observed in both mouse and monkey samples. 3'-end shortmers generated in mouse and monkey liver samples ranged from 1.40 to 13.03% and from 0.97 to 9.97%, respectively. 5'-end shortmers generated in mouse and monkey liver samples ranged from 4.90 to 15.41% and from 1.24 to 7.48%, respectively. The results suggest that both 3'-exonuclease and 5'-exonuclease were responsible for metabolizing eluforsen in *in vivo* mouse and monkey liver.

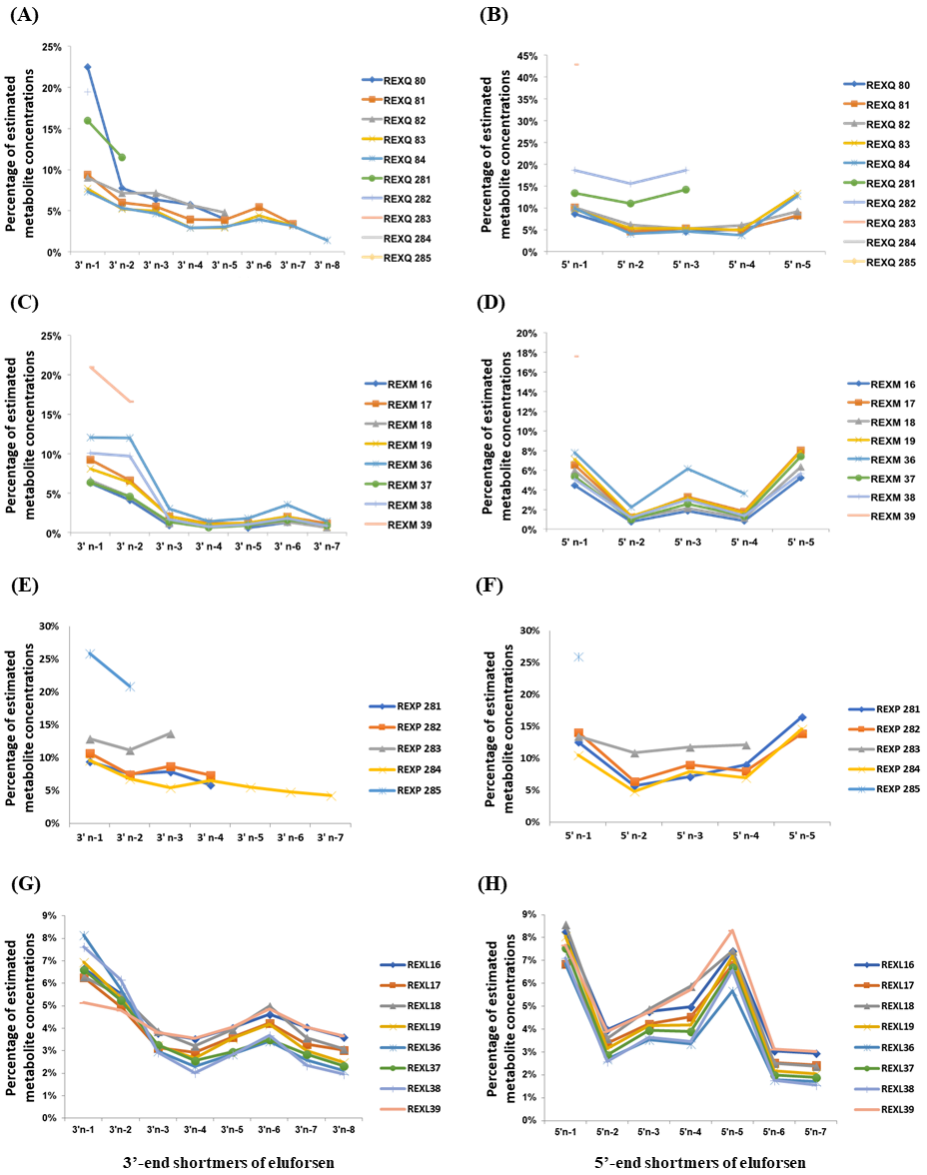

Figure 5 Trends of generation of eluforsen metabolites in *in vivo* liver and lung samples of mice and monkeys. (A) 3'-end shortmers in mouse liver samples. (B) 5'-end shortmers in mouse liver samples. (C) 3'-end shortmers in monkey liver samples. (D) 5'-end shortmers in monkey liver samples. (E) 3'-end shortmers in mouse lung samples. (F) 5'-end shortmers in mouse lung samples. (G) 3'-end shortmers in monkey lung samples. (H) 5'-end shortmers in monkey lung samples.

As shown in **Figure 5A and B** for mouse samples and **Figure 5 C and D** for monkey samples, trends of metabolite generation were very similar between samples. Of note, the 5' n-3 and 5' n-5 shortmers were present at higher amounts than expected based on the presence of other shortmers. As these metabolites had an adenine at the end of their sequence, this observation may suggest that adenine provides increased nuclease stability compared to the other nucleotides in the sequence.

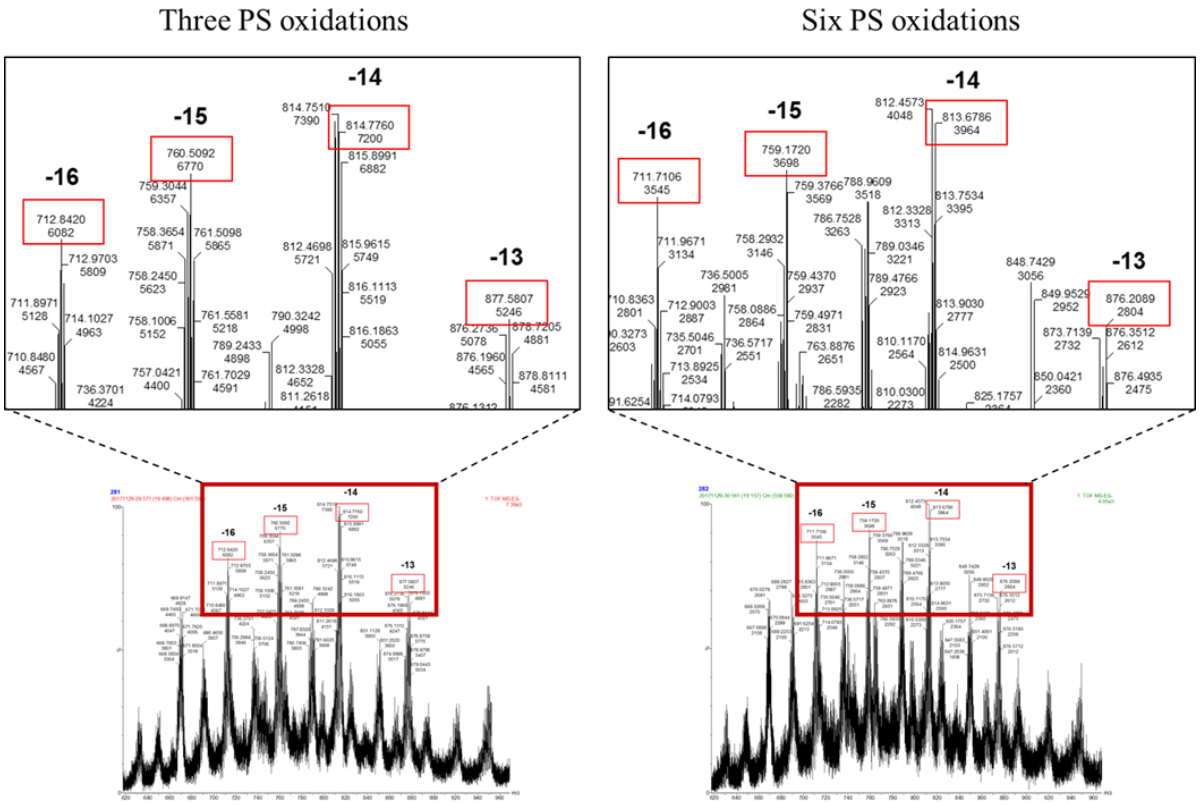

Supplementary Figure 3. Examples of MS spectra to confirm the presence of some oxidations of phosphorothioate backbone in mouse lung samples.

Higher levels of eluforsen and its metabolites were observed in mouse and monkey lung samples than in the liver samples. Interestingly, the identifiable presence of some oxidations (1-6) of the phosphorothioate backbone were identified in mouse lung samples (**Supplementary Figure**

3). Therefore, different precursor ion series were used to identify metabolites based on the number of oxidations of the phosphorothioate backbone as shown in **Table 2**. As before, different charge states were selected as precursor ions to avoid overlapped *m/z* series for each analyte. 3'-end shortmers (from n-1 to n-7) and 5'-end shortmers (from n-1 to n-5) were observed in mouse lung samples and 3' end shortmers (from n-1 to n-8) and 5' end shortmers (from n-1 to n-7) were observed in the monkey lung samples **(Table 3)**. 3'-end shortmers generated in mouse and monkey lung samples ranged from 4.20 to 12.09% and from 2.78 to 6.72 %, respectively. 5'-end shortmers generated in mouse and monkey lung samples ranged from 6.94 to 19.88 % and from 2.25 to 7.62%, respectively. Like the result of liver samples, these results suggest that both 3'-exonuclease and 5'-exonuclease were essential for metabolizing eluforsen in mouse and monkey lung. **Figure 5E and F** for mouse samples, and **Figure 5G and H** for monkey samples suggest similar tendencies of metabolite generation between samples. While both 3'-and 5'-shortmers were observed, conversion of a 2'-*O*Me to a hydroxyl group, and simple loss of any of the bases (depurination or depyrimidation) were not identified in the *in vivo* samples. Consistent with the results from the liver samples an increased prevalence of 5' n-3 and 5' n-5 shortmers was also observed in lung samples.

Discussion

Ion-pair reversed-phase liquid chromatography mass spectrometry (IP-RP-LC-MS) has been routinely used in the development of oligonucleotide-based therapeutics. To improve mobile phase systems with good chromatographic separation and enhanced MS signal intensity for the metabolite identification of eluforsen, various alkylamines and fluorinated modifiers have been investigated in this study as previously reported (Chen and Bartlett 2013, McGinnis, Grubb et al.

2013, Basiri, van Hattum et al. 2017). Ultimately, 15 mM DMCHA containing 25 mM HFIP was chosen as our buffer after comprehensive investigation to assess the effect of alkylamines and fluorinated alcohols on both chromatographic separation and MS signal intensity.

Employing effective sample preparation methods that combine one or two techniques between proteinase K digestion, LLE, SPE, and magnetic bead approaches, have been successfully used for the isolation of oligonucleotides prior to LC-MS analysis (Zhang, Lin et al. 2007, Ye and Beverly 2011, Chen and Bartlett 2012, McGinnis, Cummings et al. 2013). Proteinase K digestion has been widely used to remove proteins during the oligonucleotide analysis of biological samples using LC-MS (Chen and Bartlett 2012, McGinnis, Cummings et al. 2013) and this approach was associated with more than 90% recovery (McGinnis, Cummings et al. 2013). Due to difficulties associated with the loss of affinity of a variety of metabolites from a capture strand, the magnetic bead approach was not applied in the metabolite identification process despite its high specificity and good recovery (80-95%) (Ye and Beverly 2011). To maximize coverage of metabolites of eluforsen, SPE, with a recovery range of 60-80% (Chen and Bartlett 2012) was therefore used for relatively non-specific extraction of metabolites generated in biological samples after proteinase K digestion. Using this approach, we found more metabolites than using a magnetic bead approach.

Owing to the mass spectral complexity of larger macromolecules, analysis of therapeutic oligonucleotides face many technical challenges (McGinnis, Chen et al. 2012). While small molecule analysis often has a single *m/z* species for identification that can be chosen, larger macromolecules provide complex primary mass spectra. Specifically, the monoisotopic mass of eluforsen is 11461.18 which is approximately 1.5 times higher than other therapeutic oligonucleotides (e.g. Spinraza®: 7501 Da (2016), Kynamro®: 7594.9 Da (2016)), resulting in the production of higher charge states than that of smaller oligonucleotides. In terms of technical

aspects, mass spectral complexity of the 33-mer eluforsen was shown to have overlapping signals at the same *m/z* values from isotopic distributions as well as metabolites commonly generated by sequential removal of nucleotides from the full-length oligo. Hence, careful selection of charge states and *m/z* values were necessary to unambiguously identify eluforsen and its metabolites.

Examination of the metabolic profiles of eluforsen indicated that it was not degraded by endo- and exonucleases after 48 hr (**Figure 2**) with these nucleases *in vitro*. Phosphorothioate modification that substitutes a sulfur atom for a non-bridging oxygen in the phosphodiester backbone of oligonucleotides is known to provide nuclease resistance (Campbell, Bacon et al. 1990, Hoke, Draper et al. 1991, Gao, Han et al. 1992, Crooke 1993, Crooke and Lebleu 1993, Brown, Kang et al. 1994, Crooke, Graham et al. 1995, Crooke, Graham et al. 2000). Hence, the phosphorothioate molecule was stable against *in vitro* nucleolytic degradation. It has been reported that the phosphorothioate groups of both the *R*p- and *S*p-diastereomers were resistant against the staphylococcal nucleases, DNase I and II (Spitzer and Eckstein 1988), and Iwamoto et al. have shown that *S*p linkages increase the metabolic stability relative to *R*p linkages in rat liver homogenates (Iwamoto, Butler et al. 2017). 2'-ribose modification also results in resistance to nuclease-mediated degradation (Seth, Siwkowski et al. 2009, Seth, Vasquez et al. 2010, Pallan, Allerson et al. 2012). Therefore, a fully 2'-*O*-methyl ribose modification provides increased stability of eluforsen against degradation by endonucleases, whereas MOE gapmers were found to be initially metabolized by endonucleases and then exonucleases to produce chain-shortened metabolites (Rosie, Kim et al. 2006, Baek, Yu et al. 2010, Crooke and Geary 2013).

Eluforsen was metabolized by cellular nucleases in mouse liver homogenates, which was consistent with the metabolism of other phosphorothioate oligonucleotides in rat liver homogenates (Crooke, Graham et al. 2000). The different results obtained between purified

enzymes and liver homogenate might be due to the presence of other molecules and enzymes in liver homogenate that may enhance the interaction between the oligonucleotides and endo-exonucleases but this needs further investigation. The result that only 3'-end shortmers were observed suggests that the metabolism of eluforsen occurred mainly through 3'-exonuclease activity in mouse liver homogenates. Specifically, the fact that pyrimidine-rich oligonucleotides can be metabolized faster (Crooke, Graham et al. 2000) may explain why the 3'-poly(U) tail was observed as the most metabolically active portion in mouse liver homogenates.

It was demonstrated that both 3'-exonuclease and 5'-exonuclease were responsible for metabolism of eluforsen in *in vivo* liver and lung tissues from mice and monkeys (**Figure 5**). In the *in vivo* data, increased concentrations of 5' n-3 and 5' n-5 shortmers appeared to result from increased stability from the presence of adenine. The result can be explained by the fact that pyrimidine nucleotides (U, C) were metabolized faster than purines (A, G) (Crooke, Graham et al. 2000). It is still unknown whether metabolites can be generated by the simultaneous activities of both nucleases. However, no metabolites were observed resulting from losses of nucleotides from both ends of the molecule. Overall, the typical pattern of chain-shortened metabolites observed in other systems (Crooke 1992, Crooke and Bennett 1996, Crooke, Graham et al. 2000, Rosie, Kim et al. 2006, Geary 2009, Baek, Yu et al. 2010, Geary, Baker et al. 2015) was shown in this study. Additionally, some identifiable oxidations of phosphorothioates, substitutions of sulfur for oxygen, were detected in *in vivo* mouse lung samples. It has been well known that nucleolytic degradation is a central metabolic pathway for oligonucleotides (Crooke 1998, Crooke, Graham et al. 2000). Our result shows that eluforsen is metabolized through oxidative metabolic pathways in *in vivo* mouse lungs. While oligonucleotides are not primarily metabolized via flavin-containing monooxygenases (FMOs) or cytochromes P450 driven metabolic oxidation processes (Geary,

Leeds et al. 1997, Crooke 1998, Nicklin, Craig et al. 1998), there have been some observations that phosphorothioates undergo metabolic oxidation in *in vivo* samples (COHEN, BOURQUE et al. 1997, Nicklin, Craig et al. 1998).

Comparison of the metabolites generated in mice and monkeys, showed the similar tendencies of metabolite generation between the two species. The results are consistent with a previous study of the phosphorothioate oligonucleotide (ISIS 2503), where similar patterns of metabolites were observed in the plasma of mice and monkeys (Yu, Geary et al. 2001). As shown in **Table 3**, the sum of mean percentages of 3'-end shortmers in mouse liver, monkey liver, mouse lung, and monkey lung samples were 43.08%, 24.86%, 51.58%, and 32.01% equivalents, respectively. The sum of mean percentages of 5'-end shortmers in mouse liver, monkey liver, mouse lung, and monkey lung samples were 46.16%, 20.35%, 59.88%, and 31.26% equivalents, respectively. Overall, metabolites in mice were approximately 20-30% higher than those of monkeys. The result of a more active metabolism of eluforsen in mice than in monkeys is consistent with that of a previously reported study (Yu, Geary et al. 2001). Metabolites in lung samples were approximately 10% higher than those in liver samples. Eluforsen and its metabolites showed greater accumulation in the lung relative to liver after inhalation administration. Increased drug concentrations within target organs is a pivotal factor for the development of delivery strategies (Rani and Paliwal 2014).

Since 2'-*O*-ribose modified-PS oligonucleotides like eluforsen have a predictive metabolism via exonuclease resulting in chain shortening of the sequence from the 3'- and/or 5'-end, the metabolites do not differ qualitatively between animal species and humans. The identified metabolites in tissues of the animal species are therefore considered to reflect metabolites that may be present in humans following inhalation exposure to eluforsen. Since systemic exposure following inhalation administration of eluforsen in humans is negligible (data not shown),

metabolites in human plasma will also be negligible. The metabolite profile of eluforsen is sufficiently characterized in lung and liver of animal species, and additional studies in human material are not considered to provide additional relevant information.

The impact of the modifications on the metabolism patterns of oligonucleotides has been reported in several studies. Kynamro®, a 2'-*O*-MOE gapmer, is initially metabolized by endonucleases and then exonucleases to produce chain-shortened metabolites (Rosie, Kim et al. 2006, Baek, Yu et al. 2010, Crooke and Geary 2013). Spinraza®, a phosphorothioate-modified oligonucleotides with 2'-*O*-MOE ribose modifications throughout the PS backbone, is primarily metabolized by 3'- and 5'-exonucleases (2016). In our study, eluforsen was predominantly metabolized by 3'- and 5'-exonuclease-mediated hydrolysis producing chain-shortened metabolites which is consistent with the results from Spinraza® (2016).

Conclusion

We have developed an LC-MS method for analysis of fully phosphorothioated 2-'*O*-Me modified oligonucleotides and its metabolites generated in *in vitro* and *in vivo* studies. The metabolism of eluforsen was evaluated in *in vitro* test systems with nucleases and mouse liver homogenates, and *in vivo* liver and lung samples of mice and monkeys following inhalation administration. We have confirmed that the full phosphorothioate oligonucleotide with 2'-*O*-methyl ribose modification offers increased stability against base hydrolysis by nucleases. Purified enzymes were not able to digest eluforsen. Incubation with liver homogenate lead to generation of n-1 to n-8 from the 3'-end while no metabolites were formed from the 5'-end. Chain-shortened metabolites from both 3'-and 5'-end were formed in *in vivo* liver and lung of both species (mice and monkeys) and the results indicated that similar metabolites were generated in the two species.

Ultimately, we believe that these metabolism studies will contribute toward improving the identification of metabolites from other modified therapeutic oligonucleotides and thereby advance non-clinical drug safety evaluations for this important class of therapies.

Acknowledgments. This work was supported by ProQR Therapeutics.

CHAPTER 5

APPENDIX

IN VITRO METABOLISM OF 2'-RIBOSE UNMODIFIED AND MODIFIED PHOSPHOROTHIOATE OLIGONUCLEOTIDE THERAPEUTICS USING LIQUID CHROMATOGRAPHY-MASS SPECTROMETRY [4]

[4] Jaeah Kim, Noha M. El Zahar, and Michael G. Bartlett.
To be submitted to *Analytical and Bioanalytical Chemistry*.

Abstract

The antisense oligonucleotides (ASOs) have been touted as an emerging therapeutic class to treat genetic disorders and infections. The evaluation of metabolic stability of antisense oligonucleotides during biotransformation is critical due to concerns regarding drug safety. In this study, we developed an LC-MS/MS method offering good selectivity with a high-quality separation to identify each oligonucleotide metabolite. The method was applied to a variety of *in vitro* systems including endo/exonuclease, mouse liver homogenates, and human liver microsomes and the metabolic stability of unmodified vs. modified ASOs were compared. Phosphodiesters generated a unique $H_2PO_4^-$ fragment at *m/z* 97 and a PO_3^- fragment at *m/z* 79, whereas phosphorothioates produced a specific PO_2S^- fragment at *m/z* 95. Typical patterns of chain-shortened metabolites generated by 3'-exonulceases were observed in phosphodiester and phosphorothioate ASOs while endonuclease activity was observed in gapmers that showed relatively more resistance to nuclease degradation. The degradation of each ASO occurred more slowly corresponding to the degree of chemical modifications. Our findings provide further understanding of the impact of modifications on the metabolic stability of ASOs, which facilitates similar development of future ASO therapeutics.

Introduction

Significant progress has been made in oligonucleotide-based therapeutics for the treatment of a wide range of diseases. Approval of eight therapeutic oligonucleotides by the US Food and Drug Administration demonstrates the increasing clinical use of short oligonucleotides as treatments. To date, formivirsen (Vitravene®, 1998), pegaptanib (Macugen®, 2004), mipomersen (Kynamro®, 2013), eteplirsen (Exondys 51®, 2016), defibrotide (Defitelio®, 2016), nusinersen (Spinraza®, 2016), patisiran (Onpattro®, 2018), and inotersen (Tegsedi®, 2018) are all currently approved. Additionally, a conditional marketing authorization was granted to volanesorsen (Waylivra®, 2019) by the European Medicines Agency. Among these diverse synthetic oligonucleotides—includes an aptamer, antisense oligonucleotides (ASOs), and small interfering ribonucleic acids (siRNAs)—six products are ASOs that are small fragments of single-strand deoxyribonucleic acid (DNA) or ribonucleic acid (RNA) (Geary, Rosie et al. 2007, Mansoor and Melendez 2008). ASOs are typically 15-25 nucleotides in length (Dias and Stein 2002, Bartlett, Kim et al. 2019) and bind to complementary sequences on the target mRNA. This binding causes the down-regulation of expression of a specific gene related to a disease (Sannes-Lowery and Hofstadler 2003) by supporting RNase H activity followed by the decay of the target RNA (Geary, Rosie et al. 2007, Crooke and Geary 2013).

Unmodified ASOs with phosphodiester (PO) backbones (**Figure 1**) are extremely susceptible to degradation by nucleases in biological fluids (Blackburn 2006, Bartlett, Kim et al. 2019) and can barely penetrate the cell membrane with a net negative charge (Lysik and Wu-Pong 2003, Chan, Lim et al. 2006), thereby making them further challenging to use for therapeutic applications. The need to circumvent nuclease-mediated degradation, improve tissue half-life, and to increase the affinity and potency of ASOs have led to various chemical modifications (Chan,

Lim et al. 2006, Faria and Ulrich 2008). The first-generation ASOs (**Figure 1**) containing a sulfur group (phosphorothioates) (Verma 2018), amines (phosphoramidates) (Blackburn 2006), or methyl group (methyl phosphonates) (Miller, Cassidy et al. 2000, Blackburn 2006, Verma 2018) were modified by replacing a non-bridging oxygen in the phosphate group (Mansoor and Melendez 2008). This modification in the phosphate backbone provides more nuclease-resistance and longer plasma half-lives relative to phosphodiester ASOs (Sayers, Olsen et al. 1989, Milligan, Matteucci et al. 1993, Mansoor and Melendez 2008, Deleavey and Damha 2012), but may slightly reduce its target mRNA binding affinity due to the decreased melting temperature of the ASO-mRNA heteroduplex (Crooke 2000). The first ASO drug, formivirsen, is a 21-mer phosphorothioate (PS) ASO designed for the inhibition of cytomegalovirus replication (1998).

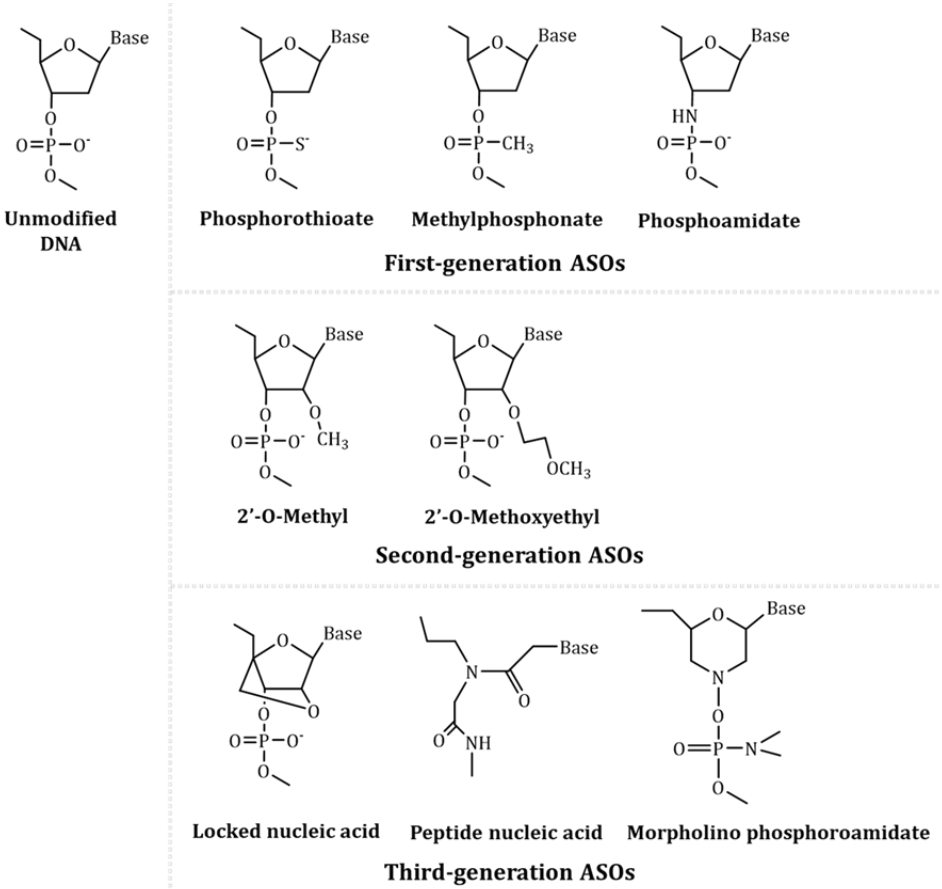

Figure 1. Structure of unmodified oligonucleotides and first-, second-, and third-generation ASOs.

Second-generation ASOs (**Figure 1**), including mipomersen, nusinersen, and inotersen, are modified at the 2'-position of the ribose with alkyl groups such as 2'-*O*-methyl (OME) and 2'-*O*-methoxyethyl (MOE), and these modifications further improve the binding affinity with target mRNA and nuclease resistance (Crooke and Geary 2013, Lee, Awano et al. 2017, Verma 2018). Nusinersen is a fully 2'-*O*-MOE and phosphorothioate-modified ASO, while mipomersen, inotersen, and volanesorsen are 5-10-5 gapmers with 2'-*O*-MOE-modified bases at each of the 5'- and 3'-ends and ten internal nucleotides placed between the modified ends. This chimeric ASO (gapmer) supports RNase H activity on the central gap for target-specific mRNA degradation while fully-modified 2'-OME and 2'-MOE modifications do not elicit target mRNA cleavage by RNase H (Crooke 1992, Altmann, Fabbro et al. 1996, Geary, Norris et al. 2015). Third-generation ASOs (**Figure 1**), including the recently approved eteplirsen, a third-generation phosphorodiamidate morpholino ASO, have been primarily developed with locked nucleic acid, peptide nucleic acid, and morpholino phosphoroamidates substitutions (Mansoor and Melendez 2008, Verma 2018).

While the chemical modifications of therapeutic oligonucleotides provide improved nuclease resistance and higher affinity targeting, those modifications may cause alterations in the biological activity and metabolism of the oligonucleotides (Deleavey and Damha 2012). During non-clinical drug safety evaluations in the drug development process, the investigation of drug metabolism in animals is vital to identifying and characterizing drug metabolites whose nonclinical toxicity needs to be evaluated in order to adequately predict potential risk in humans. To better understand the metabolism of ASOs, *in vitro* systems (e.g., liver homogenates, microsomes, and hepatocytes) have been commonly used to evaluate the metabolic stability. They also provide testing systems for screening and selecting potential drug candidates (Crooke, Graham et al. 2000, Baek, Yu et al. 2010, Studzińska, Rola et al. 2016).

For the metabolic profiling of ASOs, LC-MS/MS methods have the capability to distinguish between full-length oligonucleotides and their truncated metabolites, unlike many hybridization-ELISA methods (Basiri and Bartlett 2014). Hence, we developed an appropriate LC-MS/MS method to identify metabolites and successfully applied the method to better understand the impact of modifications of 2'-ribose and backbones on the generation of metabolites after *in vitro* incubation with purified nucleases, mouse liver homogenates, and human liver microsomes (HLM). In the method, we used a unique mobile phase system consisting of an alkylamine and a fluorinated alcohol that are commonly applied to enhance the response of oligonucleotides when using LC-MS with electrospray ionization (Beverly, Hartsough et al. 2005, Ye and Beverly 2011, Chen and Bartlett 2012, Basiri and Bartlett 2014, Ewles, Goodwin et al. 2014, Elzahar, Magdy et al. 2018, Bartlett, Kim et al. 2019).

Table 1. Sequences and modifications of the four oligonucleotides used in the study.

No.	Sequence (5'→3')	Backbone & 2'-O-ribose chemistry	Cytoside modification
Oligo 1	TCCGTCATCGCTCCTCAGGG	PO&deoxyribose	None
Oligo 2	AGCATAGTTAACGAGCTCCC	PO&deoxyribose	None
Oligo 3 (ISIS 2503)	TCCGTCATCGCTCCTCAGGG	PS&deoxyribose	None
Oligo 4 (ISIS 329993)	AGCATAGTTAACGAGCTCCC	PS&5-10-5 MOE*	Methyl-cytosine

* MOE refers to "Methoxyethyl" ribose modification. 5-10-5 refers to five MOE ribose on each "wing" or end of the sequence with ten deoxyribose in the middle.

Materials and methods

***Chemicals and reagents*.** The two unmodified deoxyribose oligonucleotides were purchased from Eurogentec S.A. (Seraing, Belgium) as 20-mer DNAs (5'-TCCGTCATCGCTCCTCAGGG-3' and 5'-AGCATAGTTAACGAGCTCCC-3') as shown in **Table 1**. The two therapeutic oligonucleotides were acquired from Ionis Pharmaceuticals (Carlsbad, CA) as a 20-mer phosphorothioate-modified DNA (5'-TCCGTCATCGCTCCTCAGGG-3'), and a 20-mer phosphorothioate-modified DNA gapmer (5'-A*G*C*A*T*AGTTAACGAG*C*T*C*C*C-3') where the asterisk (*) indicates 2'-*O*-modifications (**Table 1**). All alkylamines including N, N-dimethylcyclohexylamine (DMCHA), N, N-diisopropylethylamine (DIEA), as well as 1,1,1,3,3,3-hexafluoro-2-propanol (HFIP), LC-MS grade water, and methanol were obtained from Sigma Aldrich (St. Louis, MO, USA). Additionally, tetrahydrofuran (THF), magnesium acetate, dithiothreitol (DTT), ethylenediaminetetraacetic acid (EDTA), tris (2-carboxyethyl) phosphine (TCEP), guanidine hydrochloride, Triton X-100, ammonium bicarbonate (NH_4HCO_3), and nicotinamide adenine dinucleotide phosphate (NADPH) were supplied from Sigma Aldrich (St. Louis, MO, USA). 1,1,1,3,3,3-hexafluoro-2-methyl-2-propanol (HFMIP) was purchased from Fisher Scientific (Toronto, ON, Canada). DNase I and Exonuclease I were supplied from New England Biolabs (Ipswich, MA, USA) and Proteinase K was purchased from Gold Biotechnology (St. Louis, MO, USA). Mouse liver were acquired from BioIVT (Westbury, NY, USA). Human liver microsomes were obtained from Sekisui XenoTech, LLC (Kansas City, KS, USA).

***In vitro metabolic stability assessment using purified enzymes: DNase I (endonuclease) and Exonuclease I (exonuclease)*.** 1 µg of oligonucleotide was incubated with 20 units of either *DNase I* (20/0) or *Exonuclease I* (0/20) at 37 °C for 1, 24 and 48 hours. As a positive control, Oligo 2, an unmodified DNA, was incubated under the same conditions as the modified oligonucleotides,

Oligo 3 and Oligo 4. Additionally, Oligo 2, 3 and 4 were incubated in the buffer only without endo/exonuclease for 1, 24, and 48 hours to serve as negative controls.

***In vitro metabolic stability assessment on mouse liver homogenates*.** The 10 mL of homogenization buffer (100 mM Tris-HCl (pH 8.0), 1 mM magnesium acetate, and 1x penicillin/streptomycin mixture) was added into 5 grams of mouse liver tissues and placed in a glass vessel. The mouse liver tissues were homogenized mechanically using a Polytron (Kinematica AG, Lucerne, Switzerland). To make several 400 µL aliquots of liver homogenate, 50 µL of liver homogenate was further diluted with 350 µL of the homogenization buffer. 4 µL of oligonucleotide (100 µg/mL) was added into each tube and incubated for 0, 1, 8, 24, 72, 120, and 168 hours for the determination of *in vitro* metabolic stability.

***In vitro metabolic stability assessment on human liver microsomes*.** The buffer (100 mM Tris-HCl (pH 8.0), 1 mM magnesium acetate, and 1x penicillin/streptomycin) was prepared and 3 mM NADPH was added to aliquots of the buffer. 100 µg/mL of oligonucleotides were incubated with 1 mg/mL of liver microsomes for 0, 1, 8, 24, 72, 120, and 168 hours for the investigation of metabolic stability.

Proteinase K digestion. The proteinase K digestion was performed to digest unwanted proteins including nucleases in biological samples. The buffer consisted of 60 mM Tris, 400 mM guanidine hydrochloride, 100 mM EDTA, and 0.1% Triton X-100 (pH 9.0) was prepared and stored at 4 °C. 20 µL of digestion buffer with 20 mM DTT added before use and 15 µL of proteinase K containing 200 mg/mL in water for the samples were added into per 100 µL of each sample. All samples were vortexed for 1 min, then incubated with shaking (250 g) at 55 °C for 3 h. Subsequently, samples were processed with solid-phase extraction (SPE).

Solid-phase extraction. After the proteinase K digestion, SPE was applied for oligonucleotide isolation from biological samples using Phenomenex Clarity OTX cartridges (Phenomenex, Torrance, CA). As previously described (Chen and Bartlett 2012), 50 mM ammonium acetate with (pH 5.5 adjusted with acetic acid) in water was prepared for the equilibration buffer. The equilibration buffer was mixed with acetonitrile in a 1:1 ratio to make the wash buffer. 50 mL of a solution containing 100 mM ammonium bicarbonate and 1 mM TCEP in water at pH 9.5 was mixed with 40 mL of acetonitrile and 10 mL of THF for use as the elution buffer. The Clarity OTX cartridges were conditioned using 1 mL of methanol followed by 1 mL of equilibration buffer. The samples digested by proteinase K were mixed with 900 µL of the Clarity OTX buffer and then loaded onto the columns. Subsequently, the cartridges were washed using 2 mL × 2 of washing buffer. Analytes were eluted with 0.5 mL × 2 of elution buffer and then the eluents were evaporated to near dryness under vacuum. The dried samples were reconstituted with deionized water and then analyzed by LC-MS/MS.

LC-MS conditions. A Waters Acquity UPLC (ultrahigh performance liquid chromatography) system was used in combination with a Waters Synapt G2 Q-TOF mass spectrometer (Waters, Milford, MA) equipped with an electrospray ionization (ESI) source to analyze samples. A Phenomenex Clarity 2.6 µm Oligo-XT 100Å, 2.1 x 100 mm column (Phenomenex, Torrance, CA) at 60 °C was used for the chromatographic separation. The injection volume and flow rate were 15 µL and 0.4 mL/min, respectively. Mobile phase A consisted of 30 mM DMCHA and 100 mM HFIP in 5% methanol. Mobile phase B was 95% methanol. The gradient conditions for Oligo 1 and Oligo 2 were as follows (time (in minutes), % mobile phase B): (0.00, 10), (2.00, 10), (9.00, 18), (13.00, 40), (13.01, 60), (18.00, 60), (18.01, 10), (23.00, 10). The gradient conditions for Oligo 3 and Oligo 4 were as follows (time (in minutes), % mobile phase B): (0.00, 15), (3.00, 15), (12.00, 30), (12.01,

50), (17.00, 50), (17.01, 15), (23.00, 15). The UPLC solvent flow-through was diverted to waste from the mass spectrometer for the initial 1 minute and after the final 10 minutes of each run. The capillary voltage, the cone voltage, and the extraction cone voltage were -2.0 kV, 25 V, and 2 V, respectively. The source temperature and the desolvation temperature were 125 °C and 450 °C, respectively. The flow rate of the desolvation gas (N_2) was 1000 L/h. The MS^E sensitivity mode was applied for the MS data acquisition with a 1s scan time. The low collision energy was input to a zero value and high collision energy ramping was set from 20 to 30 eV.

Data analysis. The oligonucleotide mass assembler (OMA) (Nyakas, Blum et al. 2013) was used to obtain predicted *m/z* values for possible metabolites generated from full-length oligonucleotides.

Results

Optimization of Chromatography.

An ion-pair reverse-phase (IP-RP) LC coupled to ESI-MS that has been widely applied for oligonucleotide analysis was selected in this study (Murphy, Brown-Augsburger et al. 2005, McCarthy, Gilar et al. 2009, Basiri and Bartlett 2014). Chromatographic separation and electrospray ionization efficiency in negative ionization mode need to be balanced during the development of the LC-MS method. Babak et al. (Basiri, van Hattum et al. 2017) showed the use of DMCHA as an optimal ion-pairing agent for phosphorothioate-containing oligonucleotides by LC-MS method. HFIP was used as the counter ions in this weak acid-base system. The low boiling point (49 °C) of HFIP helps the ionization of oligonucleotides in the ESI source (Chen, Mason et al. 2013). Even though HFMIP showed better MS signal intensity in the previous study (Basiri, van Hattum et al. 2017), the combination of DMCHA and HFIP was chosen due to the shorter shelf-life of the buffer containing DMCHA and HFMIP. Methanol was utilized as an organic

modifier due to the low solubility of HFIP in acetonitrile (Chen, Mason et al. 2013). Our final conditioned mobile phase consisted of 30 mM DMCHA and 100 mM HFIP after optimization of concentrations and testing of DIEA/HFIP buffers. Chromatographic separation was achieved for each metabolite with high resolving power as shown in **Figure 2**. The difference in retention time was more than 0.3 min between one metabolite and another metabolite that differed in length by a single nucleotide.

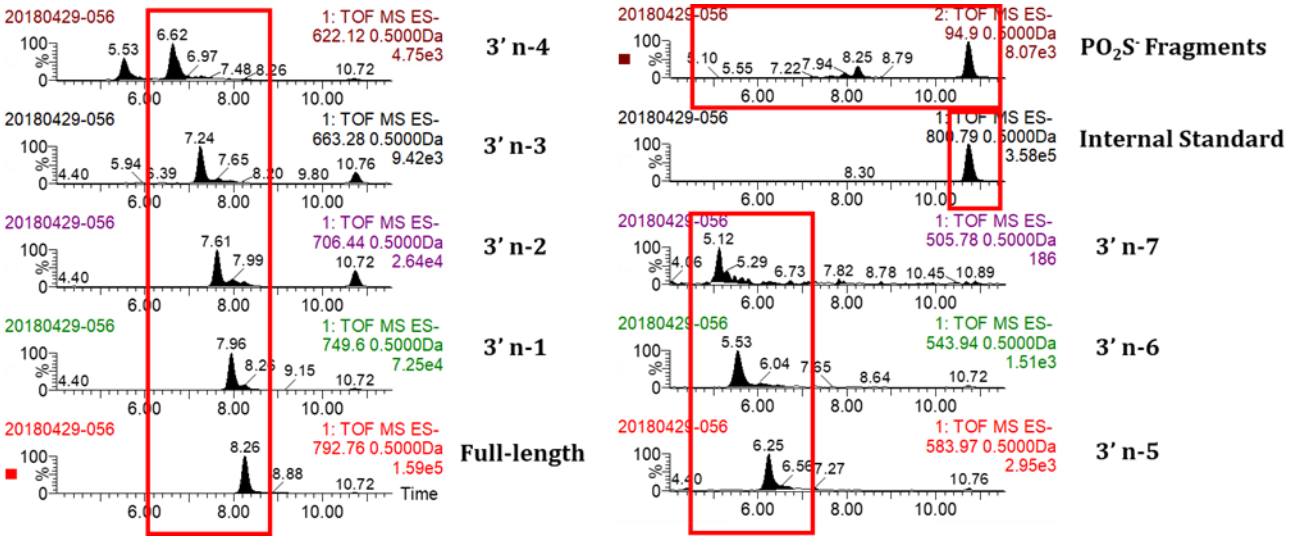

Figure 2. Representative extracted ion chromatograms of a full-length ASO and its 3'-end shortmers in samples incubated with mouse liver homogenate.

Identification of ASO metabolites

Effective metabolite characterizations can be achieved using extracted-ion chromatograms (EIC) with predicted molecular formulas (Ruan, Peterman et al. 2008). From a predictive list of *m/z* values generated using the OMA software, a specific *m/z* of a precursor ion at a certain charge state was selected and extracted to generate each EIC for the determination of each metabolite. With the high-quality separation of the method, metabolite identification was performed readily

for each compound without effort to avoid assignments due to the overlapping of *m/z* series from multiple metabolites with similar retention times. Accurate quantifications have been unavailable due to the variance of ionization efficiency for metabolites and the absence of standards for all metabolites (Husser, Brink et al. 2017). However, to estimate the relative amounts of each compound in a timely manner, the signal intensities of compounds were optimized using internal standards; Oligo 3 was used as an internal standard for Oligo 1, 2, and 4, and Oligo 4 was used for Oligo 1.

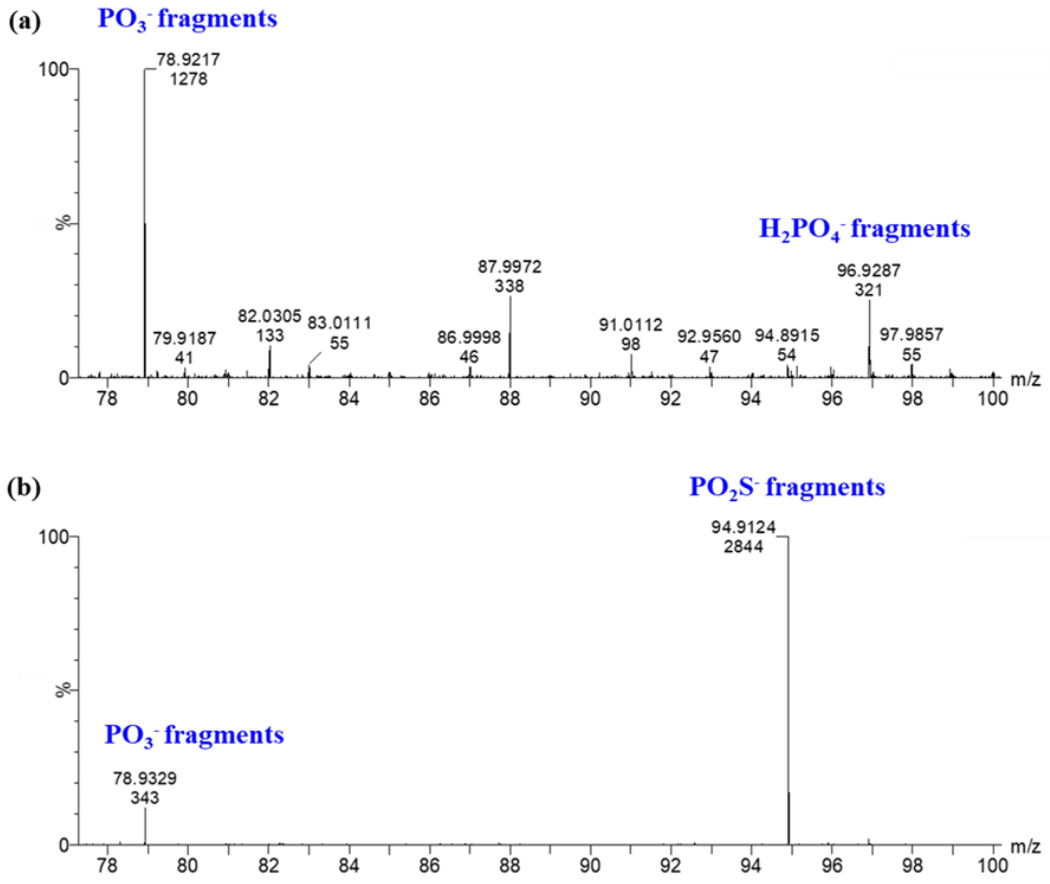

Figure 3. MS/MS product ions of PO_3^- (at *m/z* 79) $H_2PO_4^-$ (at *m/z* 97) and PO_2S^- (at *m/z* 95) fragment ions in the phosphodiester- and phosphorothioate-containing oligonucleotides. (a) PO-containing oligonucleotides. (b) PS-containing oligonucleotides.

Additionally, distinguishable MS/MS product ions (i.e. PO_3^-, $H_2PO_4^-$ and PO_2S^- fragment ions) were observed in the phosphodiester- and phosphorothioate-containing oligonucleotides (**Figure 3**). PO_3^- fragment ion at *m/z* 79 and $H_2PO_4^-$ fragment ion at *m/z* 97 were dominantly observed in the phosphodiester-containing oligonucleotides. In the phosphorothioate-containing oligonucleotides, PO_2S^- fragment ion at *m/z* 95 was mainly shown while an approximately 8 times lower amount of PO_3^- fragment ion at *m/z* 79 was observed, these findings could be attributed to ubiquitous endogenous oligonucleotides.

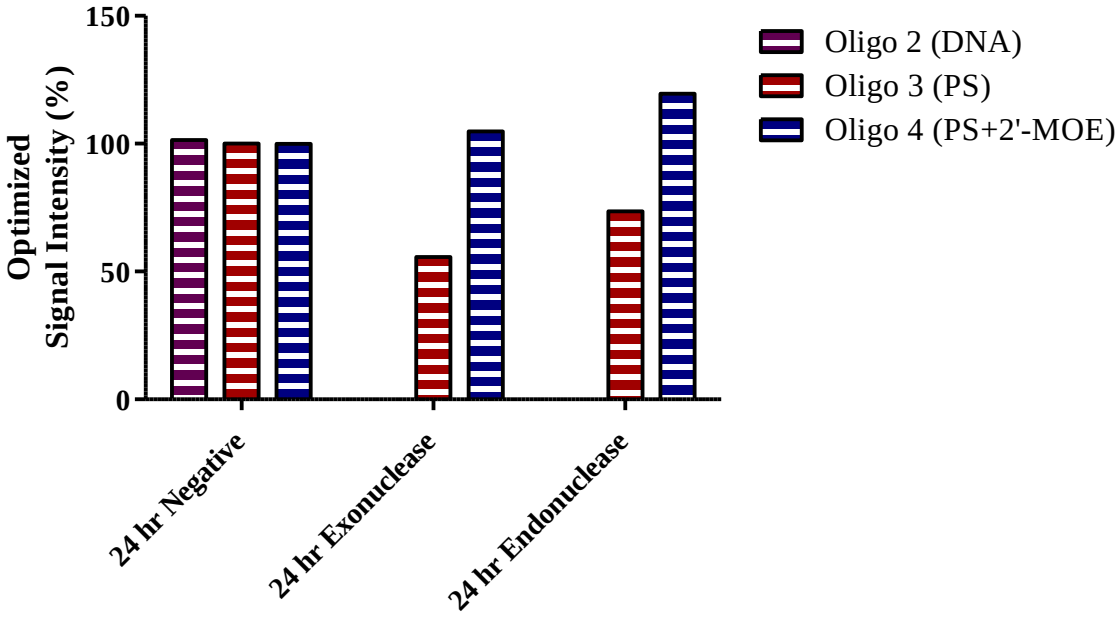

Figure 4. Determination of *in vitro* metabolic stabilites of ASOs used in this study on purified endo- and exonucleases.

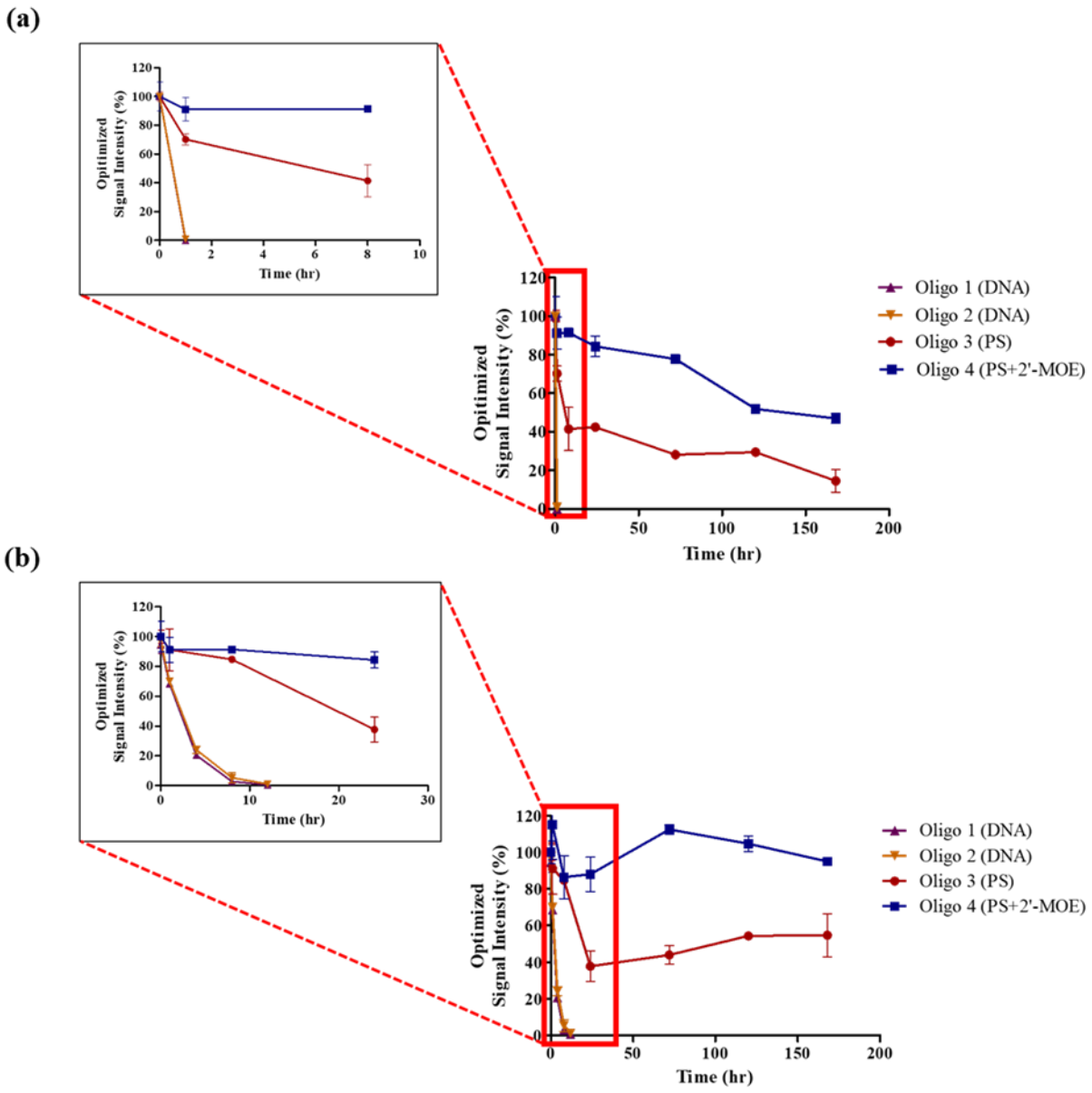

Figure 5. Determination of *in vitro* metabolic stabilites of ASOs on mouse liver homogenates and human liver microsomes. (a) Mouse liver homogenates. (b) Human liver microsomes.

Determination of *in vitro* metabolic stabilities of ASOs with endo/exonucleases (n=3), mouse liver homogenates (n=2), and human liver microsomes (n=2)

Phosphodiester oligonucleotide. Oligo 1 and 2 are phosphodiester-containing DNAs, which were incubated with purified endo- (*DNase I*), exonuclease (*Exonuclease I*) enzymes, mouse liver homogenates, or human liver microsomes. As shown in **Figure 4**, the metabolic stability of the unmodified ASO was poor after a 24-hour incubation with endo/exonuclease enzymes. In fact, it was totally degraded after only 1 hour of incubation with these enzymes. After incubation with mouse liver homogenates, Oligo 1 and 2 were also degraded within 1 hour (**Figure 5a**). The results are not surprising since unmodified oligonucleotides are good substrates for nucleases (Blackburn 2006). The unmodified ASOs were totally degraded after 12 hours of incubation with human liver microsomes as shown in **Figure 5b**, where 3'-end shortmers (from n-1 to n-9) were observed in the samples. The result confirmed that 3'-exonucleases are the critical enzymes responsible for metabolizing unmodified oligonucleotides in human liver microsomes.

Phosphorothioate ASO. After a 24-hour incubation with endo/exonuclease enzymes, the phosphorothioate modified DNA (Oligo 3) was degraded by approximately 45% and 27% by exonucleases and endonucleases, respectively (**Figure 4**), in comparison with negative controls. Only 3'-end shortmers (from n-1 to n-6) were observed in the samples incubated with exonucleases. In the samples incubated with mouse liver homogenates after a series of shorter time incubations (0, 1, 8, 24, 72, 120, and 168 hours), only 3'-end shortmers (from n-1 to n-8) but not 5'-end shortmers were mainly produced by endogenous 3'-exonucleases in mouse liver as shown in **Figure 5a**. Additionally, 3'-end shortmers (from n-1 to n-4) were observed in the samples incubated with human liver microsomes as shown in **Figure 5b**. This result suggests that 3'-

exonuclease is the primary enzyme that metabolizes oligo 3 in *in vitro* purified enzymes, mouse liver homogenates, and human liver microsomes.

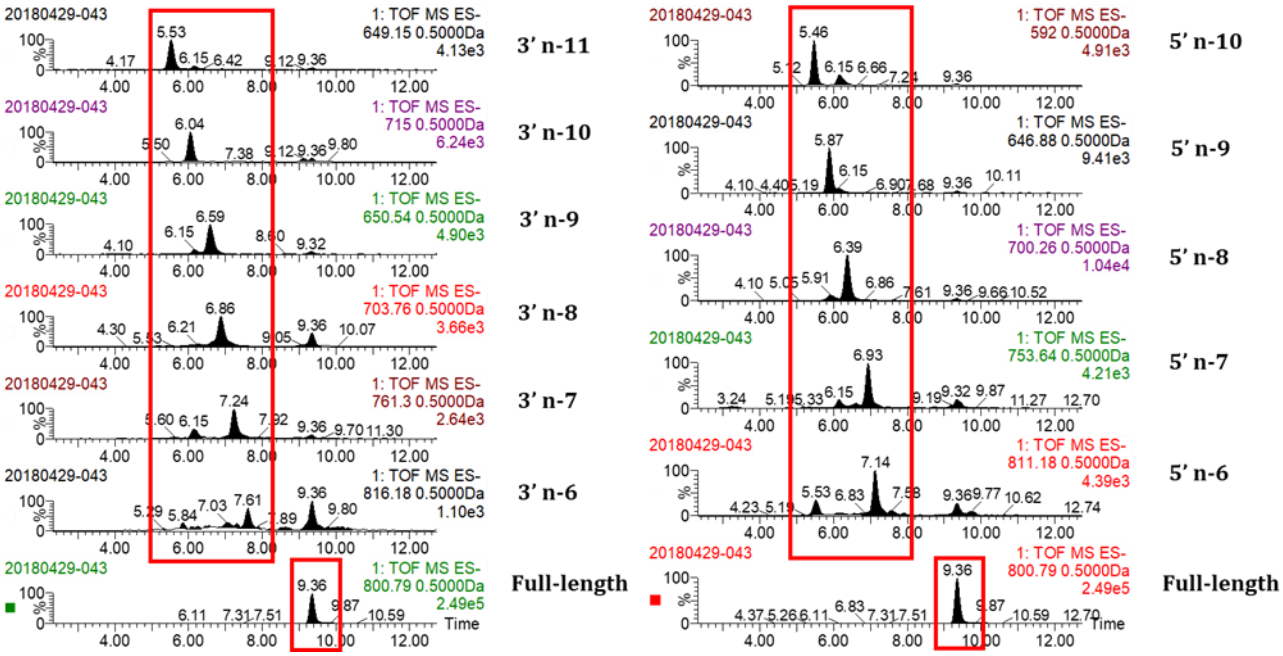

Figure 6. Extacted ion chromatogram of the Oligo 4 and its metabolites in the samples incubated with mouse liver homogenates for 72 hours. From 3'n-6 to 3'n-11 and from 5'n-6 to 5'n-10 were observed in the samples.

Phosphorothioate and 2'-*O*-MOE chimeric ASO (gapmer). The phosphorothioate and 2'-*O*-MOE modified DNA (Oligo 4) did not show any metabolism (**Figure 4**) after a 24-hour incubation with endo/exonuclease enzymes. After incubation with mouse liver homogenates, metabolites from 3'n-6 to 3'n-11 and from 5'n-6 to 5'n-10 were produced as shown in **Figure 6**. The result suggests that the cleavages were initiated in the unmodified regions of the 2'-ribose by endonucleases followed by exonuclease degradation. This result is consistent with the previous observation for the metabolism of mipomersen (gapmer) (Crooke and Geary 2013). This result

suggests that 2'-ribose MOE modification may prevent metabolic reactions with 3'- and 5'-exonucleases. Interestingly, there was no metabolism observed in the samples incubated with human liver microsomes (**Figure 5b**). The result confirmed that the gapmer is not metabolized by CYP450 enzymes that are traditional drug metabolizing enzymes, which is consistent with that of previous studies for mipomersen (Crooke and Geary 2013).

Discussions

Oligonucleotide biotransformation mainly takes places in the liver and endo/exonucleases are the major enzymes responsible for metabolizing these oligonucleotides (Crooke, Graham et al. 2000, Geary 2009). The results from reliable *in vitro* methods can be applicable for the prediction of biological response in *in vivo* systems and thereby indirectly provide extrapolation of phenomena in the human body. Hence, *in vitro* liver homogenates and microsomes (Crooke, Graham et al. 2000, Baek, Yu et al. 2010, Shemesh, Yu et al. 2016) have been commonly utilized to mimic *in vivo* systems for the metabolic investigation of oligonucleotides. To evaluate *in vitro* metabolic stabilities of ASOs and the impact of chemical modification on their metabolism, the ASOs used in the study were incubated in parallel with endo/exonucleases, mouse liver homogenates, and human liver microsomes.

As expected, a rapid clearance of phosphodiester oligonucleotides was observed after incubations with purified enzymes and mouse liver homogenates within 1 hour, and human liver microsome within 12 hours (**Figure 4** and **5**). In the human liver microsome samples, the formation of 3'-end shortmers (from n-1 to n-9) occurred as a result of 3'-exonuclease mediated metabolism.

A phosphorothioate oligonucleotide (Oligo 3) was slightly metabolized by purified enzymes with the formation of 3'-end shortmers (from 3'n-1 to n-6) while a phosphorothioate and 2'-*O*-

MOE chimeric ASO (Oligo 4) was not metabolized by these enzymes. After incubations with mouse liver homogenates, the degradation rate of the Oligo 3 was faster than that of Oligo 4. Additionally, the 3'-end shortmers (from n-1 to n-8) were observed in the Oligo 3 samples while 3'-end shortmers (from n-6 to n-11) and 5'-end shortmers (from n-6 to n-10) were produced in the Oligo 4 samples. These results indicated that the improved metabolic stability by MOE modification on each end was highly resistant to exonucleases, and thereby it was initially cleaved by endonucleases following a long exposure time and then metabolized by exonucleases. In other words, metabolites were not produced by exonucleases within the five MOE moieties on both sides. The only samples in which we observed verifiable metabolites generated by 5'-exonucleases after cleavages by endonucleases were the Oligo 4 samples incubated with mouse liver homogenates. This result is interesting since identifiable 5'-end shortmers were not detected in other *in vitro* samples.

Overall, we confirmed that chemical modifications on oligonucleotides caused alterations in their metabolism, and the high degree of modifications showed slower degradation rates and more complex metabolism. The degradation of ASOs was mediated primarily by 3'-exonucleases with the formation of chain-shortened metabolites in the *in vitro* systems except when Oligo 4 was incubated with mouse liver homogenates. Therefore, further studies in *in vivo* systems will be required for more comprehensive investigations of metabolic stabilities of modified oligonucleotides. At a certain point, shorter metabolites might not all be detected due to limited chromatographic retention under the conditions need to retain the large full-length oligonucleotide and/or less abundance. Additionally, oxidative metabolites from phosphorothioate backbones and depurination/depyrimidation were not found in this study.

Interestingly, we showed that the lack of metabolism of highly modified Oligo 4 in human liver microsomes could originate from the fact that MOE modifications provided increased metabolic stability against enzymes found in human liver microsomes. Additionally, the result is consistent with the previous study that mipomersen, a gapmer, was not metabolized in *in vitro* human liver microsomes (Crooke and Geary 2013). Therefore, to elucidate whether this phenomenon was attributed to the components in the microsomes or differences in species specific, further investigations using mouse liver microsomes or human liver S9 fraction may be needed.

Although the pharmacological properties of these metabolites are unknown and the toxicities including potential off-target effects by metabolites of ASOs have not been investigated yet, the elucidation of metabolic stability is the initial basis to predict any safety risks in human.

Conclusion

We have presented a new mobile phase composition consisting of 30 mM DMCHA and 100 mM HFIP that provides an efficient high-resolution chromatographic separation using LC-MS. The method had good selectivity for use in the identification of full-length oligonucleotides and their metabolites and thereby determine the effect of chemical modifications on *in vitro* metabolic stabilities of ASOs. We used an effective sample preparation method using Proteinase K digestion followed by SPE to maximize coverage of the metabolites. We have reported the comparison of unmodified and 2'-ribose modified phosphorothioate oligonucleotides in metabolite generation by *in vitro* incubation with purified nucleases, mouse liver homogenates, and human liver microsomes. Unique features of MS/MS fragments were observed in phosphodiester and phosphorothioate oligonucleotides. The modifications on the phosphodiester backbone and/or 2'-*O*-ribose position influenced the metabolic stability against endo- and/or exonucleases. Given

these findings, we believe that the information would contribute toward identifying metabolites of 2’-ribose modified phosphorothioate oligonucleotides and advance non-clinical drug safety evaluations.

CHAPTER 6

CONCLUSIONS

In this dissertation, various novel analytical methods were developed for the bioanalysis of small and large molecules, especially thiamine-related molecules and therapeutic oligonucleotides. Subsequently, these methods were applied for various pharmaceutical and biological studies, as appropriate. The results from Chapter 2 involve the development and application of an LC-UV method for the quantifications of two lipophilic thiamine derivatives, benfotiamine and sulbutiamine, in cancer cells and cell media. To date, there are no other methods available for the determination of benfotiamine and sulbutiamine from biological matrices. We validated the method in accordance with the current U.S. FDA guidelines for bioanalytical method validation (e.g., selectivity, linearity, sensitivity, precision, and accuracy) and applied the method to the identification of both intracellular and extracellular levels of these compounds in order to evaluate their effect on cancer cell proliferation.

In Chapter 3, we introduced the use of isotopically-labeled compounds to track the conversion of intracellular thiamine into its phosphorylated forms in order to explore the metabolic fate of thiamine. To date, there are no other methods available for addressing unanswered questions related to the cofactor and non-cofactor roles of thiamine in cancer progression as it had previously not been possible to determine how this pathway was altered. Therefore, we developed a novel ion-pair LC-MS method to simultaneously quantitate underivatized thiamine, stable-isotope labeled thiamine, thiamine monophosphate, and thiamine pyrophosphate. In this method, we introduced hexylamine as an ion-pairing agent with an effective separation of analytes and

amprolium as a proper internal standard. We validated the method with the bioanalytical validation criteria set by the U.S. FDA and applied the method to explore the metabolic fate of intracellular thiamine in cancer cells by tracking stable-isotope labeled molecules. The observation from this study suggests an unexplored role for thiamine in cancer.

In Chapter 4, we described the development of an LC-MS method and its application for *in vitro* and *in vivo* metabolite identification of eluforsen with semi-quantitative estimation of their amounts. In this study, we presented successful oligonucleotide bioanalysis using the combination of proteinase K digestion and anion-exchange SPE. We confirmed that a highly-specific capture strand utilizing an immunoaffinity approach cannot bind to shorter metabolites after a certain point, suggesting that this approach is limited when applied to metabolite identification studies. Due to the mass spectral complexity of the 33-mer eluforsen, we carefully selected charge states and *m/z* values for each metabolite to estimate relative concentrations of metabolites. As a result, we showed that chain-shortened metabolites of eluforsen by 3'- and 5'-exonucleases were produced in both *in vitro* and *in vivo* systems. We believe that the observation can further be utilized for metabolism studies of 2'-ribose-modified phosphorothioate oligonucleotides during the development of oligonucleotide therapeutics.

The results presented in Chapter 5 confirmed that the chemical modifications of ASOs influenced their metabolic stability in biological samples. We showed that a mobile phase consisting of 30 mM DMCHA and 100 mM HFIP resulted in high-quality chromatographic retention and resolution. With the method, we demonstrated the difference in metabolic stability between a phosphodiester-containing ASO, a PS-modified ASO, and a 2'-MOE-PS gapmer. Ultimately, we believe that these studies can provide significant insights into many investigations that involve the further study of the metabolic stability of other modified therapeutic

oligonucleotides, helping advanced preclinical drug safety evaluations for the therapeutic applications of ASOs.

Although the actual application of LC-MS in *in vivo* and *in vitro* metabolic stability studies of therapeutic oligonucleotides have been discussed in this dissertation, further studies are necessary to overcome the limitations in these studies. For instance, despite the finding that the combination of proteinase K digestion and anion-exchange SPE provided reasonable metabolite coverage, a comprehensive investigation using these presented LC-MS methods to establish better sample preparation methods to maximize extraction efficiency of metabolites are required to improve capabilities for this purpose.

We only conducted metabolite identification of eluforsen in *in vivo* liver and lung samples from mice and monkeys because these organs are the major target organs of eluforsen as well as the main organs involved in metabolism of xenobiotics. Nevertheless, metabolite identification of eluforsen in other organs from other animals is required to fully demonstrate LC-MS for metabolite identifications of therapeutic oligonucleotides. The need for a high level of sensitivity can be followed to detect the least abundant parent drugs and their metabolites in these other organs. To achieve better ionization efficiency in MS and improve chromatographic separations for therapeutic oligonucleotides, various studies are being currently conducted either regarding ion-pairing agents and fluorinated alcohols or changes in the mode of separation methods (e.g. HILIC) without IPs. The next steps will also involve a variety of efforts in these investigations especially on sensitivity as well as selectivity of the methods.

Utilizing the presented methods, the next investigations will involve biomarker analysis, impurity profiling, quantitative bioanalysis, and metabolism studies of other oligonucleotides. Regarding metabolism studies, in the same manner that spectral search engines using libraries in

protein analysis, the development of MS and MS/MS spectral libraries of metabolite standards should be highly anticipated for rapid metabolite identification. Additionally, the comparison of results of traditional qPCR or hELISA studies to better demonstrate the advantages of LC-MS applications in these studies is necessary for other therapeutic oligonucleotides. Our findings presented in this dissertation can be used by other researches to further understand the design of metabolism studies of oligonucleotides.

REFERENCES

US Food and Drug Administration (1998). Approval Letter of Vitravene Injection

US Food Drug Administration (2008). Guidance for Industry–Safety Testing of Drug Metabolites

European Medicines Agency (2013). European public assessment reports: Orphan medicines.

US Food and Drug Administration (2013). List of orphan designations and approvals.

US Food and Drug Administration (2016). FDA Product label. SPINRAZA (nusinersen) injection, for intrathecal use.

Kastle Therapeutics Llc (2016). KYNAMRO- mipomersen sodium injection, solution

Abdelwahab, N. S. and N. F. Farid (2014). "Validated HPLC-DAD method for stability study of sulbutiamine HCl." Rsc Advances **4**(58): 30523-30529.

Adithya, B. P. and M. Vijayalakshmi (2012). "Development and validation of RP-HPLC method for the estimation of Benfotiamine in bulk and dosage form." Int. J. Pharm. Chem. Biol. Sci **2**: 354-360.

Albala´-Hurtado, S., M. T. Veciana-Nogue´s, M. a. Izquierdo-Pulido and A. Marine´-Font (1997). "Determination of water-soluble vitamins in infant milk by high-performance liquid chromatography." Journal of Chromatography A **778**(1): 247-253.

Altmann, K.-H., D. Fabbro, N. Dean, T. Geiger, B. Monia, M. Müllert and P. Nicklin (1996). Second-generation antisense oligonucleotides: structure—activity relationships and the design of improved signal-transduction inhibitors, Portland Press Limited.

Annesley, T. M. (2003). "Ion Suppression in Mass Spectrometry." Clinical Chemistry **49**(7): 1041-1044.

Ashcroft, A. E. (2007). Ionization methods in organic mass spectrometry, Royal Society of Chemistry.

Azarani, A. and K. H. Hecker (2001). "RNA analysis by ion-pair reversed-phase high performance liquid chromatography." Nucleic acids research **29**(2): E7-E7.

Babaei-Jadidi, R., N. Karachalias, N. Ahmed, S. Battah and P. J. Thornalley (2003). "Prevention of incipient diabetic nephropathy by high-dose thiamine and benfotiamine." Diabetes **52**(8): 2110-2120.

Baek, M.-S., R. Z. Yu, H. Gaus, J. S. Grundy and R. S. Geary (2010). "In vitro metabolic stabilities and metabolism of 2′-O-(methoxyethyl) partially modified phosphorothioate antisense oligonucleotides in preincubated rat or human whole liver homogenates." Oligonucleotides **20**(6): 309-316.

Bartlett, M. G., J. Kim, B. Basiri and N. Li (2019). "Sample Preparation for LC-MS Bioanalysis of Oligonucleotides." Sample Preparation in LC-MS Bioanalysis.

Basiri, B. and M. G. Bartlett (2014). "LC–MS of oligonucleotides: applications in biomedical research." Bioanalysis **6**(11): 1525-1542.

Basiri, B., J. M. Sutton, B. S. Hanberry, J. A. Zastre and M. G. Bartlett (2016). "Ion pair liquid chromatography method for the determination of thiamine (vitamin B1) homeostasis." Biomedical Chromatography **30**(1): 35-41.

Basiri, B., H. van Hattum, W. D. van Dongen, M. M. Murph and M. G. Bartlett (2017). "The role of fluorinated alcohols as mobile phase modifiers for LC-MS analysis of oligonucleotides." Journal of The American Society for Mass Spectrometry **28**(1): 190-199.

Berg, J. M., J. Tymoczko and L. Stryer (2002). "The citric acid cycle oxidizes two-carbon units." Biochemistry.

Bettendorff, L. (1994). "The Compartmentation of Phosphorylated Thiamine Derivatives in Cultured Neuroblastoma-Cells." Biochimica Et Biophysica Acta-Molecular Cell Research **1222**(1): 7-14.

Bettendorff, L. (1994). "The compartmentation of phosphorylated thiamine derivatives in cultured neuroblastoma cells." Biochimica et Biophysica Acta (BBA) - Molecular Cell Research **1222**(1): 7-14.

Bettendorff, L., L. Weekers, P. Wins and E. Schoffeniels (1990). "Injection of sulbutiamine induces an increase in thiamine triphosphate in rat tissues." Biochem Pharmacol **40**(11): 2557-2560.

Bettendorff, L. and P. Wins (1994). "Mechanism of thiamine transport in neuroblastoma cells. Inhibition of a high affinity carrier by sodium channel activators and dependence of thiamine uptake on membrane potential and intracellular ATP." J Biol Chem **269**(20): 14379-14385.

Beverly, M., K. Hartsough and L. Machemer (2005). "Liquid chromatography/electrospray mass spectrometric analysis of metabolites from an inhibitory RNA duplex." Rapid communications in mass spectrometry **19**(12): 1675-1682.

Bitsch, R., M. Wolf, J. Moller, L. Heuzeroth and D. Gruneklee (1991). "Bioavailability Assessment of the Lipophilic Benfotiamine as Compared to a Water-Soluble Thiamin Derivative." Annals of Nutrition and Metabolism **35**(5): 292-296.

Blackburn, G. M. (2006). Nucleic acids in chemistry and biology, Royal Society of Chemistry.

Brown, D. A., S.-H. Kang, S. M. Gryaznov, L. DeDionisio, O. Heidenreich, S. Sullivan, X. Xu and M. I. Nerenberg (1994). "Effect of phosphorothioate modification of oligodeoxynucleotides on specific protein binding." Journal of Biological Chemistry **269**(43): 26801-26805.

Campbell, J. M., T. A. Bacon and E. Wickstrom (1990). "Oligodeoxynucleoside phosphorothioate stability in subcellular extracts, culture media, sera and cerebrospinal fluid." Journal of biochemical and biophysical methods **20**(3): 259-267.

Chan, J. H., S. Lim and W. F. Wong (2006). "Antisense oligonucleotides: from design to therapeutic application." Clinical and experimental pharmacology and physiology **33**(5-6): 533-540.

Chen, B. and M. Bartlett (2012). "A one-step solid phase extraction method for bioanalysis of a phosphorothioate oligonucleotide and its 3′ n-1 metabolite from rat plasma by uHPLC–MS/MS." The AAPS journal **14**(4): 772-780.

Chen, B. and M. G. Bartlett (2013). "Evaluation of mobile phase composition for enhancing sensitivity of targeted quantification of oligonucleotides using ultra-high performance liquid chromatography and mass spectrometry: application to phosphorothioate deoxyribonucleic acid." Journal of Chromatography A **1288**: 73-81.

Chen, B., S. F. Mason and M. G. Bartlett (2013). "The Effect of Organic Modifiers on Electrospray Ionization Charge-State Distribution and Desorption Efficiency for Oligonucleotides." Journal of The American Society for Mass Spectrometry **24**(2): 257-264.

Cheng, X., D. Ma, G. Fei, Z. Ma, F. Xiao, Q. Yu, X. Pan, F. Zhou, L. Zhao and C. Zhong (2018). "A single-step method for simultaneous quantification of thiamine and its phosphate esters in whole blood sample by ultra-performance liquid chromatography-mass spectrometry." Journal of Chromatography B **1095**: 103-111.

Chokkathukalam, A., D.-H. Kim, M. P. Barrett, R. Breitling and D. J. Creek (2014). "Stable isotope-labeling studies in metabolomics: new insights into structure and dynamics of metabolic networks." Bioanalysis **6**(4): 511-524.

Chomczynski, P. and N. Sacchi (1987). "Single-step method of RNA isolation by acid guanidinium thiocyanate-phenol-chloroform extraction." Analytical Biochemistry **162**(1): 156-159.

COHEN, A. S., A. J. BOURQUE, B. H. WANG, D. L. SMISEK and A. BELENKY (1997). "A nonradioisotope approach to study the in vivo metabolism of phosphorothioate oligonucleotides." Antisense and Nucleic Acid Drug Development **7**(1): 13-22.

Comin-Anduix, B., J. Boren, S. Martinez, C. Moro, J. J. Centelles, R. Trebukhina, N. Petushok, W. N. P. Lee, L. G. Boros and M. Cascante (2001). "The effect of thiamine supplementation on tumour proliferation - A metabolic control analysis study." European Journal of Biochemistry **268**(15): 4177-4182.

Comín-Anduix, B., J. Boren, S. Martinez, C. Moro, J. J. Centelles, R. Trebukhina, N. Petushok, W. N. P. Lee, L. G. Boros and M. Cascante (2001). "The effect of thiamine supplementation on tumour proliferation: a metabolic control analysis study." European Journal of Biochemistry **268**(15): 4177-4182.

Coulier, L., R. Bas, S. Jespersen, E. Verheij, M. J. van der Werf and T. Hankemeier (2006). "Simultaneous quantitative analysis of metabolites using ion-pair liquid chromatography− electrospray ionization mass spectrometry." Analytical chemistry **78**(18): 6573-6582.

Crooke, R. (1993). "Cellular uptake, distribution and metabolism of phosphorothioate, phosphorodiester and methylphosphonate oligonucleotides. In" Antisense Research and Applications"(ST Crooke and B. Lebleu, eds.)." Antisense Research and Applications. Boca Raton, FL: CRC **427**.

Crooke, R. (1998). In vitro cellular uptake, distribution, and metabolism of oligonucleotides. Antisense Research and Application, Springer**:** 103-140.

Crooke, R. M., M. J. Graham, M. E. Cooke and S. T. Crooke (1995). "In vitro pharmacokinetics of phosphorothioate antisense oligonucleotides." Journal of Pharmacology and Experimental Therapeutics **275**(1): 462-473.

Crooke, R. M., M. J. Graham, M. J. Martin, K. M. Lemonidis, T. Wyrzykiewiecz and L. L. Cummins (2000). "Metabolism of antisense oligonucleotides in rat liver homogenates." Journal of Pharmacology and Experimental Therapeutics **292**(1): 140-149.

Crooke, S. T. (1992). "Therapeutic applications of oligonucleotides." Annual review of pharmacology and toxicology **32**(1): 329-376.

Crooke, S. T. (1998). Basic principles of antisense therapeutics. Antisense research and application, Springer**:** 1-50.

Crooke, S. T. (2000). Progress in antisense technology: the end of the beginning. Methods in enzymology, Elsevier. **313:** 3-45.

Crooke, S. T. and C. F. Bennett (1996). "Progress in antisense oligonucleotide therapeutics." Annual Review of Pharmacology and Toxicology **36**(1): 107-129.

Crooke, S. T. and R. S. Geary (2013). "Clinical pharmacological properties of mipomersen (Kynamro), a second generation antisense inhibitor of apolipoprotein B." British Journal of Clinical Pharmacology **76**(2): 269-276.

Crooke, S. T. and B. Lebleu (1993). Antisense research and applications, CRC Press.

Dai, G., X. Wei, Z. Liu, S. Liu, G. Marcucci and K. K. Chan (2005). "Characterization and quantification of Bcl-2 antisense G3139 and metabolites in plasma and urine by ion-pair reversed phase HPLC coupled with electrospray ion-trap mass spectrometry." Journal of Chromatography B **825**(2): 201-213.

Dattagupta, J. K., T. Fujiwara, E. V. Grishin, K. Lindner, P. C. Manor, N. J. Pieniazek, R. Saenger and D. Suck (1975). "Crystallization of the fungal enzyme proteinase K and amino acid composition." J Mol Biol **97**(2): 267-271.

de Koning, W. and K. van Dam (1992). "A method for the determination of changes of glycolytic metabolites in yeast on a subsecond time scale using extraction at neutral pH." Analytical biochemistry **204**(1): 118-123.

Deleavey, G. F. and M. J. Damha (2012). "Designing chemically modified oligonucleotides for targeted gene silencing." Chemistry & biology **19**(8): 937-954.

Deng, P., X. Chen, G. Zhang and D. Zhong (2010). "Bioanalysis of an oligonucleotide and its metabolites by liquid chromatography–tandem mass spectrometry." Journal of Pharmaceutical and Biomedical Analysis **52**(4): 571-579.

Dias, N. and C. Stein (2002). "Antisense oligonucleotides: basic concepts and mechanisms." Molecular cancer therapeutics **1**(5): 347-355.

Doneanu, C. E., W. Chen and J. C. Gebler (2009). "Analysis of oligosaccharides derived from heparin by ion-pair reversed-phase chromatography/mass spectrometry." Analytical chemistry **81**(9): 3485-3499.

Douzenis, A., I. Michopoulos and L. Lykouras (2006). "Sulbutiamine, an 'innocent' over the counter drug, interferes with therapeutic outcome of bipolar disorder." World Journal of Biological Psychiatry **7**(3): 183-185.

Elzahar, N., N. Magdy, A. M. El-Kosasy and M. G. Bartlett (2018). "Degradation product characterization of therapeutic oligonucleotides using liquid chromatography mass spectrometry." Analytical and bioanalytical chemistry **410**(14): 3375-3384.

Eram, M. S. and K. Ma (2013). "Decarboxylation of pyruvate to acetaldehyde for ethanol production by hyperthermophiles." Biomolecules **3**(3): 578-596.

Erich, S., T. Anzmann and L. Fischer (2012). "Quantification of lactose using ion-pair RP-HPLC during enzymatic lactose hydrolysis of skim milk." Food chemistry **135**(4): 2393-2396.

Ewles, M., L. Goodwin, A. Schneider and T. Rothhammer-Hampl (2014). "Quantification of oligonucleotides by LC-MS/MS: the challenges of quantifying a phosphorothioate oligonucleotide and multiple metabolites." Bioanalysis **6**(4): 447-464.

Faria, M. and H. Ulrich (2008). "Sugar boost: when ribose modifications improve oligonucleotide performance." Current opinion in molecular therapeutics **10**(2): 168-175.

FDA (2001). "Guidance for Industry." Guidance for Industry: Bioanalytical Method Validation.

FDA (2013). "Draft Guidance for Industry." Draft Guidance for Industry: Bioanalytical Method Validation.

(2013). Draft Guidance for industry: Bioanalytical method validation

(2018). Guidance for Industry: Bioanalytical Method Validation

Fenn, J., M. Mann, C. Meng, S. Wong and C. Whitehouse (1989). "Electrospray ionization for mass spectrometry of large biomolecules." Science **246**(4926): 64-71.

Ganapathy, V., S. B. Smith and P. D. Prasad (2004). "SLC19: the folate/thiamine transporter family." Pflügers Archiv **447**(5): 641-646.

Gao, W., F. Han, C. Storm, W. Egan and Y.-C. Cheng (1992). "Phosphorothioate oligonucleotides are inhibitors of human DNA polymerases and RNase H: implications for antisense technology." Molecular Pharmacology **41**(2): 223-229.

Geary, R. S. (2009). "Antisense oligonucleotide pharmacokinetics and metabolism." Expert Opinion on Drug Metabolism & Toxicology **5**(4): 381-391.

Geary, R. S., B. F. Baker and S. T. Crooke (2015). "Clinical and Preclinical Pharmacokinetics and Pharmacodynamics of Mipomersen (Kynamro(®)): A Second-Generation Antisense Oligonucleotide Inhibitor of Apolipoprotein B." Clinical Pharmacokinetics **54**: 133-146.

Geary, R. S., B. F. Baker and S. T. Crooke (2015). "Clinical and preclinical pharmacokinetics and pharmacodynamics of mipomersen (Kynamro®): a second-generation antisense oligonucleotide inhibitor of apolipoprotein B." Clinical pharmacokinetics **54**(2): 133-146.

Geary, R. S., J. M. Leeds, S. P. Henry, D. K. Monteith and A. A. Levin (1997). "Antisense oligonucleotide inhibitors for the treatment of cancer: 1. Pharmacokinetic properties of phosphorothioate oligodeoxynucleotides." Anti-cancer drug design **12**(5): 383-393.

Geary, R. S., D. Norris, R. Yu and C. F. Bennett (2015). "Pharmacokinetics, biodistribution and cell uptake of antisense oligonucleotides." Advanced drug delivery reviews **87**: 46-51.

Geary, R. S., Z. Y. Rosie and A. A. Levin (2007). Basic principles of the pharmacokinetics of antisense oligonucleotide drugs. Antisense drug technology, CRC Press**:** 192-224.

Greb, A. and R. Bitsch (1998). "Comparative bioavailability of various thiamine derivatives after oral administration." International Journal of Clinical Pharmacology and Therapeutics **36**(4): 216-221.

Guo, W., J. Sheng and X. Feng (2015). "13C-metabolic flux analysis: an accurate approach to demystify microbial metabolism for biochemical production." Bioengineering **3**(1): 3.

Hammes, H. P., X. Du, D. Edelstein, T. Taguchi, T. Matsumura, Q. Ju, J. Lin, A. Bierhaus, P. Nawroth, D. Hannak, M. Neumaier, R. Bergfeld, I. Giardino and M. Brownlee (2003). "Benfotiamine blocks three major pathways of hyperglycemic damage and prevents experimental diabetic retinopathy." Nat Med **9**(3): 294-299.

Hanberry, B. S., R. Berger and J. A. Zastre (2014). "High-dose vitamin B1 reduces proliferation in cancer cell lines analogous to dichloroacetate." Cancer Chemother Pharmacol **73**(3): 585-594.

Hilz, H., U. Wiegers and P. Adamietz (1975). "Stimulation of proteinase K action by denaturing agents: application to the isolation of nucleic acids and the degradation of 'masked' proteins." Eur J Biochem **56**(1): 103-108.

Hoke, G. D., K. Draper, S. M. Freier, C. Gonzalez, V. B. Driver, M. C. Zounes and D. J. Ecker (1991). "Effects of phosphorothioate capping on antivense oligonucleotide stability, hybridization and antiviral efficacy versus herpes simplex virus infection." Nucleic acids research **19**(20): 5743-5748.

Husser, C., A. Brink, M. Zell, M. B. Müller, E. Koller and S. Schadt (2017). "Identification of GalNAc-Conjugated Antisense Oligonucleotide Metabolites Using an Untargeted and Generic Approach Based on High Resolution Mass Spectrometry." Analytical Chemistry **89**(12): 6821-6826.

Iwamoto, N., D. C. D. Butler, N. Svrzikapa, S. Mohapatra, I. Zlatev, D. W. Y. Sah, Meena, S. M. Standley, G. Lu, L. H. Apponi, M. Frank-Kamenetsky, J. J. Zhang, C. Vargeese and G. L. Verdine (2017). "Control of phosphorothioate stereochemistry substantially increases the efficacy of antisense oligonucleotides." Nature Biotechnology **35**: 845.

Jang, C., L. Chen and J. D. Rabinowitz (2018). "Metabolomics and Isotope Tracing." Cell **173**(4): 822-837.

Jeanpierre, M. (1987). "A rapid method for the purification of DNA from blood." Nucleic Acids Res **15**(22).

Jemal, M. (2000). "High-throughput quantitative bioanalysis by LC/MS/MS." Biomedical Chromatography **14**(6): 422-429.

Johnson, J. L., W. Guo, J. Zang, S. Khan, S. Bardin, A. Ahmad, J. X. Duggan and I. Ahmad (2005). "Quantification of raf antisense oligonucleotide (rafAON) in biological matrices by LC-MS/MS to support pharmacokinetics of a liposome-entrapped rafAON formulation." Biomedical Chromatography **19**(4): 272-278.

Jonus, H. C., B. S. Hanberry, S. Khatu, J. Kim, H. Luesch, L. H. Dang, M. G. Bartlett and J. A. Zastre (2018). "The Adaptive Regulation of Thiamine Pyrophosphokinase-1 Facilitates Malignant Growth During Supplemental Thiamine Conditions." Oncotarget **9**(83): 35422-35438.

Kim, J., C. P. Hopper, K. H. Connell, P. Darkhal, J. A. Zastre and M. G. Bartlett (2016). "Development of a novel method for the bioanalysis of benfotiamine and sulbutiamine in cancer cells." Analytical Methods **8**(28): 5596-5603.

Lee, T., H. Awano, M. Yagi, M. Matsumoto, N. Watanabe, R. Goda, M. Koizumi, Y. Takeshima and M. Matsuo (2017). "2'-O-Methyl RNA/Ethylene-Bridged Nucleic Acid Chimera Antisense Oligonucleotides to Induce Dystrophin Exon 45 Skipping." Genes **8**(2): 67.

Lin, Z. J., W. Li and G. Dai (2007). "Application of LC–MS for quantitative analysis and metabolite identification of therapeutic oligonucleotides." Journal of pharmaceutical and biomedical analysis **44**(2): 330-341.

Loew, D. (1996). "Pharmacokinetics of thiamine derivatives especially of benfotiamine." International Journal of Clinical Pharmacology and Therapeutics **34**(2): 47-50.

Lu, J. and E. L. Frank (2008). "Rapid HPLC measurement of thiamine and its phosphate esters in whole blood." Clinical chemistry **54**(5): 901-906.

LU'O'NG, K. V. Q. and L. T. H. NGUYỄN (2013). "The role of thiamine in cancer: possible genetic and cellular signaling mechanisms." Cancer Genomics-Proteomics **10**(4): 169-185.

Lysik, M. A. and S. Wu-Pong (2003). "Innovations in oligonucleotide drug delivery." Journal of pharmaceutical sciences **92**(8): 1559-1573.

Malandrinos, G., M. Louloudi and N. Hadjiliadis (2006). "Thiamine models and perspectives on the mechanism of action of thiamine-dependent enzymes." Chemical Society Reviews **35**(8): 684-692.

Mansoor, M. and A. J. Melendez (2008). "Advances in antisense oligonucleotide development for target identification, validation, and as novel therapeutics." Gene regulation and systems biology **2**: GRSB. S418.

Mansoor, M. and A. J. Melendez (2008). "Advances in antisense oligonucleotide development for target identification, validation, and as novel therapeutics." Gene regulation and systems biology **2**: 275-295.

McCarthy, S. M., M. Gilar and J. Gebler (2009). "Reversed-phase ion-pair liquid chromatography analysis and purification of small interfering RNA." Analytical biochemistry **390**(2): 181-188.

McGinnis, A. C., B. Chen and M. G. Bartlett (2012). "Chromatographic methods for the determination of therapeutic oligonucleotides." Journal of Chromatography B **883**: 76-94.

McGinnis, A. C., B. S. Cummings and M. G. Bartlett (2013). "Ion-exchange liquid chromatography method for the direct determination of small ribonucleic acids." Analytica Chimica Acta **799**: 57-67.

McGinnis, A. C., B. S. Cummings and M. G. Bartlett (2013). "Ion exchange liquid chromatography method for the direct determination of small ribonucleic acids." Analytica chimica acta **799**: 57-67.

McGinnis, A. C., E. C. Grubb and M. G. Bartlett (2013). "Systematic optimization of ion-pairing agents and hexafluoroisopropanol for enhanced electrospray ionization mass spectrometry of oligonucleotides." Rapid Communications in Mass Spectrometry **27**(23): 2655-2664.

Mendoza, R., A. D. Miller and J. Overbaugh (2013). "Disruption of thiamine uptake and growth of cells by feline leukemia virus subgroup A." Journal of virology **87**(5): 2412-2419.

Metallo, C. M., J. L. Walther and G. Stephanopoulos (2009). "Evaluation of 13C isotopic tracers for metabolic flux analysis in mammalian cells." Journal of biotechnology **144**(3): 167-174.

Miller, P. S., R. A. Cassidy, T. Hamma and N. S. Kondo (2000). "Studies on anti-human immunodeficiency virus oligonucleotides that have alternating methylphosphonate/phosphodiester linkages." Pharmacology & therapeutics **85**(3): 159-163.

Milligan, J. F., M. D. Matteucci and J. C. Martin (1993). "Current concepts in antisense drug design." Journal of medicinal chemistry **36**(14): 1923-1937.

Murphy, A. T., P. Brown-Augsburger, R. Z. Yu, R. S. Geary, S. Thibodeaux and B. L. Ackermann (2005). "Development of an ion-pair reverse-phase liquid chromatographic/tandem mass spectrometry method for the determination of an 18-mer phosphorothioate oligonucleotide in mouse liver tissue." European Journal of Mass Spectrometry **11**(2): 209-216.

Nanaware, D. A., V. K. Bhusari and S. R. Dhaneshwar (2013). "Validated HPLC method for simultaneous quantitation of Benfotiamine and metformin hydrochloride in bulk drug and formulation." Int J Pharm Pharm Sci **5**: 138-142.

Nicklin, P., S. Craig and J. Phillips (1998). Pharmacokinetic properties of phosphorothioates in animals—absorption, distribution, metabolism and elimination. Antisense Research and Application, Springer**:** 141-168.

Nosaka, K., M. Onozuka, N. Kakazu, S. Hibi, H. Nishimura, H. Nishino and T. Abe (2001). "Isolation and characterization of a human thiamine pyrophosphokinase cDNA1." Biochimica et Biophysica Acta (BBA)-Gene Structure and Expression **1517**(2): 293-297.

Nwokeoji, A. O., A.-W. Kung, P. M. Kilby, D. E. Portwood and M. J. Dickman (2017). "Purification and characterisation of dsRNA using ion pair reverse phase chromatography and mass spectrometry." Journal of Chromatography A **1484**: 14-25.

Nyakas, A., L. C. Blum, S. R. Stucki, J.-L. Reymond and S. Schürch (2013). "OMA and OPA—Software-Supported Mass Spectra Analysis of Native and Modified Nucleic Acids." Journal of The American Society for Mass Spectrometry **24**(2): 249-256.

Pácal, L., J. Tomandl, J. Svojanovský, D. Krusová, S. Štěpánková, J. Řehořová, J. Olšovský, J. Bělobrádková, V. Tanhäuserová and M. Tomandlová (2010). "Role of thiamine status and genetic variability in transketolase and other pentose phosphate cycle enzymes in the progression of diabetic nephropathy." Nephrology Dialysis Transplantation **26**(4): 1229-1236.

Pallan, P. S., C. R. Allerson, A. Berdeja, P. P. Seth, E. E. Swayze, T. P. Prakash and M. Egli (2012). "Structure and nuclease resistance of 2',4'-constrained 2'-O-methoxyethyl (cMOE) and 2'-O-ethyl (cEt) modified DNAs." Chemical communications (Cambridge, England) **48**(66): 8195-8197.

Panuwet, P., R. E. Hunter, P. E. D'Souza, X. Chen, S. A. Radford, J. R. Cohen, M. E. Marder, K. Kartavenka, P. B. Ryan and D. B. Barr (2016). "Biological Matrix Effects in Quantitative Tandem Mass Spectrometry-Based Analytical Methods: Advancing Biomonitoring." Critical reviews in analytical chemistry / CRC **46**(2): 93-105.

Patil, S. D., D. G. Rhodes and D. J. Burgess (2005). "DNA-based therapeutics and DNA delivery systems: a comprehensive review." The AAPS journal **7**(1): E61-E77.

Portari, G. V., H. Vannucchi and A. A. Jordao (2013). "Liver, plasma and erythrocyte levels of thiamine and its phosphate esters in rats with acute ethanol intoxication: A comparison of thiamine and benfotiamine administration." European Journal of Pharmaceutical Sciences **48**(4-5): 799-802.

Puts, J., M. de Groot, M. Haex and B. Jakobs (2015). "Simultaneous determination of underivatized vitamin B1 and B6 in whole blood by reversed phase ultra high performance liquid chromatography tandem mass spectrometry." PloS one **10**(7): e0132018.

Rabbani, N. and P. J. Thornalley (2011). "Emerging role of thiamine therapy for prevention and treatment of early-stage diabetic nephropathy." Diabetes Obes Metab **13**(7): 577-583.

Rani, K. and S. Paliwal (2014). "A review on targeted drug delivery: Its entire focus on advanced therapeutics and diagnostics." Sch. J. App. Med. Sci **2**(1C): 328-331.

Ranoux, A. and U. Hanefeld (2013). "Improving transketolase." Topics in Catalysis **56**(9-10): 750-764.

Remane, D., M. R. Meyer, D. K. Wissenbach and H. H. Maurer (2010). "Ion suppression and enhancement effects of co-eluting analytes in multi-analyte approaches: systematic investigation using ultra-high-performance liquid chromatography/mass spectrometry with atmospheric-pressure chemical ionization or electrospray ionization." Rapid Communications in Mass Spectrometry **24**(21): 3103-3108.

Rosie, Z. Y., T.-W. Kim, A. Hong, T. A. Watanabe, H. J. Gaus and R. S. Geary (2006). "Cross-species pharmacokinetic comparison from mouse to man of a second generation antisense oligonucleotide ISIS 301012, targeting human ApoB-100." Drug Metabolism and Disposition.

Ruan, Q., S. Peterman, M. A. Szewc, L. Ma, D. Cui, W. G. Humphreys and M. Zhu (2008). "An integrated method for metabolite detection and identification using a linear ion trap/Orbitrap

mass spectrometer and multiple data processing techniques: application to indinavir metabolite detection." Journal of Mass Spectrometry **43**(2): 251-261.

Sannes-Lowery, K. A. and S. A. Hofstadler (2003). "Sequence confirmation of modified oligonucleotides using IRMPD in the external ion reservoir of an electrospray ionization Fourier transform ion cyclotron mass spectrometer." Journal of the American Society for Mass Spectrometry **14**(8): 825-833.

Sayers, J. R., D. B. Olsen and F. Eckstein (1989). "Inhibition of restriction endonuclease hydrolysis by phosphorothioate-containing DNA." Nucleic acids research **17**(22): 9495.

Schellenberger, A. and G. Hübner (1985). "Thiamine pyrophosphate—carrier of the catalytic function of C—C-splitting enzymes." Biochemical Education **13**(4): 160-163.

Schildkraut, I. (2001). Nuclease. Encyclopedia of Genetics. S. Brenner and J. H. Miller. New York, Academic Press**:** 1357-1358.

Seth, P. P., A. Siwkowski, C. R. Allerson, G. Vasquez, S. Lee, T. P. Prakash, E. V. Wancewicz, D. Witchell and E. E. Swayze (2009). "Short Antisense Oligonucleotides with Novel 2′−4′ Conformationaly Restricted Nucleoside Analogues Show Improved Potency without Increased Toxicity in Animals." Journal of Medicinal Chemistry **52**(1): 10-13.

Seth, P. P., G. Vasquez, C. A. Allerson, A. Berdeja, H. Gaus, G. A. Kinberger, T. P. Prakash, M. T. Migawa, B. Bhat and E. E. Swayze (2010). "Synthesis and Biophysical Evaluation of 2′,4′-Constrained 2′O-Methoxyethyl and 2′,4′-Constrained 2′O-Ethyl Nucleic Acid Analogues." The Journal of Organic Chemistry **75**(5): 1569-1581.

Shemesh, C. S., R. Z. Yu, H. J. Gaus, S. Greenlee, N. Post, K. Schmidt, M. T. Migawa, P. P. Seth, T. A. Zanardi, T. P. Prakash, E. E. Swayze, S. P. Henry and Y. Wang (2016). "Elucidation

of the Biotransformation Pathways of a Galnac(3)-conjugated Antisense Oligonucleotide in Rats and Monkeys." Molecular Therapy. Nucleic Acids **5**(5): e319.

Shin, B. H., S. H. Choi, E. Y. Cho, M.-J. Shin, K.-C. Hwang, H. K. Cho, J. H. Chung and Y. Jang (2004). "Thiamine attenuates hypoxia-induced cell death in cultured neonatal rat cardiomyocytes." Mol Cells **18**(2): 133-140.

Shin, B. H., S. H. Choi, E. Y. Cho, M. J. Shin, K. C. Hwang, H. K. Cho, J. H. Chung and Y. S. Jang (2004). "Thiamine attenuates hypoxia-induced cell death in cultured neonatal rat cardiomyocytes." Molecules and Cells **18**(2): 133-140.

Spitzer, S. and F. Eckstein (1988). "Inhibition of deoxyribonucleases by phosphorothioate groups in oligodeoxyribonucleotides." Nucleic acids research **16**(24): 11691-11704.

Stein, C., C. Subasinghe, K. Shinozuka and J. S. Cohen (1988). "Physicochemical properties of phospborothioate oligodeoxynucleotides." Nucleic acids research **16**(8): 3209-3221.

Studzińska, S., R. Rola and B. Buszewski (2016). "Development of a method based on ultra high performance liquid chromatography coupled with quadrupole time-of-flight mass spectrometry for studying the in vitro metabolism of phosphorothioate oligonucleotides." Analytical and bioanalytical chemistry **408**(6): 1585-1595.

Tretter, L. and V. Adam-Vizi (2005). "Alpha-ketoglutarate dehydrogenase: a target and generator of oxidative stress." Philosophical Transactions of the Royal Society of London B: Biological Sciences **360**(1464): 2335-2345.

Trovero, F., M. Gobbi, J. Weil-Fuggaza, M. J. Besson, D. Brochet and S. Pirot (2000). "Evidence for a modulatory effect of sulbutiamine on glutamatergic and dopaminergic cortical transmissions in the rat brain." Neurosci Lett **292**(1): 49-53.

Van Goor, F., S. Hadida, P. D. J. Grootenhuis, B. Burton, J. H. Stack, K. S. Straley, C. J. Decker, M. Miller, J. McCartney, E. R. Olson, J. J. Wine, R. A. Frizzell, M. Ashlock and P. A. Negulescu (2011). "Correction of the F508del-CFTR protein processing defect in vitro by the investigational drug VX-809." Proceedings of the National Academy of Sciences **108**(46): 18843-18848.

van Landeghem, B. A., J. Puts and H. A. Claessens (2005). "The analysis of thiamin and its derivatives in whole blood samples under high pH conditions of the mobile phase." Journal of chromatography B **822**(1-2): 316-321.

Van Reeth, O. (1999). "Pharmacologic and therapeutic features of sulbutiamine." Drugs Today (Barc) **35**(3): 187-192.

Varadi, G., Z. Zhu and S. G Carter (2015). "Efficient Transdermal Delivery of Benfotiamine in an Animal Model." ADMET and DMPK **2**(4): 272-281.

Verma, A. (2018). "Recent Advances in Antisense Oligonucleotide Therapy in Genetic Neuromuscular Diseases." Annals of Indian Academy of Neurology **21**(1): 3-8.

Vojta, J., P. Hanzlík, A. Jedlička and P. Coufal (2015). "Separation and determination of impurities in paracetamol, codeine and pitophenone in the presence of fenpiverinium in combined suppository dosage form." Journal of Pharmaceutical and Biomedical Analysis **102**: 85-92.

Volvert, M.-L., S. Seyen, M. Piette, B. Evrard, M. Gangolf, J.-C. Plumier and L. Bettendorff (2008). "Benfotiamine, a synthetic S-acyl thiamine derivative, has different mechanisms of action and a different pharmacological profile than lipid-soluble thiamine disulfide derivatives." BMC pharmacology **8**(1): 10.

Yang, F., D. Li, K. Feng, D. Hu and S. Li (2010). "Determination of nucleotides, nucleosides and their transformation products in Cordyceps by ion-pairing reversed-phase liquid chromatography–mass spectrometry." Journal of Chromatography A **1217**(34): 5501-5510.

Ye, G. and M. Beverly (2011). "The use of strong anion-exchange (SAX) magnetic particles for the extraction of therapeutic siRNA and their analysis by liquid chromatography/mass spectrometry." Rapid Commun Mass Spectrom **25**(21): 3207-3215.

Ye, G. and M. Beverly (2011). "The use of strong anion-exchange (SAX) magnetic particles for the extraction of therapeutic siRNA and their analysis by liquid chromatography/mass spectrometry." Rapid Communications in Mass Spectrometry **25**(21): 3207-3215.

Yu, R. Z., R. S. Geary, J. M. Leeds, T. Watanabe, M. Moore, J. Fitchett, J. Matson, T. Burckin, M. V. Templin and A. A. Levin (2001). "Comparison of pharmacokinetics and tissue disposition of an antisense phosphorothioate oligonucleotide targeting human Ha-ras mRNA in mouse and monkey." Journal of Pharmaceutical Sciences **90**(2): 182-193.

Zastre, J. A., B. S. Hanberry, R. L. Sweet, A. C. McGinnis, K. R. Venuti, M. G. Bartlett and R. Govindarajan (2013). "Up-regulation of vitamin B1 homeostasis genes in breast cancer." The Journal of nutritional biochemistry **24**(9): 1616-1624.

Zastre, J. A., R. L. Sweet, B. S. Hanberry and S. Ye (2013). "Linking vitamin B1 with cancer cell metabolism." Cancer & Metabolism **1**(1): 16.

Zhang, G., J. Lin, K. Srinivasan, O. Kavetskaia and J. N. Duncan (2007). "Strategies for bioanalysis of an oligonucleotide class macromolecule from rat plasma using liquid chromatography− tandem mass spectrometry." Analytical chemistry **79**(9): 3416-3424.

Zhang, J., W. S. Ahn, P. A. Gameiro, M. A. Keibler, Z. Zhang and G. Stephanopoulos (2014). "13C isotope-assisted methods for quantifying glutamine metabolism in cancer cells." Methods in enzymology **542**: 369.